NEPTUNE: a new software platform for advanced nuclear thermal hydraulics

Antoine Guelfi, Dominique Bestion, Marc Boucker, Pascal Boudier, Philippe Fillion, Marc Grandotto, Jean-Marc Hérard, Eric Hervieu, Pierre Péturaud

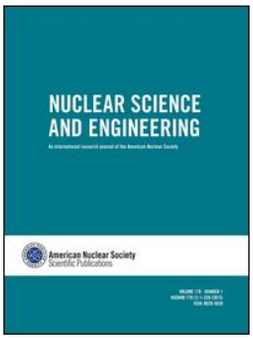

Nuclear Science and Engineering

ISSN: 0029-5639 (Print) 1943-748X (Online) Journal homepage: www.tandfonline.com/journals/unse20

NEPTUNE: A New Software Platform for Advanced Nuclear Thermal Hydraulics

Antoine Guelfi, Dominique Bestion, Marc Boucker, Pascal Boudier, Philippe Fillion, Marc Grandotto, Jean-Marc Hérard, Eric Hervieu & Pierre Péturaud

To cite this article: Antoine Guelfi, Dominique Bestion, Marc Boucker, Pascal Boudier, Philippe Fillion, Marc Grandotto, Jean-Marc Hérard, Eric Hervieu & Pierre Péturaud (2007) NEPTUNE: A New Software Platform for Advanced Nuclear Thermal Hydraulics, Nuclear Science and Engineering, 156:3, 281-324, DOI: 10.13182/NSE05-98

To link to this article: https://doi.org/10.13182/NSE05-98

Published online: 10 Apr 2017.

NUCLEAR SCIENCE AND ENGINEERING: **156**, 281–324 (2007)

NEPTUNE: A New Software Platform for Advanced Nuclear Thermal Hydraulics

Antoine Guelfi,[a]* Dominique Bestion,[b] Marc Boucker,[a] Pascal Boudier,[b] Philippe Fillion,[c] Marc Grandotto,[d] Jean-Marc Hérard,[a] Eric Hervieu,[b] and Pierre Péturaud[a]

[a]*Électricité de France, R&D Division, Fluid Mechanics, Power Generation, and Environment, 6 quai Watier, 78400 Chatou, France*
[b]*Commissariat à l'Energie Atomique, Nuclear Energy Division, DER/SSTH, CEA Grenoble, 17 rue des Martyrs, 38000 Grenoble, France*
[c]*Commissariat à l'Energie Atomique, Nuclear Energy Division, DM2S/SFME, CEA Saclay, 91191 Gif sur Yvette, France*
[d]*Commissariat à l'Energie Atomique, Nuclear Energy Division, DTN/SMTM, CEA Cadarache, 13108 Saint-Paul Lez Durance, France*

Received December 19, 2005
Accepted September 2, 2006

Abstract—*The NEPTUNE project constitutes the thermal-hydraulic part of the long-term Electricité de France and Commissariat à l'Energie Atomique joint research and development program for the next generation of nuclear reactor simulation tools. This program is also financially supported by the Institut de Radioprotection et Sûreté Nucléaire and AREVA NP. The project aims at developing a new software platform for advanced two-phase flow thermal hydraulics covering the whole range of modeling scales and allowing easy multiscale and multidisciplinary calculations. NEPTUNE is a fully integrated project that covers the following fields: software development, research in physical modeling and numerical methods, development of advanced instrumentation techniques, and performance of new experimental programs.*

The analysis of the industrial needs points out that three main simulation scales are involved. The system scale is dedicated to the overall description of the reactor. The component or subchannel scale allows three-dimensional computations of the main components of the reactors: cores, steam generators, condensers, and heat exchangers. The current generation of system and component codes has reached a very high level of maturity for industrial applications. The third scale, computational fluid dynamics (CFD) in open medium, allows one to go beyond the limits of the component scale for a finer description of the flows. This scale opens promising perspectives for industrial simulations, and the development and validation of the NEPTUNE CFD module have been a priority since the beginning of the project. It is based on advanced physical models (two-fluid or multifield model combined with interfacial area transport and two-phase turbulence) and modern numerical methods (fully unstructured finite volume solvers). For the system and component scales, prototype developments have also started, including new physical models and numerical methods.

In addition to scale-specific developments, the generalized use of multiscale calculations is also expected to be a major means to meet the industrial needs. The coexistence of different simulation scales together with the fast growth of computing power multiplies the computation possibilities. In particular, thanks to the recent progress of CFD tools, one can imagine local zooms in some critical parts of the reactor components. The NEPTUNE multiscale platform will offer advanced coupling functionalities based on state-of-the-art software architecture and new numerical coupling techniques.

Finally, despite the existence of a huge worldwide database of two-phase flow experiments, the validation of new physical models (more local, more complex) requires new experimental data. That is the reason why for several years we have been developing new instrumentation techniques such as four-sensor

*E-mail: antoine.guelfi@edf.fr

optical probes, X-ray tomography, and hot-wire anemometry. These techniques will be used for new experimental programs (currently being launched) that have been defined in connection with the high-priority industrial applications (departure from nucleate boiling, pressurized thermal shock, loss-of-coolant accident, etc.).

I. INTRODUCTION: THE NEPTUNE PROJECT

I.A. From the Industrial Needs to NEPTUNE

The NEPTUNE project was launched at the end of 2001 by Electricité de France (EDF) and the Commissariat à l'Energie Atomique (CEA) as the thermal-hydraulics part of their long-term joint research and development (R&D) program for the next generation of nuclear reactor simulation tools. This program is also financially supported by the Institut de Radioprotection et Sûreté Nucléaire (IRSN) and AREVA NP.

The whole project is built on a thorough analysis of the industrial needs, which has been carried out in recent years. At the end of the 1990s, the French partners actually started to perform a comprehensive analysis of the industrial configurations involving two-phase flows, and simultaneously they began to identify the limits of current simulation tools.[1] This work was extended to the European level within the frame of the EUROpean project for Future Advances in Science and Technology for Nuclear Engineering Thermal-hydraulic research (EUROFASTNET) concerted action,[2] which was launched during the Fifth European Framework Program FP5 (1998–2002). One of the main outcomes of the EUROFASTNET action was a state-of-the-art analysis of current thermal-hydraulic simulation tools. A priority list was also established ranking 44 industrial needs for which further scientific advances were required both in physical modeling and numerical methods. The analysis also benefited from numerous results obtained within the international framework by other projects (e.g., ASTAR, ECORA, or WAHALOADS in the European Community context[3]) and working groups (e.g., GAMA group activities for Organisation for Economic Co-operation and Development/Committee on the Safety of Nuclear Installations[4]).

The major stakes for the nuclear industry are the competitiveness of reactors (in comparison to alternative power-generation means) and the safety of nuclear power plants (NPPs). The industrial situations that were identified as priority needs are all closely connected to these two major assets for industrial companies and safety authorities. For instance, the improved prediction of departure from nucleate boiling (DNB) ranks among the high-priority needs since it is directly linked to fuel performance. In the same way, the estimation of the fluid temperature on the reactor pressure vessel (RPV) in case of a pressurized thermal shock (PTS) is a major issue when controlling the lifespan of critical components. The prediction of the maximum cladding temperature during a large-break loss-of-coolant accident (LBLOCA) is another example of prime importance for safety analysis.

In order to meet these industrial needs, the NEPTUNE project aims at preparing a new generation of two-phase flow thermal-hydraulic tools, covering the whole range of modeling scales and allowing easy multiscale and multidisciplinary calculations. To attain this ambitious objective EDF and CEA have decided to join their effort with the support of the Institut de Radioprotection et Sûrete Nucléaire (IRSN) and AREVA NP. The teams of both organizations and their expertise in the fields of physical modeling, numerical methods, code development, and experimental activities are gathered into a unique project. In addition to the considerable human potential it represents, this cooperation also ensures a more efficient coordination of the whole R&D work. This partnership between the French organizations has also been extended to neutronics, fuel thermomechanics, material behavior, and software architecture. The main objective of this large-scale collaboration is to develop a consistent set of codes enabling easy multiphysics and multiscale coupling.

The NEPTUNE project also benefits from the launching of the new European Community Integrated Project NUclear REactor SIMulation (NURESIM) (see Refs. 5 and 6), in which top-level organizations share their expertise in physical modeling and numerical methods in order to build a common software platform for nuclear reactor simulation.

I.B. A Multiscale Approach

The analysis of the industrial needs points out that different simulation scales are involved. The significant steps forward (either in physical modeling or in numerical methods) have been identified for each scale and also for the coupling between them. This is summarized below.

I.B.1. The Three Scales

In two-phase flow thermal-hydraulic analysis for nuclear applications, three main simulation scales are usually described. They can be classified as follows:

1. *system scale*: dedicated to the overall description of the reactor circuits. The main applications are safety analysis, operation studies, and real-time simulators. The

CATHARE code[7] has been developed by the same partners as for NEPTUNE and constitutes the present generation of system code used in France. It is similar to other system codes such as the TRAC/RELAP Advanced Computational Engine (TRACE) (see Ref. 8). The primary and secondary circuits of a reactor are modeled by coupling zero-dimensional (0-D), one-dimensional (1-D), and three-dimensional (3-D) modules together with submodules like walls, fuels, pumps, valves, breaks, safety systems, heat exchangers, and control systems. Pipes are modeled with 1-D modules, pipe connections with tees, large volumes by a two-node capacity module, and the 3-D module [computational fluid dynamics (CFD) in porous medium] is used for the pressure vessel. The whole reactor is modeled using a few hundred 0-D or 1-D cells, whereas the pressure vessel requires about 1000 3-D coarse cells (decimeter or meter scale). This allows simulations of all accident scenarios, including LBLOCA and small-break LOCA (SBLOCA) with a reasonable central processing unit (CPU) time (<12 h).

2. *CFD in porous medium*: often referred to as the component scale (or subchannel scale), it is dedicated to the design, safety, and operation studies for reactor cores and tubular heat exchangers (steam generators, condensers, and auxiliary exchangers). Technical objects (rod, plate, or tube bundles) are homogenized into the control volumes using the "porosity" concept. The minimum spatial resolution is fixed by the subchannel size (centimeter scale). The 3-D module of a system code (like CATHARE-3D, for instance) can be considered as a special case of component code, the main difference lying in the discretization that is used (much more refined for component studies). In France, the current generation of component codes is made of FLICA (Ref. 9), GENEPI (Ref. 10), and THYC (Ref. 11). Other renowned examples of subchannel codes are COBRA-TF (Ref. 12), NASCA (Ref. 13), and ATHOS (Ref. 14).

3. *CFD in open medium*: the average scale (millimeter or less) allows one to go beyond the limits of the component scale for a finer description of the flows. It includes turbulence modeling using a Reynolds-Averaged Navier-Stokes (RANS) approach, and new approaches similar to large eddy simulation (LES) will be envisaged. One can envisage local analyses in the critical parts of the cores, steam generators, or other components including complex geometries. It is also the only scale that is able to predict the fluid temperature field for investigating thermal shocks or thermal fatigue of the reactor structures. The development of multiphase CFD and its use for industrial applications are quite recent compared to the other scales, even though a huge international R&D effort has already been produced on this subject. Both "in-house" and "commercial" codes are currently being developed and validated. A recent synthesis on the use of two-phase CFD to nuclear reactor thermal hydraulics can be found in Ref. 15.

One may add a smaller scale to this classification: direct numerical simulation (DNS), which encounters an outstanding international interest, thanks to the fast growth of computational power. The characteristic length is less than the micrometer. It allows local simulations focusing on very small domains (e.g., containing a few bubbles or droplets). Although DNS is not expected to be used directly for industrial simulations for several years, it will help in understanding local flow phenomena and may be used for developing closure relations for more macroscopic models (see Sec. VII.A.2 for preliminary results).

I.B.2. Improving the Different Scales

Future (2010–2015) industrial calculations will still require a combined use of the three major scales (system, component, and CFD). For the latter the major steps toward the next generation lie in both new physical models and improved numerical methods. The corresponding NEPTUNE research work and the first results for each scale will be detailed in the next sections. The broad outlines are summarized below:

1. for the three "industrial" scales: the development of advanced unstructured finite volumes methods and generalization of parallelism
2. system codes and component codes: these codes have reached a very high level of maturity for industrial applications, which arises from more than 25 years of R&D. These tools will still be used for at least 10 years by engineering teams. Further progress is now mainly expected from:
   a. *system scale*: multifield modeling, interfacial area transport (IAT) (1-D and 3-D porous), improved numerical treatment of the reflooding phase in case of LOCA
   b. *component scale*: two-fluid and multifield models for porous medium
   c. *main industrial applications*: pressurized water reactors (PWRs) in operation and in accidental transients [LBLOCA, steam line break (SLB)], boiling water reactors (BWRs), experimental and propulsion reactors, steam generator tube vibrations, corrosion
3. CFD in open medium: since this scale opens promising perspectives for industrial simulations, it was a priority of NEPTUNE Phase 1 (2002–2003) to produce the first principal release of the NEPTUNE CFD module. The main identified sources of progress are now the following ones:
   a. two-phase turbulence modeling, IAT modeling, direct contact condensation, droplet or bubble polydispersion
   b. separate phase modeling, wave behavior

c. new coupling methods with macroscopic scales (local zooms) or with other disciplines (such as neutronics or chemistry)

d. main industrial applications: DNB local analysis (boiling bubbly flows in rod bundles including complex geometries such as spacer grids), PTS (turbulent jet, disperse, and separate phase flows with direct contact condensation).

I.B.3. Developing Multiscale Coupling

Beyond these developments, which remain scale-specific, the generalized use of multiscale calculations is also expected to be a major means to improve the industrial simulations. The coexistence of at least three different simulation scales together with the fast growth of computing power multiplies the computation possibilities. For more than 30 years already, many organizations have developed coupled applications for the nuclear industry (see, for instance, Refs. 16 and 17 for well-known system/subchannel coupling applications). With the recent great progress of CFD, there is a renewal of interest in the field of multiscale and multiphysics coupling. For instance, in the case of a two-phase PTS, one can use a coupling between a system code and a CFD code (open medium); the CFD calculation is required to predict the local fluid temperature in the downcomer and its evolution with time. Another interesting example is given by the local calculation in a small part of the core (using CFD in open medium) coupled with a component calculation (CFD in porous medium) for the whole domain. Various projects in the world aim at developing improved coupled systems. In the nuclear industry see, for instance, Refs. 18 and 19; another example in the field of meteorology can be found in Ref. 20. In this paper multiphysics coupling issues will not be addressed, although the NEPTUNE team is also involved in such activities.

Whatever the type of thermal-hydraulic/thermal-hydraulic coupling is (1-D/3-D, open/porous medium, two-fluid/homogeneous models, or any other combination), a multiscale software platform must fulfill at least two basic conditions:

1. At the software level, the different applications must share a unified architecture at least for the transfer of data between each other. This software architecture must be based on modern and international standards.

2. At the physical and numerical levels, new methods must be developed to couple different two-phase flow models. These methods can be classified into two families:

   a. *interfacial coupling*: The information is transmitted through an interface that delimitates two different computation domains.

   b. *volume coupling*: Different solving techniques are used on overlapping parts of the same physical domain.

   So far, only the first family has been tackled within the NEPTUNE project; the corresponding research is presented in Sec. VII.B.

I.C. Experimental Validation

Despite the existence of a huge worldwide database of two-phase flow experiments, developing new and complex physical models still requires new physical validation data. This is the reason why the NEPTUNE project also includes the following experimental activities:

1. definition of validation plans in connection with industrial situation targets (i.e., priority is given to the validation of the models that have a significant impact on the key industrial parameters)

2. development of advanced instrumentation for two-phase flow investigation such as advanced optical probes, X-ray tomography, and hot-wire anemometry

3. performance of new experiments, applying the validation plans defined above.

I.D. NEPTUNE Roadmap

The NEPTUNE project was launched at the end of 2001 after a 6-month period of intensive preparation by CEA and EDF (Phase 0).

Phase 1 actually started in 2002 and lasted 2 years (2002–2003). During this first period, the work mainly concentrated on the following:

1. the development of the first main release of NEPTUNE CFD: validation of the numerical method, benchmarking, implementation of new physical models with emphasis on DNB and PTS related models

2. the definition of the general software architecture for the NEPTUNE platform

3. the performance of first multiscale and multidisciplinary demonstration test cases

4. the launching of R&D programs (numerics, physics)

5. the definition of physical validation plans for high-priority industrial applications (DNB, PTS, LBLOCA).

Current phase (Phase 2, 2004–2006) is under way with the following priorities:

1. carrying out of the development and the validation of NEPTUNE CFD

2. extension of the scope of software development to the macroscopic scales (specifications and prototype developments for the component and system scales)

3. launching of new experimental programs in connection with the priority needs

4. continuation of the R&D program in numerical methods and physical modeling.

Since NEPTUNE aims at building new simulation tools for all the scales, it is a long-term project and final validated deliverables are expected by 2012–2015. The technical program for next phases (Phase 3, Phase 4, etc.) will be defined after the completion of Phase 2, taking into account all the technical results and the experience gained.

The rest of this paper is organized as follows:

1. In Secs. II through VI, we give a detailed presentation of NEPTUNE developments for all scales; we describe the current status of the NEPTUNE platform, and we provide the main results obtained so far.

2. In Sec. VII, we present the long-term R&D program.

3. In Sec. VIII, we focus on the experimental validation program, with a particular emphasis on the validation plan and new instrumentation techniques.

II. PHYSICAL AND NUMERICAL BASIS

II.A. Basic Sets of Equations

We consider two-phase flow models based on local instantaneous equations of fluid mechanics, derived from the basic principles of classical mechanics and thermodynamics. In an Eulerian framework, the conservation of mass, the basic law of mechanics (momentum balance), and the first principle of thermodynamics (energy conservation) can be expressed in the form of three balance equations (see, for instance, Ref. 21) as follows:

$$\frac{\partial \rho}{\partial t} + \nabla \cdot (\rho \vec{v}) = 0 \ , \tag{1}$$

$$\frac{\partial (\rho \vec{v})}{\partial t} + \nabla \cdot (\rho \vec{v}\vec{v} + p\bar{\bar{I}} - \bar{\bar{T}}) = \vec{F}_{ext} \ , \tag{2}$$

and

$$\frac{\partial}{\partial t}\left[\rho\left(u + \frac{1}{2}\vec{v}\vec{v}\right)\right] + \nabla \cdot \left[\rho \vec{v}\left(h + \frac{1}{2}\vec{v}\vec{v}\right) - \bar{\bar{T}} \cdot \vec{v} + q\right] = Q_{ext} + \vec{F}_{ext} \cdot \vec{v} \ . \tag{3}$$

These equations are valid inside each fluid phase, whereas additional jump conditions are necessary for the interfaces between two phases.

Constitutive relations are needed to express the stress tensors $\bar{\bar{T}}$ (see Nomenclature on p. 318) in terms of main variables and equations of state (EOS) are used to link thermodynamical variables ρ, T, h, and p to each other.

Because of the presence of small space and timescales involved both by turbulence and interfaces, direct simulation of these equations to solve industrial problems is still beyond the scope of current computational resources. Thus, these equations are either averaged or filtered by various processes, depending on the space and time resolution of the model.

Space averaging may contain walls in CFD for porous medium with a space filter scale greater than or equal to flow scales like the hydraulic diameter. In CFD for open medium, walls only exist at some boundaries of the calculation domain, and the space filter scale is significantly smaller than the hydraulic diameter.

Turbulent scales and scales associated with two-phase intermittency may be totally filtered like in RANS models or partially filtered like in the LES approach.

A phase averaging or a field averaging is often used, the basic equations for mass, momentum, and energy being first multiplied by a phase indicator function or a field indicator function before space, time, or ensemble averaging is applied. This may result either in a two-fluid model or in multifield models.

Modeling approaches can include additional transport equations to predict turbulence parameters ($K - \epsilon$, $R_{ij} - \epsilon$, etc.) or to characterize interfaces (interfacial area density, particle number density, etc.).

Smaller scale models may include some interface tracking/capturing methods (ITMs).

The NEPTUNE platform will include four main types of models:

1. *CFD in open medium*: Equations are time or ensemble averaged and possibly space averaged over a scale smaller than the hydraulic diameter. A phase averaging or a field averaging is used. Additional transport equations are used for turbulence and interfacial structure modeling. This approach will be used when flow parameters have to be predicted at a relatively small scale, for example, providing the transverse profiles of temperature, void fraction, and velocity in a pipe or in a subchannel in a reactor core or steam generator. The current version of NEPTUNE includes a two-fluid CFD tool for open medium, but the solver may receive multifield models (see Sec. III.A.1).

2. *3-D models for porous medium*: Equations of CFD in open medium are further space averaged over a scale larger than the hydraulic diameter. A porosity parameter appears in the equations and the computing cell size may be equal to or larger than the hydraulic diameter so that each cell contains walls. The transfers with the wall have

to be modeled in the right side of balance equations. This approach is used for calculating reactor cores, steam generators, or other tubular heat exchangers and also for the whole pressure vessel of a reactor in the system scale. Both two-fluid and multifield models are being developed for NEPTUNE CFD in porous medium.

3. *1-D model*: Equations of CFD in open medium are further space averaged over the cross section of the flow. The transfers with the wall have to be modeled in the right side of balance equations. Such a 1-D model is used in the system scale for modeling pipe flow and any flow in a reactor component when there is a privileged direction of flow. Both two-fluid and multifield models are being developed for the NEPTUNE 1-D model.

4. *0-D model*: Equations of CFD in open medium are further space averaged over the whole volume of the component. This very simplified approach is still often used in the system scale because of its low CPU cost.

Considering the CPU cost of 3-D CFD and the foreseeable improving efficiency of computers, the use of 1-D and 0-D models in system codes will still be necessary in most applications for at least the next two decades, the use of two-phase CFD being restricted to local zooms on some components for some specific issues.

Equations are given here in their primary form, for CFD in open medium when a two-fluid model is used, with $k = g, l$ denoting gas and liquid phases:

$$\frac{\partial}{\partial t}(\alpha_k \rho_k) + \nabla\cdot(\alpha_k \rho_k \vec{v}_k) = \Gamma_k \ , \tag{4}$$

$$\frac{\partial}{\partial t}(\alpha_k \rho_k \vec{v}_k) + \nabla\cdot(\alpha_k \rho_k \vec{v}_k \vec{v}_k - \alpha_k(\bar{\bar{T}}_k^m + \bar{\bar{T}}_k^{\mathrm{Re}}) + \alpha_k p_k \bar{\bar{I}}) = \vec{F}_{ki} + \Gamma_k \vec{v}_{ki} + \vec{F}_k^{ext} \ , \tag{5}$$

and

$$\frac{\partial}{\partial t}\left[\alpha_k \rho_k \left(e_k + \frac{1}{2}\vec{v}_k^2\right)\right] + \nabla\cdot\left[\alpha_k \rho_k \vec{v}_k \left(e_k + \frac{1}{2}\vec{v}_k^2\right) - \alpha_k \bar{\bar{T}}_k \cdot \vec{v}_k + \alpha_k p_k \vec{v}_k + \alpha_k (q_k^m + q_k^t)\right] = Q_{ki} + \Gamma_k \left(e_{ki} + \frac{1}{2}\vec{v}_{ki}^2\right) + \vec{F}_{ki}\cdot\vec{v}_{ki} + \vec{F}_k^{ext}\cdot\vec{v}_k + Q_k^{ext} \ . \tag{6}$$

Interfacial jump conditions are written as follows:

$$\sum_{k=g,l} \Gamma_k = 0 \ ; \quad \sum_{k=g,l} \Gamma_k \vec{v}_{ki} + \vec{F}_{ki} = 0 \ ;$$

$$\sum_{k=g,l} \left[Q_{ki} + \Gamma_k \left(e_{ki} + \frac{1}{2}\vec{v}_{ki}^2\right) + \vec{F}_{ki}.\vec{v}_{ki} \right] = 0 \ . \tag{7}$$

The energy balance equation is written in the total energy form, which is the sum of the internal energy e_k and the kinetic energy. In addition, the following trivial relation between the phase fractions holds:

$$\sum_{k=g,l} \alpha_k = 1 \ . \tag{8}$$

When models exist for $\bar{\bar{T}}_k$, Γ_k, $\vec{F}_{ki}$, $\vec{v}_{ki}$, q_k, Q_{ki}, e_{ki} seven unknowns remain: $\alpha\ (=\alpha_g), p_g, p_l, v_g, v_l, e_g, e_l$.

In the single-pressure approach, an additional algebraic relation is written between p_g and p_l to close the system. Notice that in the momentum and energy equations above, the interfacial pressure p_i contributions do not appear explicitly but through the interfacial momentum transfer term $\vec{F}_{ki}$, which can be split into two parts as follows:

$$\vec{F}_{ki} = \vec{M}_{ki} + p_i \nabla \alpha_k \ . \tag{9}$$

II.B. Basic Numerical Methods

II.B.1. A Common Framework: Finite Volume on Unstructured Meshes

Within the current NEPTUNE platform, the numerical methods used to solve the open-medium CFD–governing equations [Eqs. (4), (5), and (6)] share the same general spatial discretization framework of finite volumes on unstructured meshes. This allows the use of arbitrarily shaped cells (tetrahedrons, hexahedrons, prisms, pyramids, etc.) when combined with a face-based data structure. Nonmatching connections between cells are supported, provided that some local quality criteria are met.

Approximations of all variables are computed at the cell center of the finite volumes, while fluxes are exchanged at cell interfaces. Numerical consistency and precision for diffusive and advective fluxes for nonorthogonal and irregular cells are taken into account through a choice of gradient reconstruction techniques.

Based on this common framework, several choices can be made for time discretization and, moreover, for the method used to solve the set of coupled equations within a time step.

Indeed, mainly two methods are currently used for CFD in the NEPTUNE platform: a pressure-based method (also badly nicknamed "elliptic method") that is used in NEPTUNE CFD V1.0 (see Sec. III.A.1), and a hyperbolic method used in the OVAP module (see Sec. III.A.2). Note

that both methods are used to solve the system of Eqs. (4) through (7) with the single-pressure form ($p = p_l = p_g$).

III. NEPTUNE CFD IN OPEN MEDIUM

III.A. Numerical Methods

III.A.1. NEPTUNE CFD V1.0

The NEPTUNE CFD V1 numerical method stems from the class of well-known pressure-based methods used in single-phase flow solvers.[22] In this approach, mass, momentum, and energy are coupled by an iterative procedure within a time step. The system of Eqs. (4) through (7) is solved in two major fractional steps:

1. a prediction of phase velocities using the momentum equations
2. the coupling between phase fractions, pressure, and energy through mass and energy equations and a simplified form of momentum equations.

One major advantage of this algorithm is that it allows one to solve multifluid models (which were found necessary for several key industrial applications) with mass, momentum, and energy equations for an arbitrary number of m physical fields, not only the classical two-fluid model. We present below an overview of the algorithm described in more details in Ref. 23.

III.A.1.a. First Step: Velocities Prediction

During that step, $3m$ convection-diffusion equations with source terms are solved, one for each velocity component of each phase. These equations derive from partially linearized momentum equations, written for each increment $\delta\vec{v}_k^* = \vec{v}_k^* - \vec{v}_k^n$:

$$\rho_k^n \frac{\delta\vec{v}_k^*}{\Delta t} - \frac{\delta\vec{v}_k^*}{\alpha_k^n}\nabla\cdot(\alpha_k^n \rho_k^n \vec{v}_k^n) + (\delta\vec{v}_k^* \otimes \alpha_k^n \rho_k^n \vec{v}_k^n) - \sum_{l=1}^{m} \frac{\partial}{\partial\vec{v}_l}\left[\frac{\vec{F}_k'^m}{\alpha_k^n} + \vec{S}_k^n\right]\delta\vec{v}_l^* = \vec{B}_k^{exp} \tag{10}$$

and

$$\vec{B}_k^{exp} = \frac{\vec{v}_k^n}{\alpha_k^n}\nabla\cdot(\alpha_k^n \rho_k^n \vec{v}_k^n) - \frac{1}{\alpha_k^n}\nabla\cdot(\vec{v}_k^n \otimes \alpha_k^n \rho_k^n \vec{v}_k^n) - \nabla p^n + \rho_k^n \vec{g} + \frac{\vec{F}_k'^n}{\alpha_k^n} + \vec{S}_k^n \ . \tag{11}$$

In this system, the jacobian matrices $\partial(\vec{F}_k'/\alpha_k)/\partial\vec{v}_l$ represent the implication of interfacial transfer terms, which are taken into account only if they act as return-to-equilibrium terms and are easy to derive.

III.A.1.b. Second Step: Mass-Momentum-Energy Coupling

During this step, the advective and diffusive parts of the momentum equations are "frozen" using the predicted velocities $\vec{v}_k^*$, while the local and first-order differential terms, depending on pressure and phase fractions, are taken into account in an implicit way. The following reduced form of the momentum equation is considered:

$$\alpha_k^{n+1}\rho_k^n \frac{\vec{v}_k^{n+1} - \vec{v}_k^*}{\Delta t} - \sum_{l=1}^{m}\left[\frac{\partial\vec{S}_k'}{\partial\vec{v}_l}\right]^n (\vec{v}_l^{n+1} - \vec{v}_l^*) - \sum_{l=1}^{m}\left[\frac{\partial\vec{S}_k'}{\partial\alpha_l}\right]^n \delta\alpha_l^{n+1} + \sum_{l=1}^{m}\left[\frac{\partial\vec{S}_k'}{\partial(\nabla\alpha_l)}\right]^n \nabla\delta\alpha_l^{n+1} + \alpha_k^{n+1}\nabla\delta p^{n+1} = 0 \ , \tag{12}$$

with $\delta\alpha_l^{n+1} = \alpha_l^{n+1} - \alpha_l^n$ and $\vec{S}_k'$ gathering the interfacial momentum transfer and other source terms. These equations are coupled with the mass and energy equations, for which time discretization writes the following:

$$\frac{\alpha_k^{n+1}\rho_k^{n+1} - \alpha_k^n\rho_k^n}{\Delta t} + \nabla\cdot(\alpha_k^{n+1}\rho_k^n\vec{v}_k^{n+1}) = \Gamma_k^{n+1} \tag{13}$$

and

$$\frac{\alpha_k^{n+1}\rho_k^{n+1}H_k^{n+1} - \alpha_k^n\rho_k^n H_k^{n+1}}{\Delta t} + \nabla\cdot(\alpha_k^{n+1}\rho_k^n\vec{v}_k^{n+1}H_k^{n+1/2}) = \Gamma_k^{n+1/2}H_k^{n+1/2} + Q_{ki}^{n+1/2} + \alpha_k^{n+1/2}\frac{p^{n+1} - p^n}{\Delta t} \ . \tag{14}$$

In Eq. (14), the energy balance is written for the total enthalpy

$$H_k = \underbrace{e_k + p/\rho_k}_{h_k} + \tfrac{1}{2}\vec{v}_k^2 \ .$$

In order to couple Eqs. (12) through (14) in an efficient way, and considering that most applications concern low Mach number flows, it is necessary to reach the following goals:

1. fitting the Courant-Friedrichs-Levy number to material velocity rather than to the acoustic speed, by approximating velocities in an implicit way in the mass equations and pressure in momentum equations
2. ensuring that if a phase fraction tends toward zero (phase disappearance), the phase fraction is kept positive, and other variables of this phase tend toward controlled values (typically one needs to

define a bounded value of the velocity as the ratio of the momentum over the mass fraction, which may become cumbersome when the mass fraction vanishes)

3. coupling at best heat and mass transfers, which depend on pressure, energies and phase fractions, in a strongly nonlinear manner.

Velocity variables are first eliminated by introducing the reduced momentum equations into the mass equations. Additional simplifications are necessary for obtaining tractable coupled equations between pressure and volume fractions. To this end, implicit coupling between phase fractions inside the space divergence is not taken into account in Eq. (12). This leads to the following m equation nonlinear system for pressure p^{n+1} and phase fractions α_k^{n+1}:

$$\frac{\alpha_k^{n+1}\rho_k^{n+1} - \alpha_k^n \rho_k^n}{\Delta t} + \nabla\cdot(\alpha_k^{n+1}\rho_k^n \vec{v}_k^{n+1}) = \Gamma_k^{n+1} \quad , \quad (15)$$

with

$$\vec{v}_k^{n+1} = \vec{w}_k - \boldsymbol{R_k}\nabla\alpha_k^{n+1} - \boldsymbol{D_k}\nabla p^{n+1} \quad . \quad (16)$$

The system formed by Eqs. (14) and (15), closed with the constraint on the phase fractions $\sum_{k=1}^m \alpha_k^{n+1} = 1$, is solved thanks to an iterative procedure that is summarized below.

First, there is an initialization step:

$$i = 0 \quad , \quad p^{(i)} = p^n \quad , \quad \alpha_k^{(i)} = \alpha_k^n \quad , \quad H_k^{(i)} = H_l^n \quad ,$$

$$\vec{v}_k^{(i)} = \vec{v}_k^* \quad , \quad \rho_k^{(i)} = \rho_k(p^{(i)}, h_k^{(i)}, \ldots) \quad . \quad (17)$$

Then, iterations get started, in which the (i) values are sought from the previous $(i-1)$ values:

1. *Enthalpy prediction for all phases*. Enthalpy equations [Eq. (14)] are solved for the unknown $\delta H_k^{(i)}$. Then, thermophysical properties are updated.

2. *Volume fraction predictions*. Equation (15) is solved for the unknowns $\alpha_k^{(i)}$, in the following form:

$$\frac{\alpha_k^{(i)}\rho_k^{(i)} - \alpha_k^n\rho_k^n}{\Delta t} + \nabla\cdot(\alpha_k^{(i)}\rho_k^n(\vec{w}_k - \boldsymbol{D_k}\nabla p^{(i-1)}) - \alpha_k^{(i-1)}\rho_k^n \boldsymbol{R_k}\nabla\alpha_k^{(i)}) = \Gamma_k^{(i)} \quad . \quad (18)$$

When using a first-order upwind scheme for the convective part, and classical implicit two-point fluxes for diffusive terms, positive values of the void fraction are guaranteed. This also ensures convergence of approximations of the void fraction toward the true solution when using orthogonal or Voronoi meshes (see Ref. 24).

3. *Correction step with a pressure equation*. If the predicted volume fractions, which are all positive, do not respect constraint on phase fractions sum $\sum_{k=1}^m \alpha_k^{n+1} = 1$, a correction step is needed to adjust velocities through the gradient of the pressure increment $-\boldsymbol{D_k}\nabla\delta p^{(i)}$:

$$\frac{\alpha_k^{(i+1/2)}\rho_k^{(i+1/2)} - \alpha_k^{(i)}\rho_k^{(i)}}{\Delta t} + \mathrm{div}(-\alpha_k^{(i)}\rho_k^n \boldsymbol{D_k}\nabla\delta p^{(i)}) = \Gamma_k^{(i+1/2)} - \Gamma_k^{(i)} \quad . \quad (19)$$

All unknowns are expressed in terms of the pressure increment $\delta p^{(i)}$, using, in a simplified manner, the above equations, the energies equations, and the EOS. Then, by prescribing $\sum_{k=1}^m \alpha_k^{(i+1/2)} = 1$, we obtain an elliptic pressure equation on pressure increment. The right side is proportional to default or excess in phase fractions $\sum_{k=1}^m \alpha_k^{(i)} - 1$. Pressure and velocities are updated using the following:

$$\begin{cases} p^{(i)} = p^{(i-1)} + \delta p^{(i)} \\ \vec{v}_k^{(i)} = \vec{w}_k - \boldsymbol{R_k}\nabla\alpha_k^{(i)} - \boldsymbol{D_k}\nabla p^{(i)}. \end{cases} \quad (20)$$

4. *Convergence test*. The overall convergence of the procedure is controlled by a test on the predicted phase fraction sum constraint. If $|1 - \sum_{k=1}^m \alpha_k^{(i)}| \leq \varepsilon$, then the iterative procedure stops and

$$p^{n+1} = p^{(i)} \quad , \quad \alpha_k^{n+1} = \alpha_k^{(i)} \quad , \quad H_k^{n+1} = H_k^{(i)} \quad ,$$

$$\vec{v}_k^{n+1} = \vec{v}_k^{(i)} \quad , \quad \rho_k^{n+1} = \rho_k^{(i)} \quad ; \quad (21)$$

otherwise, the procedure goes back to step (1), with incrementation of (i).

When the procedure converges, all increments should tend toward zero, and the volume constraint is satisfied. If the procedure does not converge for a given number of cycles (about three to ten) and a given precision on volume conservation constraint, the time step is reduced and the procedure is restarted. There are several ways to couple Eqs. (14) and (15), see Ref. 25. The present approach, based on a global phasic continuity, is suitable for obtaining a very good balance for each mass balance equation, with or without mass transfer.

The spatial discretization is classical. As stated in II.B, approximations of all variables are computed at the cell centers of the finite volumes, while fluxes are computed at cell interfaces. Convective fluxes are approximated using upwind second-order schemes based on classical slope limiters. In order to increase the accuracy of diffusive fluxes, a special gradient reconstruction procedure is used,[26,27] which is valid for irregular and nonorthogonal cells.

III.A.2. OVAP

The OVAP code, which is part of the NEPTUNE CFD platform, benefits from a truly modular and extensible architecture that allows one to efficiently integrate new numerical methods and physical models. It provides finite volume approximations of solutions for two-phase flow models including a two-fluid model and a general multifield two-phase flow model. The governing equations of the standard two-fluid model have been recalled above while the reader is referred to Ref. 28 to see details of the overall multifield model. Moreover, the two-fluid model can be augmented by an IAT equation or the MUltiple-SIze Group (MUSIG) model. The keystone of the OVAP algorithm pertains to the use of an extension of the Roe's approximate Riemann solver[29] and the characteristic flux schemes to the frame of nonconservative hyperbolic systems arising when computing two-phase flow models.[30,31] Just as their single-phase counterparts, these schemes are characterized by low numerical diffusion, high resolution of shocks and contact discontinuities, and conservation properties through a finite volume formulation. They also provide some natural way to implement boundary conditions. However, the application of the generalized Roe scheme to the numerical simulation of two-phase flow models requires an efficient computation of the absolute value or the sign of the system matrix. In most of the two-phase flow models, this matrix has a nontrivial eigenstructure and the eigen decomposition is often ill-conditioned. The OVAP code uses a general, fast, and robust algorithm[32] avoiding the diagonalization process and enabling one to perform numerical simulation of complex systems such as multifield models. Implicit upwinding techniques are used in the code, and preconditioning techniques have been implemented, including incomplete LU (Lower triangular/Upper triangular), incomplete Choleski, and diagonal preconditioners. The library of algebraic solvers also offers various possibilities, among which is the Generalized Minimal RESidual (GMRES) type algorithm. Recently, the module has benefited from the introduction of schemes to account for diffusive effects on unstructured meshes. The whole is under extensive validation. For further details, the reader is referred to Refs. 28, 33, and 34.

III.B. Physical Models

III.B.1. General Framework for Physical Modeling in NEPTUNE CFD V1.0

In version V1.0 of the NEPTUNE CFD module for open medium, priority was given to the modeling of boiling bubbly flows for DNB investigations and of physical phenomena in cold leg and downcomer for PTS investigations. Prior to giving the details of the physical models dedicated to these two applications, the governing equations for a two-phase flow system in an open medium, with the single-pressure hypothesis $p = p_l = p_g$, are recalled in the form used in NEPTUNE CFD V1.0. These equations derive from the primary equations [Eqs. (4), (5), and (6)] by a splitting of interfacial transfer terms, revealing their physical nature and thus making them easier to model. They form a general framework where several terms, mainly interfacial transfer ones, still have to be related to primary variables by means of models depending on the flow features.

The mass balance equations are written as

$$\frac{\partial}{\partial t}(\alpha_k \rho_k) + \nabla\cdot(\alpha_k \rho_k \vec{v}_k) = \Gamma_k \ , \tag{22}$$

where Γ_k is the volumetric production rate of phase k due to phase change, including nucleation at walls.

The momentum balance equations are written in a nonconservative form as

$$\begin{aligned}\alpha_k \rho_k \left[\frac{\partial \vec{v}_k}{\partial t} + \vec{v}_k\cdot\nabla\vec{v}_k\right] &= \nabla\cdot[\alpha_k(\bar{\bar{T}}_k^m + \bar{\bar{T}}_k^{\mathrm{Re}})] \\ &\quad - \alpha_k\nabla p + \vec{M}_{ki} + \alpha_k \rho_k \vec{g} \\ &\quad + \Gamma_k(\vec{v}_{ki} - \vec{v}_k) \ ,\end{aligned} \tag{23}$$

where the first term in the right side contains the molecular stress tensor $\bar{\bar{T}}_k^m$ and the turbulent Reynolds stress tensor $\bar{\bar{T}}_k^{\mathrm{Re}}$, and the third term $\vec{M}_{ki}$ is the averaged interfacial momentum transfer term, to the exclusion of the mean pressure contribution [Eq. (9)].

The total enthalpy balance equations are written as

$$\begin{aligned}&\frac{\partial}{\partial t}(\alpha_k \rho_k H_k) + \nabla\cdot(\alpha_k \rho_k H_k \vec{v}_k) \\ &\quad = \alpha_k \frac{\partial p}{\partial t} - \nabla\cdot(\alpha_k(q_k^m + q_k^t)) + \nabla\cdot(\alpha_k \bar{\bar{T}}_k^m\cdot\vec{v}_k) \\ &\qquad + \alpha_k \rho_k \vec{g}\cdot\vec{v}_k + \vec{M}_{ki}\vec{v}_{ki} + \Gamma_k\left(h_{ki} + \vec{v}_{ki}\cdot\vec{v}_k - \frac{v_k^2}{2}\right) \\ &\qquad + a_i q_{ki} + Q_{k,ext} \ ,\end{aligned} \tag{24}$$

with $H_k = h_k + \frac{1}{2}v_k^2 = e_k + \frac{1}{2}v_k^2 + (p/\rho_k)$.

The molecular and turbulent heat fluxes for phase k are respectively noted q_k^m and q_k^t, while q_{ki} is the interfacial heat flux.

The turbulence modeling of a phase that can be considered as a continuous medium is described by a $K-\epsilon$ model, which is written here in a general form:

$$\begin{aligned}&\frac{\partial}{\partial t}(\alpha_k \rho_k K_k) + \nabla\cdot(\alpha_k \rho_k K_k \vec{v}_k) \\ &\quad = \nabla\cdot\left(\alpha_k \rho_k \frac{\nu_{tk}}{Pr_{tK}}\nabla K_k\right) - \alpha_k \rho_k \epsilon_k \\ &\qquad + \alpha_k \bar{\bar{T}}_k^{\mathrm{Re}} : \nabla\vec{v}_k + K_{ki}\Gamma_k + P_{Ki} + P_K^{\mathrm{IAC}}\end{aligned} \tag{25}$$

and

$$\frac{\partial}{\partial t}(\alpha_k \rho_k \epsilon_k) + \nabla\cdot(\alpha_k \rho_k \epsilon_k \vec{v}_k) = \nabla\cdot\left(\alpha_k \rho_k \frac{\nu_{tk}}{Pr_{t\epsilon}}\nabla\epsilon_k\right) - C_{\epsilon 2}\alpha_k \rho_k \frac{\epsilon_k^2}{K_k} + C_{\epsilon 1}\frac{\epsilon_k}{K_k}\alpha_k \bar{\bar{T}}_k^{\mathrm{Re}} : \nabla\vec{v}_k - \frac{2}{3}\alpha_k \rho_k \epsilon_k \nabla\cdot\vec{v}_k + \epsilon_{ki}\Gamma_k + P_{\epsilon i} \quad , \tag{26}$$

where the Reynolds stress tensor and the turbulent eddy viscosity are given by

$$\bar{\bar{T}}_k^{\mathrm{Re}} \equiv -\rho_k \overline{\vec{u}'\vec{u}'}^k = \rho_k \nu_{tk}(\nabla\vec{v}_k + \nabla^T\vec{v}_k) - \frac{2}{3}\rho_k(K_k + \nu_{tk}\nabla\cdot\vec{v}_k)\bar{\bar{I}} \tag{27}$$

and

$$\nu_{tk} \equiv C_\mu \frac{K_k^2}{\epsilon_k} \quad . \tag{28}$$

P_{Ki} and $P_{\epsilon i}$ are terms for the turbulence production induced by interfacial friction, while P_K^{IAC} is a source term due to coalescence and breakup of bubbles.

III.B.2. Physical Models for Boiling Bubbly Flows

In view of modeling boiling bubbly flows up to DNB occurrence, it was first considered that a special attention should be paid to all phenomena affecting the void repartition and the heat transfers. Since all forces acting on the bubbles depend on the bubble size, it was considered necessary to predict this size with a sufficient accuracy. Since the turbulence affects not only heat diffusion but also the bubble size through coalescence and breakup, it was also considered necessary to have a good prediction of the turbulent fields. The modeling choices were made with respect to these requirements together with the general concern of not being too complex for a first approach.

The selected modeling of boiling bubbly flows[35] for NEPTUNE CFD V1.0 is based on the six balance equations [Eqs. (22), (23), and (24)] of the two-fluid model. A $K-\epsilon$ model is added to predict the turbulence in the liquid phase. A transport equation for bubble interfacial area concentration (IAC) is also written to characterize both a mean bubble diameter and the interfacial transfer area. In such a flow, the IAC evolves rapidly because of many physical phenomena: bubble nucleation and collapse, bubble growing due to phase change and gas expansion, bubble coalescence and breakup. At the same time, the IAC is transported by the flow. The complete model has been tested in comparison with air-water data in a vertical pipe and boiling Freon data in a heated pipe.[35–38]

The $K-\epsilon$ turbulence model for the liquid phase in bubbly flows includes the effect of bubble-induced turbulence.[36] The specific models for bubbly flows are in fact due to the terms P_{Ki}, $P_{\epsilon i}$, and P_K^{IAC} in Eqs. (25) and (26).

The term P_K^{IAC} accounts for the energy exchange between the interfacial free energy and the liquid turbulent kinetic energy due to bubble coalescence and breakup. It is divided in two parts: $P_K^{\mathrm{IAC}} = -\sigma(\Phi_{a_i}^{CO} + \Phi_{a_i}^{BK})$, the terms $\Phi_{a_i}^{CO}$ and $\Phi_{a_i}^{BK}$ denoting respectively the sink and source terms of IAC due to bubble turbulent coalescence and breakup (σ is the surface tension).

The source terms P_{Ki} and $P_{\epsilon i}$ corresponding to the turbulence produced and dissipated in bubble wakes are modeled as

$$P_{Ki} = -(\vec{M}_g^D + \vec{M}_g^{MA})(\vec{v}_g - \vec{v}_l) \tag{29}$$

and

$$P_{\epsilon i} = C_{\epsilon 3}\frac{P_{Ki}}{\tau} \quad , \quad \tau = \left(\frac{d_s^2}{\epsilon_l}\right)^{1/3} \quad , \tag{30}$$

where τ is a characteristic time for the bubble-induced turbulence, and $\vec{M}_g^D$ and $\vec{M}_g^{MA}$ are the averaged drag and added mass forces exerted on the dispersed phase in the momentum equations.

In Eqs. (25) and (26), the default values of the different coefficients are taken from single-phase flow classical modeling: $\mathrm{Pr}_t = 0.9$, $\mathrm{Pr}_{tK} = 1$, $\mathrm{Pr}_{t\epsilon} = 1.3$, $C_{\epsilon 1} = 1.44$, $C_{\epsilon 2} = 1.92$, and $C_{mu} = 0.09$ (see Ref. 39). The value of the constant $C_{\epsilon 3}$ has been adjusted to 0.6.

The interfacial momentum transfer term is the sum of the drag force, the added mass force, the lift force, and a turbulent bubble dispersion force:

$$\vec{M}_{ki} = \vec{M}_k^D + \vec{M}_k^{MA} + \vec{M}_k^L + \vec{M}_k^{DT} \quad , \tag{31}$$

$$\vec{M}_g^D = -\vec{M}_l^D = -\tfrac{1}{8}a_i \rho_l C_D |\vec{v}_g - \vec{v}_l|(\vec{v}_g - \vec{v}_l) \quad , \tag{32}$$

$$\vec{M}_g^{MA} = -\vec{M}_l^{MA} = -C_{MA}\alpha\frac{1+2\alpha}{1-\alpha} \times \rho_l\left[\left(\frac{\partial\vec{v}_g}{\partial t} + \vec{v}_g\cdot\nabla\vec{v}_g\right) - \left(\frac{\partial\vec{v}_l}{\partial t} + \vec{v}_l\cdot\nabla\vec{v}_l\right)\right] \quad , \tag{33}$$

$$\vec{M}_g^L = -\vec{M}_l^L = -C_L\alpha\rho_l(\vec{v}_g - \vec{v}_l) \wedge Rot(\vec{v}_l) \quad , \tag{34}$$

and

$$\vec{M}_g^{DT} = -\vec{M}_l^{DT} = -C_{DT}\rho_l K_l \nabla\alpha \quad . \tag{35}$$

The added mass force does not play a significant role in the first selected applications to adiabatic and boiling flows, but both lift and turbulent dispersion forces may have a dominant role on the void distribution.

Considering now heat and mass transfers, the liquid to interface heat transfer is responsible for vaporization and condensation of bubbles and is modeled through a Nusselt number function of Reynolds, Prandtl, and Jakob numbers:

$$a_i q_{li} = h_{li} a_i (T_{sat} - T_l) \quad \text{and} \quad h_{li} = \frac{\lambda}{d_s} \text{Nu} \ , \tag{36}$$

$$\text{Nu} = \text{Nu}(\text{Re}, \text{Pr}, \text{Ja}) \ , \tag{37}$$

and

$$\text{Ja} = \frac{\rho_l C_{pl} (T_l - T_{sat})}{\rho g L} \ , \quad \text{Re} = \frac{d_s U_r}{\nu_l} \ ,$$

$$\text{Pr} = \frac{\nu_l}{a_l} \ . \tag{38}$$

Wall heat transfer is divided classically[40] into three parts for convective heat flux q_c, heat flux due to the quenching effect q_q, and heat flux used for phase change by bubble nucleation q_e:

$$q_w = q_c + q_q + q_e \ , \tag{39}$$

where q_c is expressed by log law wall function, and q_e is a function of the bubble frequency of detachment f, the bubble detachment diameter d_{nuc}, and the active nucleation site density N, which are correlated as follows:

$$q_e = f \frac{\pi}{6} d_{nuc}^3 \rho_g L N \ . \tag{40}$$

The interfacial mass transfer term is given by

$$\Gamma_g = -\Gamma_l = \frac{-q_{li} - q_{gi} + q_e}{H_g - H_l} \ . \tag{41}$$

The interfacial area equation can be derived[37] from a Liouville equation for the bubble probability density function:

$$\frac{\partial a_i}{\partial t} + \nabla \cdot (a i \vec{V}_i) = \frac{2}{3} \frac{a_i}{\alpha \rho_g} \left(\Gamma_{g,i} - \alpha \frac{d\rho_g}{dt} \right) + \pi d_{nuc}^2 \Phi_n^{NUC} + \Phi_{a_i}^{CO} + \Phi_{a_i}^{BK} \ , \tag{42}$$

with four source terms for mass transfer and density change effects, nucleation, coalescence, and breakup. In this first approach, the simplifying assumptions of spherical bubbles with a single bubble size given by d_s are made. The Sauter mean diameter d_s and bubble number density n are related to the IAC and the void fraction by the following relations:

$$d_s = \frac{6\alpha}{a_i} \quad \text{and} \quad n = \frac{\alpha}{\pi d_s^3 / 6} = \frac{1}{36\pi} \frac{a_i^3}{\alpha^2} \ . \tag{43}$$

The nucleation term is directly calculated from the wall nucleation models. Coalescence and breakup models were proposed by Yao and Morel.[38]

The results obtained with this model were compared with DEBORA tests for subcooled boiling with measurements of transverse profiles of void fraction, mean diameter d_s, and liquid temperature. The agreement is qualitatively good and quantitatively reasonable (see Sec. III.C.2). More interesting are the analyses of all sensitivity tests that were performed for both adiabatic and boiling bubbly flows:

1. The turbulence characteristics may be strongly affected by the presence of bubbles, and the current modeling is an extrapolation of the single-phase $K - \epsilon$ models by adding interfacial production and dissipation terms. Results are rather sensitive to the $C_{\epsilon 3}$ coefficient, and it is difficult to find a universal value for this term. Further progress would require one to model separately the turbulence produced by wall shear layers and the turbulence produced in bubble wakes, which may have very different scales. This approach has been followed in a recent thesis work.[41]

2. The local interfacial structure is currently characterized using the information provided by a transport equation for a bubble number density or an IAC. Original coalescence and breakup models without fitting coefficients[38] yield good predictions in boiling flows with good shape for void and mean diameter profiles. However it seems that none of the available coalescence and breakup models has a very wide range of validity, and further modeling effort is required. Another shortcoming of the presented model is the assumption of a single bubble size. For example, when the bubbles arrive in the core of the duct in a boiling channel, they condense because the liquid is locally subcooled. If all these bubbles have locally the same size, they will condense at the same speed and hence their diameter will decrease accordingly. If they have different sizes, the small bubbles will condense and collapse more rapidly, leaving the bigger ones, which increase the averaged bubble size. Therefore, the assumption of a single bubble size can lead to an underestimation of this bubble mean size in this case. The modeling of boiling bubbly flows with several bubble sizes should be addressed in future studies.

3. The formulation of lift and turbulent diffusion forces are still not generic, and more universal models are still to be developed.

4. Wall functions for momentum and energy equations are still taken from single-phase models, whereas

flow processes near the wall are significantly different in two-phase flow.

A first step has been achieved in modeling boiling bubbly flows (see also Sec. III.C.2 for computational results), and several ways for improving the modeling have been identified.

III.B.3. Physical Models for PTS Investigations

In PWRs, a class of transient events has been identified in which a rapid cooldown of the reactor vessel coincides with high internal pressure levels; this situation corresponds to a PTS (Refs. 42–44). Such an event produces high stresses and relatively low temperatures at the inner surface of the RPV. Because of the high stresses and the reduced fracture toughness near the inner surface caused by irradiation, preexisting flaws can propagate through the wall and cause vessel failure. SBLOCA scenarios exist with an emergency core cooling system (ECCS) injection in a partially or totally uncovered cold leg where the main heat source to the liquid is due to steam condensation in the cold leg and in the top of the downcomer.[45] Depending on the temperature of the mixture, the cold leg and the downcomer might be subjected to a thermal shock, which has to be withstood by the structure without brittle fracture risk. For RPV aging one must evaluate more precisely the liquid temperature evolution during the injection in order to not overestimate the thermal shock and justify a greater lifespan of the vessel. In this context, two-phase CFD methods with turbulence and adequate interfacial transfer models are useful, since they can provide the temperature field in the liquid and the thermal load on the reactor structure for such uncovered cold-leg configurations.

Because of the resulting heating of the water, condensation of steam is a key phenomenon that must be handled by the simulations. Condensation is mainly dependent on the interfacial structure and on the turbulent mixing in the liquid phase. The achieved work has focused on slow transients following an SBLOCA with a rather simple interfacial structure of the stratified flow in the cold leg. The main objective was the prediction of the liquid temperature field, which depends mainly on interfacial heat and mass transfer related to direct contact condensation of steam on a subcooled liquid and on the turbulence diffusion within the liquid. Many research works indicate that turbulence behavior near the interface plays a dominant role for the interfacial transfers. For ECCS injection cases, the turbulence mainly comes from the effect of the water jet and shear at the wall and at the gas-liquid interface. Thus, as a first step to simulate such scenarios, separate effects in simple geometry were investigated, i.e., interfacial friction and turbulence production, interfacial heat transfer, and turbulence in a water pool induced by a water jet, in order to establish and validate the developed models.

Two-phase CFD in open medium with a two-fluid model [Eqs. (22), (23), and (24)] was used for predicting local flow parameters of a stratified flow in a horizontal channel with or without condensation at the free surface.[46] Any point of a stratified flow is either single-phase gas, single-phase liquid, or two-phase in the free surface region with possible interfacial waves, and our purpose is to use a single set of equations for all cases. Such equations in the two-phase region of the interface are also assumed to filter all interfacial wave phenomena, and the resulting void fraction may allow one to predict the average free surface location. Single-phase gas region and single-phase liquid region can then be treated as single-phase flows with a moving boundary at the free surface and solid boundaries along the walls. Only the two-phase region equations are coupled with both single-phase regions and contain interfacial transfers between phases.

For modeling the turbulent stresses in momentum equations and turbulent heat transfers in energy equations, the rather simple $K-\epsilon$ model [Eqs. (25) and (26)] for each phase was selected to be first evaluated in such flow conditions. In single-phase regions, the classical formulation of single-phase $K-\epsilon$ equations is used with constants as recommended by Schiestel.[39] In the two-phase region, additional terms due to the interface have to be modeled. The turbulent stress tensor of phase k is assumed to depend only on local strain of phase k even in the two-phase region, and to be independent on phase change.

As already mentioned, the major issue when dealing with free surface flows is to correctly handle the tiny two-phase region corresponding to the interface. First, one has to calculate the IAC a_i to express the interfacial transfers of momentum and heat. As a first step, we assume a horizontal flat interface. The possible presence of interfacial waves is not taken into account, but according to the averaging of the equation, only the average interface position is calculated and the effects of waves could be later modeled as surface roughness effects like in wall friction (or wall heat transfer) models. In single-phase gas and single-phase liquid domains, a_i is set to zero. For a grid containing a stratified interface, the diffusion terms in momentum and energy are replaced by interfacial transfer terms that may be seen as boundary conditions for each phase, using extended wall functions. In $K-\epsilon$ equations diffusion terms are set to zero to satisfy the nondiffusion conditions across the interface. The interface is treated as a moving boundary for the gas region and the liquid region, and the wall function method is applied like for solid boundaries.

In a turbulent stratified flow, the interfacial heat transfer is controlled by turbulence in the vicinity of an interface. Part of this turbulence originates from wall shear regions and part is due to the turbulence production at the interface by interfacial friction and interfacial waves. Several models for interfacial friction and for interfacial

heat transfer were evaluated.[47–49] Results were reported by Yao et al.[46] The interfacial transfers were validated against air-water stratified flow experimental data of Fabre et al.[50] and steam-water stratified flow data with condensation of Lim et al.[51] in horizontal channel of rectangular cross section. Although some reasonable predictions were obtained[46] for the liquid velocity, turbulent kinetic energy, and shear profiles in the liquid layer, available heat transfer models could not predict correctly the significant increment of condensation when the interface changes from glossy to wavy. The complex interactions between interfacial waves, interfacial shear, interfacial heat transfer, and interfacial turbulence should be further investigated.

III.C. Validation and Demonstration Cases

The assessment process of NEPTUNE CFD V1 has involved both verification against a wide range of numerical and physical benchmarks and validation of physical models for bubbly flows and separate-phase flows.

III.C.1. Basic Numerical and Physical Tests

The definition of a set of physical and numerical test cases and the corresponding acceptability criteria to be fulfilled were thoroughly established, which helped a lot during the early stage of development. This work was motivated by the following ideas. It is well-known that the transport equations solved in the multiphase codes are rather more complex than those in single-phase codes, the origin of this difference lying mainly in the complex interactions between the different length and timescales involved. The potentialities of the numerics in multiphase codes are thus difficult to estimate without the help of computational results. Our approach consists of performing some calculations in situations as simple as possible yet related to the scope of codes devoted to nuclear safety analysis. We therefore tried to choose single-effect cases, in which one physical phenomenon is uppermost. In a second step, we defined guidelines for an efficient performing of the calculations. Thirdly, on the basis of our experience in multiphase flow computational analysis, we defined heuristic criteria to be fulfilled by computational results, and we illustrated them with results from more than 15 benchmarks.[52] Among the criteria detailed in this reference, the first one states that the algorithms should neither lead to missing the representation of a key phenomenon nor lead to making unphysical phenomena appear. Other checked criteria are commonly used requirements: accuracy of mass and energy balances, low numerical diffusion, and low CPU time and memory. The robustness of the algorithms with respect to different flow conditions were also verified (high variation of pressure, phase appearance and disappearance).

Among the test cases, one can find, for instance, fast depressurization of a pipe (Super Canon experiment[53]), complete phase separation, sloshing in a tank (Maschek et al. experiment[54]), Ransom faucet flow, two-phase water-hammer, and shock tube. Two of these benchmarks are addressed below as examples.

The Super Canon experiment[53] was set up to simulate a double-ended guillotine LOCA of a PWR primary circuit. It consists of a horizontal cylindrical piece of pipe where the pressure drops from 150 bars to 1 bar in <0.5 s, because of the opening of one end of the pipe. The liquid flashes and a pressure wave propagates from the break opening to the far end of the pipe in a two-phase medium. Initially, the tube is filled with degassed undersaturated water at 150 bars and at a temperature of 300°C. On Fig. 1, one can see the time-evolution profile of the pressure at two different locations in the pipe (in the center and near the open end). Both CFD results and measurement data are provided, as well as CATHARE results, which are presented for reference. It is rather difficult for both 1-D models (CATHARE) and 3-D models (NEPTUNE, OVAP) to be very accurate in such a fast transient when using available standard interfacial transfer closure laws. However, this case allowed us to check successfully the robustness of the numerical method with regard to rapid pressure variations in the presence of phase change, and the accuracy of mass and energy balances.

In the Maschek et al. experiment,[54] the sloshing of water takes place in a cylindrical pool, which is initially divided in two concentric parts. In the inner cylinder, there is a water column that is higher than the water level in the external one. The initial state of the system is presented in Fig. 2. When the water column is released, a sloshing motion of the liquid is initiated between the symmetry axis and the outer wall of the cylindrical pool. The main goal of the simulation is to compute the free surface flow and to predict the motion of the free surface correctly. Measurements of the water level peaks at the center of the pool and at the wall, as well as the time at which these peaks occur, are available for comparison with computational results. Figure 3 shows the water fraction fields when water level reaches peaks at the centerline of the pool and at the wall. Mesh refinement showed that the computation of the wall peak converged toward the experimental values (height and time). Results for the central peaks were less satisfactory when refining the mesh. This was attributed to the fact that the symmetry boundary condition at the central axis cannot represent the real physical phenomenon.

III.C.2. Validation of Physical Models

The validation of physical models implemented in NEPTUNE CFD V1 addressed mainly bubbly flows (adiabatic and boiling flows) on the one hand, and flow patterns related to PTS on the other hand (free surface flows, condensation, and two-phase jets). The major difficulty

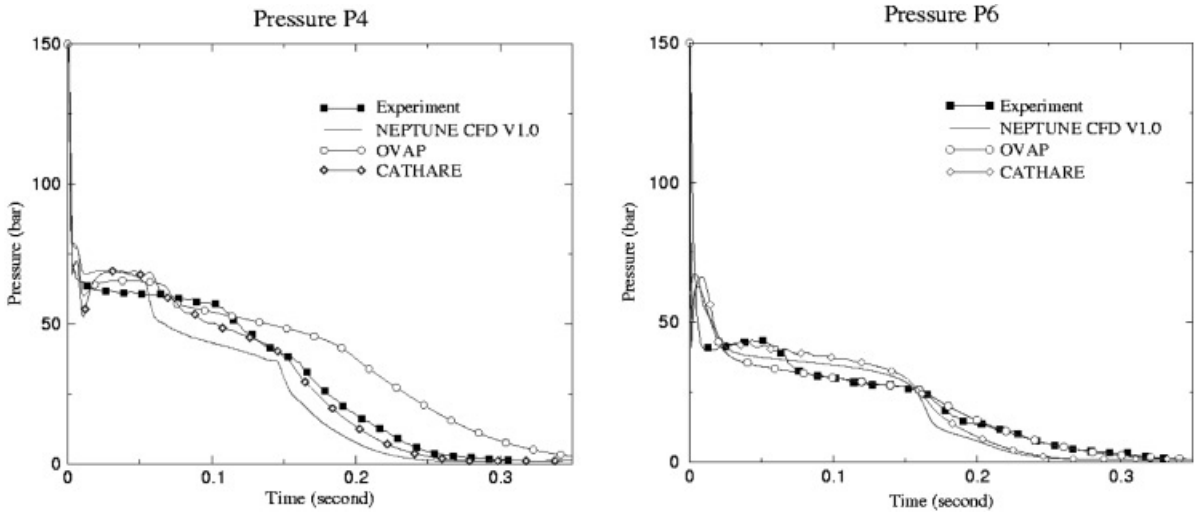

Fig. 1. Super Canon test case: pressure evolution at two locations along the pipe (P4 = middle of the pipe, P6 = open end).

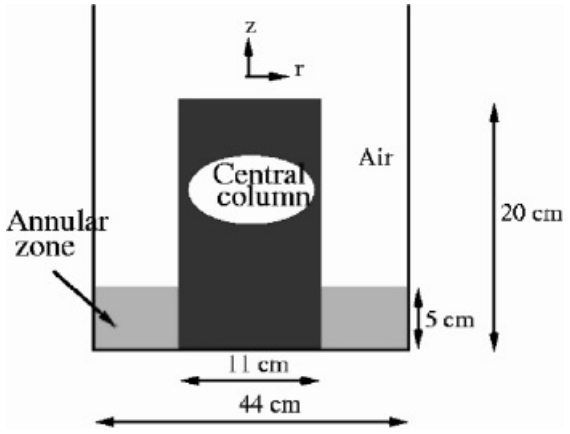

Fig. 2. Maschek test case: experimental layout.

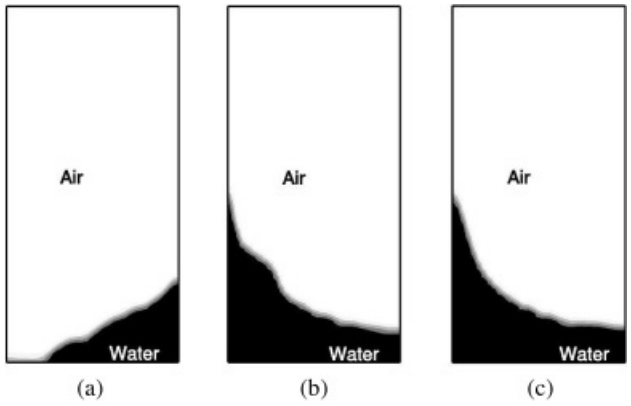

Fig. 3. Maschek test case: computational maxima of the calculation performed with NEPTUNE CFD on a 33 × 45 cartesian mesh, represented by the water fraction field: (a) first motion toward the wall; (b) first peak; (c) second peak; (2-D axisymmetrical computation).

when dealing with heat transfer and high pressure is that experimental data providing local measurements needed for the validation of the local scale modeling are rare. Considering the complexity of the phenomena involved, the validation of the first version of NEPTUNE CFD was performed so as to know which kind of flows the present modeling is able to predict, and to give hints for improvements in those cases where it fails to give good quantitative results. Below are presented some examples illustrating this process.

III.C.2.a. Validation Against Bubbly Flows in a Sudden Expansion

The experiment of Fdhila[55] is an adiabatic air/water bubbly flow upwardly directed in a sudden expansion. The small tube inner diameter is equal to 50 mm, whereas the large tube inner diameter is equal to 100 mm. Figure 4 illustrates a comparison between calculation results (continuous line) and the experimental radial profiles (square symbols) taken at an axial distance equal to 25 cm downstream from the sudden area enlargement and close upstream from the reattachment point.[56] The inlet superficial liquid and gas velocities (measured at the bottom of the smaller pipe) are equal to 1.57 and 0.3 m/s, respectively. The compared quantities are the void fraction, the liquid mean axial and radial velocities, and the liquid turbulent kinetic energy. A relatively good agreement was found between the calculated profiles and the experimental ones. Although no lift force was used in this calculation, there is a trend to overestimate the amount

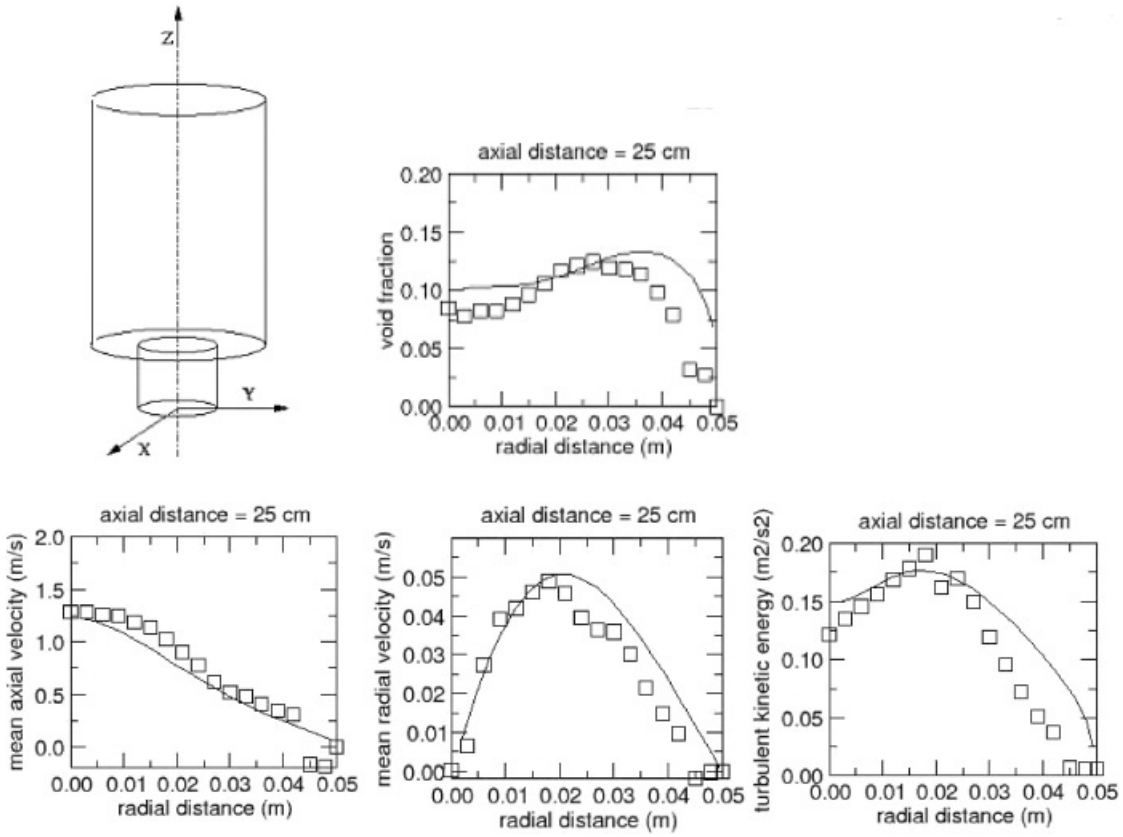

Fig. 4. Fdhila experiment: comparison of calculated (continuous line) and experimental radial profiles (square symbols) of the void fraction, the liquid mean axial and radial velocities, and the liquid turbulent kinetic energy.

of air captured in the recirculation zone and to diffuse too much turbulence in this zone.

III.C.2.b. Validation Against Parallel Boiling Bubbly Flows

The ability to predict boiling flow in simple geometry can be tested by means of the DEBORA experiment.[57] In this experiment, R-12 was adopted as the working fluid to simulate the PWR conditions under low pressure. Some liquid R-12 flows upwardly inside a vertical pipe having an internal diameter equal to 19.2 mm. The whole pipe can be divided axially into two parts: the heated section (3.485-m length) and the adiabatic outlet section (0.365-m length). In the DEBORA-3 test selected here, pressure is equal to 26.2 bars, the flow rate to 2000 $kg/m^2 \cdot s^{-1}$ and the inlet temperature to 61.5°C (26°C under saturation). Vapor bubbles are generated by nucleation on the wall surface and condense into the subcooled liquid when they are far from the wall. Experimental data are measured on one radial profile (taken at 70% of the heated section length) and one axial profile located near the wall. The availability of radial profiles, including void fraction, under boiling conditions, makes the DEBORA experiments very valuable for validation of local scale models. The computations presented here were made using an axisymmetrical domain because of the corresponding symmetry of the flow. In the computations, the IAC equation for bubbles is taken into account. In Fig. 5 the liquid temperature and void fraction profiles are compared to the experimental ones, using the standard form of the models and a fine mesh (40 cells in the radial direction, 220 in the axial direction). One can see that the numerical results are in good agreement with the experiment only from a qualitative point of view. The liquid temperature is slightly overpredicted, while the vapor production is overestimated near the wall. Accordingly, the wall temperature (not shown here) is overestimated. This suggests that the wall heat transfer for nucleate boiling conditions has some shortcomings, which may involve both the thermal wall functions and the model for flux distribution between liquid heating and vapor production.

Another noteworthy validation case for parallel boiling flows was recently performed, featuring an R-113 boiling flow in an annulus-shaped pipe.[58]

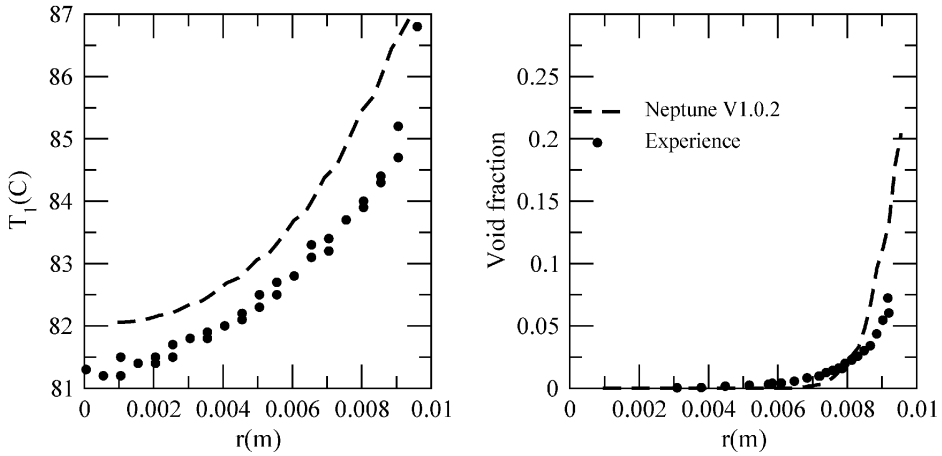

Fig. 5. DEBORA-3 experiment: comparison of computed and experimental radial profiles of liquid temperature and void fraction.

III.C.2.c. Test of Boiling Flows in Complex Geometry

Here we consider a boiling bubbly flow through a mixing device featuring the effect of a fuel assembly spacer grid equipped with mixing vanes (DEBORA-mixing experiment, CEA, Grenoble). The experimental setup is basically the same as the above-mentioned DEBORA experiment, except that a mixing device is inserted into the heated tube as shown in Fig. 6. The computational domain includes the total heated section upstream from the mixing device and a short part downstream. The mesh is made of 186 000 cells, mainly hexahedrons and a few prisms. In this case, fixed-size bubbles are considered (0.3 mm in diameter). The computation results[59] compared favorably with the experimental ones, particularly in that the global effect of the mixing vanes was observed. In fact, the steam is produced at the wall, but as the flow passes through the mixing device most steam bubbles migrate from the wall to the center of the blades' wakes, because of pressure difference (see Fig. 6). Once they are entrained in a subcooled part of the flow, the steam bubbles will condense. Although the vapor production is rather low in this test (the maximum void fraction is $<10\%$), the predicted void fraction level downstream from the mixing vanes is in good agreement with the measurements.

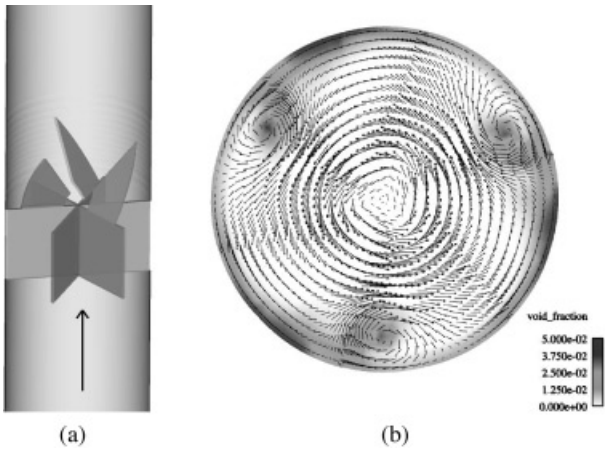

Fig. 6. DEBORA-mixing experiment: (a) sketch of the mixing device; (b) void fraction and liquid velocity fields 20 mm downstream from the vanes.

III.C.2.d. Validation Against PTS-Related Experiments

Models have been firstly assessed by means of separate effect test results, as reported above in Sec. III.B.3. Then, the simulation of an experiment coupling many effects (namely the COSI experiment[60,61]) was studied. In the COSI experiment, the injection of cold water, during a PWR postulated accident, was experimentally simulated; the loop represents, with scale $\frac{1}{100}$ in volume, a part of a cold leg (118 mm in diameter), with a safety injection, and a vertical pipe representing the top of the downcomer (Fig. 7). Generally, the vapor comes from the left side of the pipe, cold water is injected by the safety system, and liquid water flows down in the downcomer (right side of the pipe). A weir was located at the extremity of the pipe, before the downcomer, in order to set a water minimum level. Depending on the tests, the pressure was either 0.2 or 0.7 MPa. Condensation occurs at the surface of this stratified flow and on the jet itself before mixing. Most of the runs are steady-state ones. In this experiment, an emphasis is placed on the global condensation rate and on the liquid temperature. The temperature profiles in vertical direction perpendicular to the pipe axis are measured at eight axial positions along the pipe. The temperature profiles obtained by NEPTUNE CFD V1 show very good tendencies, compared

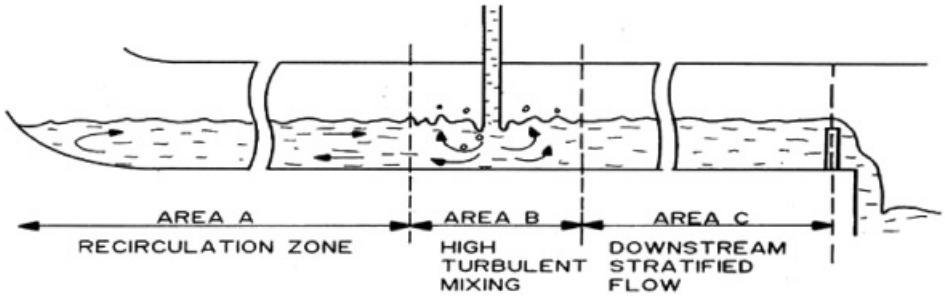

Fig. 7. Flow configuration in COSI tests.

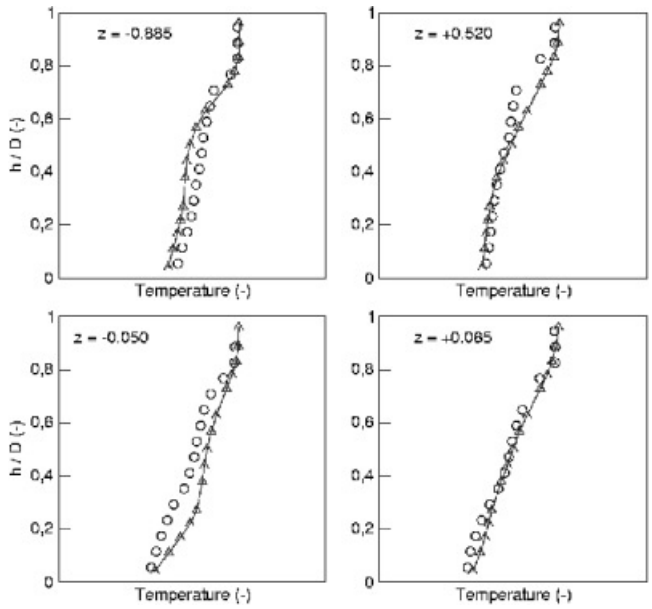

Fig. 8. Example of COSI test simulation with NEPTUNE: Calculated temperature profiles (solid line with triangles) along vertical diameters are compared to measured values (circles) at four sections with abscissa $z = -0.885$, -0.05, 0.065, and 0.52 m ($z = 0$ at ECCS injection). The two or three uppermost measured temperatures are equal to saturation temperature and are assumed to be in pure steam flow.

with the experimental results (Fig. 8). The results show the robustness of NEPTUNE CFD V1 in the case of a stratified flow with direct contact condensation. The effect of physical models and of the mesh on the simulations are being investigated.

IV. NEPTUNE CFD IN POROUS MEDIUM

As already pointed out in Sec. I, the current generation of component codes in France (FLICA4, GENEPI, THYC) has reached a very high level of maturity and will still be used for about a decade. That is the reason why the development of new component modules during the first years of the NEPTUNE project has not been claimed as a priority. The total costs could also have become prohibitive. Nonetheless, the main directions toward improved component codes are already known, and some prototype developments have started. This chapter provides a synthesis of what can be anticipated for the future.

IV.A. NEPTUNE 3-D Porous Solvers

IV.A.1. Applications

The development of new 3-D porous solvers, which will cover component and 3-D system applications, is being planned. The specifications of the physical models and numerical schemes are being written. The first applications for this new solver will concern both PWRs and BWRs.

IV.A.2. Physical Modeling

The current activity focuses on both a two-fluid model and a three-field model with some effort on the following:

1. a rigorous derivation of averaged equations in porous medium approach
2. a 3-D formulation of closure laws. For the two-fluid model, the first set of closure laws results mainly from the extension of the two-fluid 1-D model (CATHARE) to the 3-D model and from the extension of 3-D homogeneous equilibrium models (HEMs)/homogeneous relaxation models (HRMs) (FLICA4, GENEPI, THYC) to the two-fluid model.
3. a turbulence modeling in porous medium (see Sec. V)
4. IAT modeling (see Sec. V)
5. three-field model for dryout investigations (for BWR) and for PWR LBLOCA applications (see Sec. V).

IV.A.3. Numerical Schemes

To go beyond the limitations of the spatial discretization of current codes (structured meshes for CATHARE and THYC, semistructured extruded hybrid meshes for FLICA4, hexahedrons for GENEPI), the numerical schemes will be totally unstructured. The plan is to extend the current unstructured finite volume schemes of the CFD in open medium modules (NEPTUNE CFD V1.0, OVAP) to take into account the porosity.

IV.B. Preprocessing

A new preprocessor for the component scale is under development. This preprocessor will provide the same textual interface, Python, as provided for the other components of the NEPTUNE platform (see Sec. VI.A) to offer the possibility to develop easy extensions for complex studies. It will also provide a graphical interface using the SALOME platform.[62] One of the major components of the NEPTUNE preprocessor, Technological Object (TechObj), is already available. TechObj is a realistic, simple, and user-friendly computer-aided design model that allows one to describe technological objects inside cores, steam generators, and heat exchangers; the user is not constrained to give the averaged quantities (porosity, hydraulic equivalent diameter) like in some current subchannel codes or system codes but only the real dimensions and locations of the technological objects. This component has been developed keeping in mind that a unique description must be used whatever the scale or discipline is. For example, fuel rod objects in a core could be reused for neutronics, CFD scale, or thermal behavior analyses. The preprocessor will generate also semiautomatic meshes of the core or the steam-generator and will compute the intersection between the cells of the 3-D mesh and the technological objects to provide the averaged quantities.

IV.C. Core Applications

For the core, the new component scale modules (3-D porous solver, component scale preprocessor) will also cover a wide range of applications, from experimental facilities to almost all types of reactors (PWR, BWR, RBMK, VVER, fuel-plate reactors, etc.), and for different purposes (design, safety). These features imply many constraints in terms of preprocessing, physical modeling, numerical scheme, and software conception.

IV.C.1. Local Zoom for Core Analysis

In order to obtain a better simulation of the local flow conditions around hot assemblies [in connection with critical heat flux (CHF) prediction], current codes dedicated to core analysis (FLICA4, THYC) allow computations with local zooming. Far from the hot assemblies, the cell size corresponds to the pitch size of the assemblies, and it decreases to the subchannel size within the hot assembly. Two schemes are currently used: either a nonconforming mesh (FLICA4) or a few different meshes connected to each other (THYC). The new module of the NEPTUNE platform will integrate the current schemes in a 3-D context; the local refinement will be made along the three directions.

IV.C.2. Neutronic Coupling

There are two different ways of computing reactor steady-state and transient operation with a neutronic model:

1. coupling with a 3-D neutronics code. For the current generation of core codes, some developments are being achieved with efficient but limited coupling tools. Thus, the coupling FLICA4-CRONOS2 (Refs. 63 and 64) and THYC-COCCINELLE (Refs. 11 and 65) are carried out with the ISAS (Ref. 17) and CALCIUM (Ref. 66) supervisors. A script allows one to control the data flows between the thermal-hydraulic and the neutronics codes. The new component scale modules will be coupled with the DESCARTES code[67] by the SALOME platform (see Sec. VI.A).
2. coupling with a point kinetics model.

IV.C.3. Heat Conduction in Fuel

Heat conduction in fuel will be performed either by an internal simplified module in the NEPTUNE platform (radial 1-D assumption), or an external two-dimensional (2-D) or 3-D solver. Both solvers will be coupled by a single standardized interface with the thermal-hydraulic NEPTUNE solver.

IV.D. Steam Generators and Heat Exchangers

In terms of physical modeling, the needs for these applications are similar to those for the core applications (3-D, two-fluid, and multifield modeling).

The coupling functionalities must include the following:

1. coupling with the open medium CFD module (steam generator water lane, steam generator upper area, steam generator downcomer)
2. coupling with the primary flow (inside the tubes)
3. coupling with 3-D thermal solid analysis (bundle wrapper, axial economizer).

V. SYSTEM SCALE

V.A. Turbulence Modeling and Interfacial Area Concentration Prediction

The EUROFASTNET project[2] reviewed the present generation of system codes and concluded that they have

reached a high level of maturity and are able to address the safety issues. However, some weaknesses were identified, the physical modeling being limited by the capabilities of the two-fluid six-equation model. A qualitative jump in the description of the physics is now expected from a dynamic modeling of turbulence and IAC in flows that are not fully developed and in flow regime transitions, and from more generic multifield models capable of handling more complex flow regimes.

The modeling of turbulent scales in pipes or in rod bundles (tube bundles) allows the prediction of many effects that are not modeled in previous models. Thus, the following:

1. Coalescence and breakup of bubbles or droplets are mainly affected by turbulence. Then the prediction of the interfacial area requires a good modeling of turbulent scales. In the same way, the IAC has a very significant effect on turbulent scales. Interfacial area and turbulence are fully coupled in two-phase flows and the dynamic modeling must be followed in parallel for both aspects.

2. Stratification of a bubbly flow in a horizontal channel also depends on a balance between the turbulent dispersion force and the buoyancy force acting on the bubbles. In two-fluid six-equation models, only a very simplified formulation of both effects was possible and no relaxation time associated to the process could be properly described by an algebraic criterion.

3. Flashing flows in a nozzle or at a break are nonestablished flows, which require an accurate modeling of the flashing delay related to heterogeneous nucleation. It is expected that the activation of the nucleation sites depends on pressure turbulent fluctuations, which may be estimated by a proper modeling of turbulent scales.

4. All interfacial transfers depend on turbulence through the interfacial area and transfer coefficients. Direct contact condensation may be highly affected by turbulence as shown by Janicot and Bestion,[61] and any source of turbulence—including the turbulence induced by ECCS jet—has to be taken into account for a good prediction of condensation in the PTS-related application.

5. All heat transfers with walls are also affected by the turbulence intensity. In the case of a core uncovery, the wall cooling by steam can only be modeled with established flow heat transfer coefficients in current two-fluid models, whereas a prediction of turbulent scales could model the heat transfer enhancement due to spacer grids. At the entrance of a pipe, heat transfer coefficients decrease in the region where turbulent profiles are established. Having a dynamic modeling of the turbulence intensity will allow one to model entrance effects,

6. In rod and tube bundles, turbulent mixing between subchannels depends on turbulent scales. The prediction of spacer grid effects on these turbulent scales will provide more accurate predictions when using subchannel analysis for CHF prediction.

7. All singularities in the geometry of a duct affect turbulent scales and all other flow parameters that depend on them.

A first attempt to predict turbulent velocity and length scales was made using a transport equation for the turbulent kinetic energy K and an algebraic expression of the length scale L ($K - L$ model). Then a $K - \epsilon$ model was developed with an additional term in singularities. It was first adapted for 1-D single-phase flows in pipes by comparison with spatially averaged 3-D CFD predictions. Then it was extended to single-phase flows in rod bundles with spacer grids. Figure 9 illustrates the AGATE experiment and Fig. 10 shows the prediction of turbulence decay downstream from the grid using the $K - \epsilon$ model.[68]

Then this $K - \epsilon$ model was adapted to two-phase flows, coupled with a transport equation for the IAC and validated in bubbly flow in a pipe.[68] The IAC model for bubbly flows contains differential terms for phase change and density variations, and algebraic source terms for turbulent coalescence and breakup. Figures 11 and 12 show the prediction of K and interfacial area A_i in the DEDALE experiment.[68] The DEDALE experiment is a 6-m height and 38.1-mm diameter vertical pipe. The

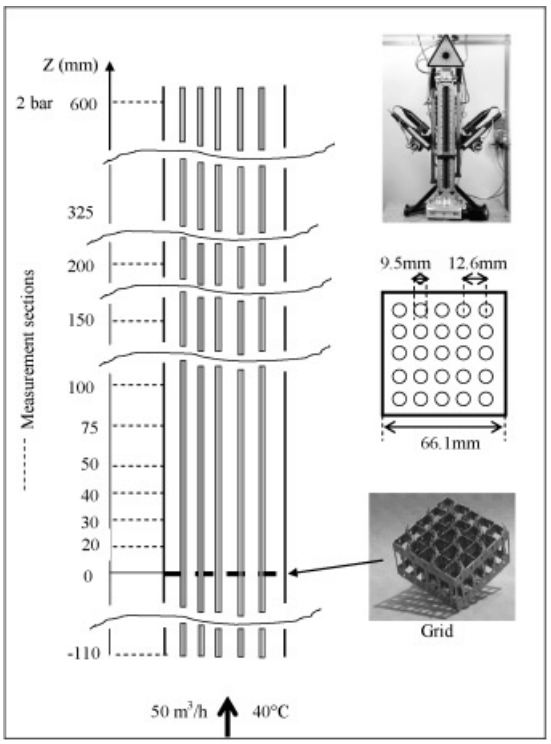

Fig. 9. Description of the AGATE experiment.

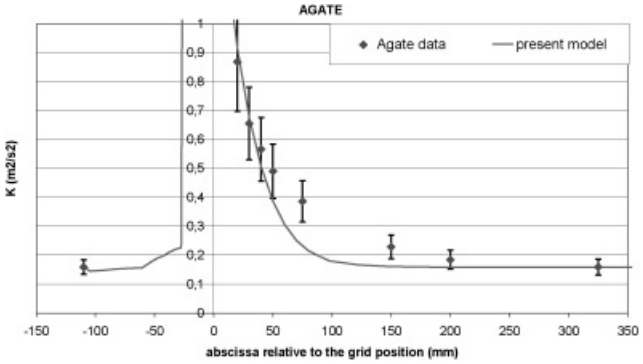

Fig. 10. AGATE experimental and computational results.

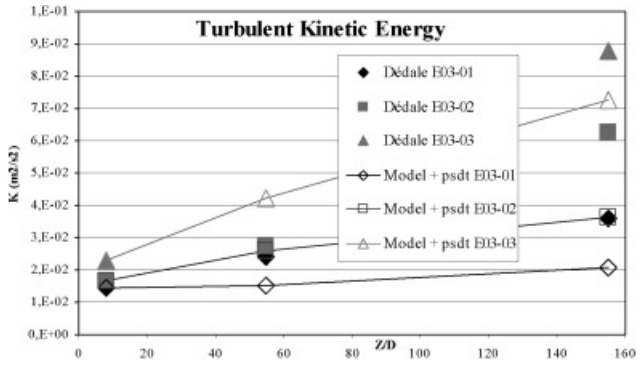

Fig. 11. DEDALE turbulent kinetic energy for tests E03.

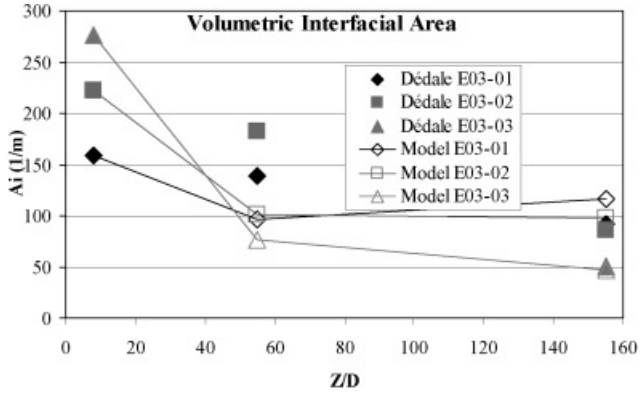

Fig. 12. DEDALE interfacial area for tests E03.

experiment is adiabatic and at atmospheric pressure. Injection of water-air mixture creates bubbly to churn flows. The instrumentation provides measurements, among other quantities, of liquid velocities, void fraction, and IAC. The radial profiles are measured at three sections $Z/D = 8/55/155$ and are spatially averaged for the current 1-D analysis. Table I gives the flow rates and cross-sectional averaged void fraction of the tests used for validation. The experimental uncertainties on interfacial area (measured by a two-sensor optical probe) and on turbulent kinetic energy (estimated from the root-mean-square value of the axial velocity component) are not given; they are probably not small, but experimental qualitative trends are considered as reliable.

TABLE I

DEDALE Experiment: Thermal-Hydraulic Parameters

	Test E03-01	Test E03-02	Test E03-03
M_l (kg/s)		0.597	
Re_l		50170	
M_g (kg/s)	1.29e−4[a]	1.94e−4	2.59e−4
α	0.074	0.112	0.150

[a]Read as 1.29×10^{-4}.

In the low-velocity tests, coalescence dominates breakup, and turbulence is mainly produced by bubble wakes. It is clear that for a significant void fraction (test E03-03) both the turbulence and the interfacial area change rather rapidly and are not established even at $Z/D = 155$. Several models for breakup and coalescence found in the literature were tested and were not able to give the right trends. Most models for coalescence and breakup use estimations of turbulent quantities (K, ϵ) provided by algebraic relations that are only valid in single-phase established flow. In these calculations, a dynamic evaluation of turbulent quantities was used, coupled with IAT. Although predictions are not very accurate for the small void fraction tests, at least the good trends are predicted when both turbulence and interfacial area are significantly changing in test E03-03, which is quite difficult to obtain. This is a first step in an attempt to develop a simple one-group model for the interfacial area in bubbly/slug/churn flows. Further comparison of the model predictions with other data banks is required.

Although interactions between interfacial area and turbulence models are very complex, such first results confirm the interest of dynamic prediction of both turbulence and interfacial area for nonestablished flows and for flow regime transitions.

V.B. Multifield Modeling

Limitations were found for some two-phase flow patterns when a phase is split into two separate fields. The annular-dispersed flow with continuous liquid along walls and droplets in the gas flow is the first example where a three-field model may improve the predicting capabilities. Valette and Jayanti[69–71] developed a three-field model and validated it against a large database including pipe flows and flows in rod bundles corresponding to the geometry of a BWR core. The model is able to predict

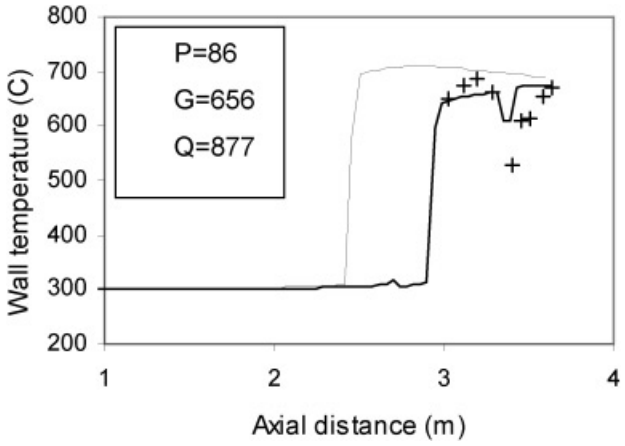

Fig. 13. Wall temperature profile in THTF rod bundle (from Ref. 71): comparison of experimental data (symbols) with a three-field model with (dark line) and without (light line) the droplet deposition enhancement model on spacer grids.

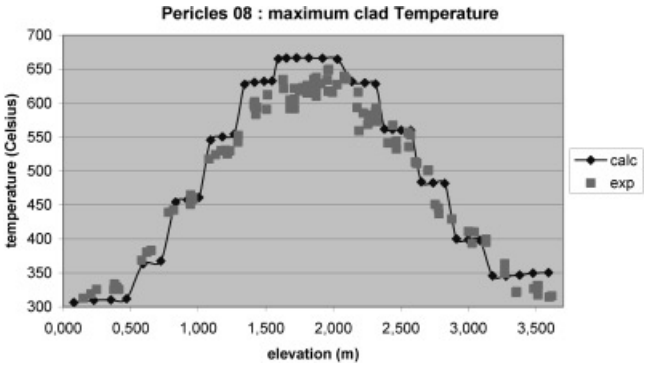

Fig. 14. Maximum clad temperature profile in PERICLES Reflooding Test 8: comparison of experiment with a three-field model prediction.

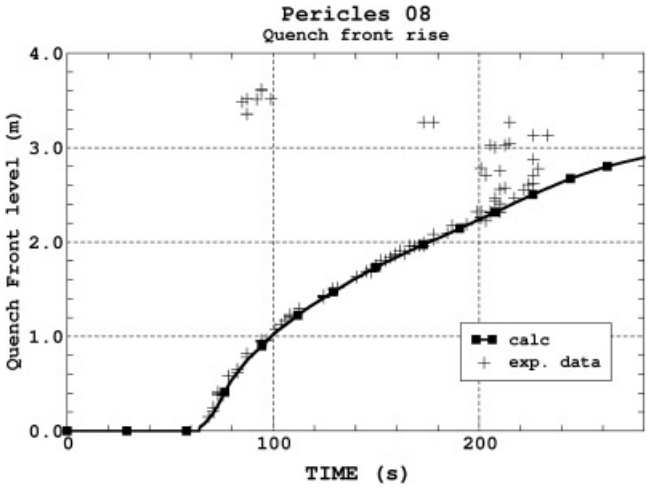

Fig. 15. Quenching time in PERICLES Reflooding Test 8: comparison of experiment with a three-field model prediction.

pressure drops, fraction of entrained liquid, dryout quality, and postdryout wall temperature for a heated flow.

Special attention was paid to the entrainment and deposition of droplets that control the fraction of entrained liquid and the film dryout. Figure 13 shows that the developed model is also able to predict the effect of spacer grids on the dryout location and on the wall temperature profile in a rod bundle.[71,72] Taking into account the enhancing effect of spacer grids in the droplet deposition process enables one to shift the dryout location onto the right position and to predict some desuperheating induced by the grid in the postdryout region. In Fig. 13 crosses mark the measured wall temperatures on the dried rods, and lines mark the calculated wall temperatures without (thin on the left) and with (thicker, right) the droplet deposition enhancement model on spacer grids.

The three-field model was then applied to the reflooding process. The standard CATHARE V2.5 reflooding model, using a refined moving grid in the heating wall in front of the quench front location, was extended and adapted to the advanced three-field description of a boiling two-phase flow. In a first step, the results of this model have been satisfactorily compared to the PERICLES-Cylindrical test section experimental results in a 1-D approach. Figure 14 shows the comparison between predicted and measured maximum wall temperatures along the PERICLES bundle. Figure 15 shows that the model is already able to predict accurately the bottom-up quench front progression. The top-down quenching model (available in the standard CATHARE version) was not activated here, which explains why quenching in the upper region of the core was not predicted. Improvements of the top-down quenching model are still required to take full benefit of the three-field model in a region where falling films coexist with droplets flowing upward. Further validation will include the rod bundle heat transfer (RBHT) tests' data provided with advanced instrumentation.

V.C. Numerical Improvements

V.C.1. Reflooding Numerical Method

In the current system scale solver CATHARE, in the case of a reflooding situation, a small 2-D thermal meshing is added to the standard calculation—namely, hydraulic calculation and 1-D radial thermal calculation—to

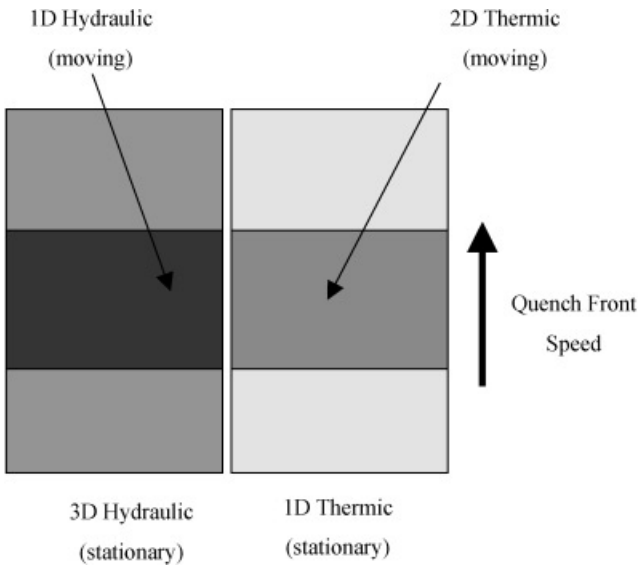

Fig. 16. NEPTUNE reflooding numerical method.

catch and model the physical stiff axial thermal gradient. For NEPTUNE system scale application, we are looking for a more powerful method based on a fine grid—hydraulic calculation coupled to a 2-D heat conduction calculation—moving along a coarse grid; see Fig. 16.

V.C.2. Three-Dimensional Solver

CATHARE uses a staggered mesh discretization method—implicit continuous Eulerian method—that handles only structured meshes. To avoid that too-strong limitation, we are also working to extend the NEPTUNE CFD solver—elliptic and colocated—to system scale applications like 3-D pressure vessel computations during an LBLOCA. Samples of lower plenum first meshing with that new 3-D solver are given in Fig. 17.

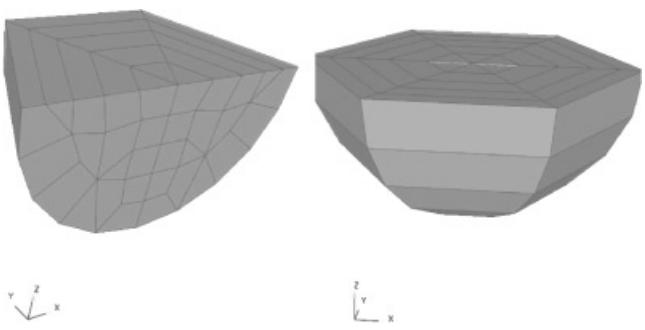

Fig. 17. Samples of lower plenum meshings (CFD solver).

V.D. Software Developments

The development of NEPTUNE system application has been specified in terms of three major evolutions [starting from the industrial system code CATHARE (Ref. 7)]:

1. the extension of physical modeling capabilities. As previously stated (see Secs. V.A and V.B) we try to extend the classical approach—two-field, six-equation modeling—of previous system scale solvers: resolution of new balance equations (mass, energy, momentum for droplets, bubbles, interfacial area, turbulent quantities) and adaptation of the existing numerical schemes in CATHARE. Software implementation of multifield-based models is already available (end of 2005) on dryout tests cases and on 1-D reflooding test cases.[70] Software implementation of interfacial area transport models is under way.[73] The multifield modeling approach will be extended to 0-D and 3-D system modules during the year 2006. An LBLOCA system scale demonstration test case using both multifield modeling and full reactor meshing is scheduled by the end of 2006.

2. advanced software architecture. CATHARE software architecture is essentially based on the FORTRAN language capabilities. Following the NEPTUNE platform architecture standards (see Sec. VI.A), the new system scale solver architecture will use multilanguage approaches, mixing Python, C++, and FORTRAN languages. The new architecture will make an extensive use of shared components available in the NEPTUNE platform (see Ref. 74). A dedicated applied programming interface will also be developed to make easier multiscale coupling (with 3-D CFD and porous scales) and multidiscipline coupling (with thermomechanics and reactor kinetics applications).

3. a new graphical user interface (GUI) for system applications. CATHARE pre- and postprocessing tools were only based on textual formats. A new GUI is under development (Fig. 18) within the SALOME software platform.[62] It will handle pre- and postprocessing of both CATHARE and NEPTUNE system applications. The main specifications of that GUI are the following:

   a. to deal with 1-D, 0-D, and 3-D modules and their walls

   b. to read/write old CATHARE input data text files

   c. to manage both preprocessing and postprocessing

   d. to be plugged in the system code either in a live mode or in a batch mode

   e. to share GUI solutions and frameworks with other NEPTUNE scales

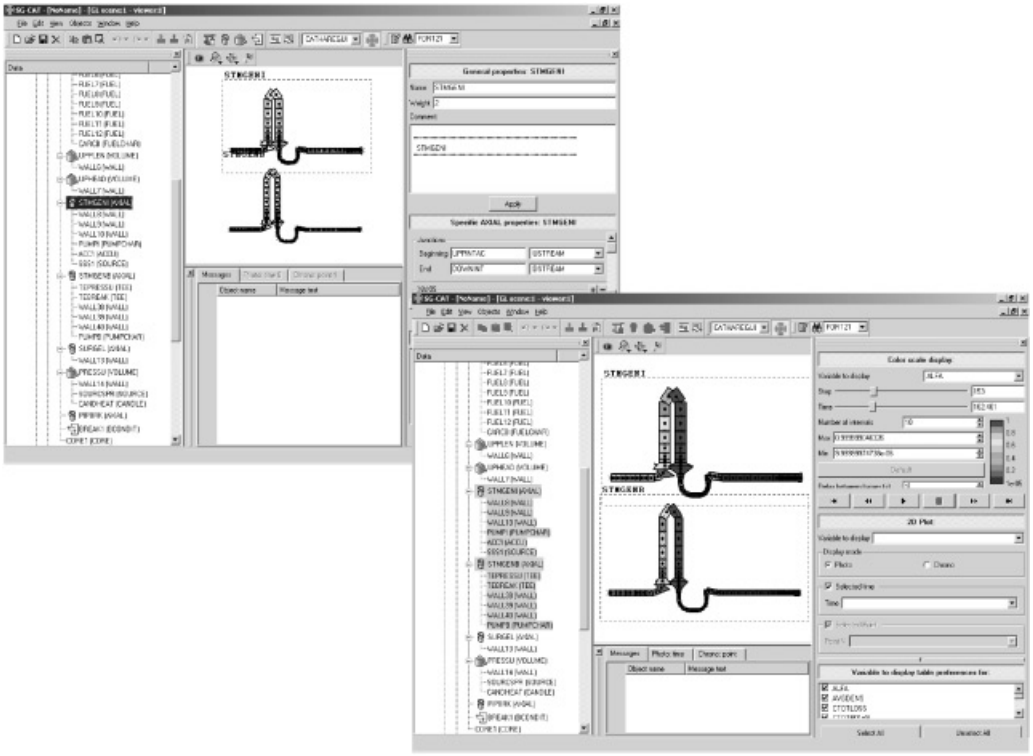

Fig. 18. Look and feel of the NEPTUNE system GUI (pre/post).

f. to share TechObj formats with other NEPTUNE scales.

At the beginning of 2006, the CATHARE/NEPTUNE system scale GUI already handles a CP1 reactor nodalization.

VI. MULTISCALE COUPLING FOR INDUSTRIAL APPLICATIONS

As already pointed out in Sec. I.B, more and more industrial simulations require multiscale calculations. During the early stages of the NEPTUNE project (2002–2003), some existing codes (as well as the new NEPTUNE CFD code) were wrapped into the platform, in order to perform first multiscale demonstration simulations. Two examples are provided below. Then Secs. VI.C and VI.D highlight the generic strategy that is being applied in terms of software architecture and numerical methods in order to improve multiscale coupling.

VI.A. Pressurized Thermal Shock Coupling Calculation

This case is a one-way coupling exercise without any physical or numerical feedback of a system scale calculation (CATHARE, wrapped into the NEPTUNE platform)—small break scenario, full reactor meshing—and a NEPTUNE CFD calculation, meshing limited to a zone near the end of the cold leg and the downcomer (Fig. 19). This work has shown the numerical feasibility of such a multiscale coupling calculation.

VI.B. Main Steam Line Break Coupling Test Case

This case is a mesh overlapping coupling exercise of a system scale calculation (CATHARE wrapped into NEPTUNE)—main SLB scenario, full reactor meshing—and a component scale calculation (FLICA4 wrapped into NEPTUNE), meshing limited to the core zone only. The coupling zone is exactly the core extension zone. Both component and system solvers are wrapped into a Python software language module, and the whole coupling computation is globally managed through the interpolation and supervision modules (Fig. 20). This work has clearly shown the ability of the fluid solvers to be wrapped in C++ and then processed as standard Python modules for the good achievement of the whole coupling test. This test has been achieved in the SALOME software environment.[62]

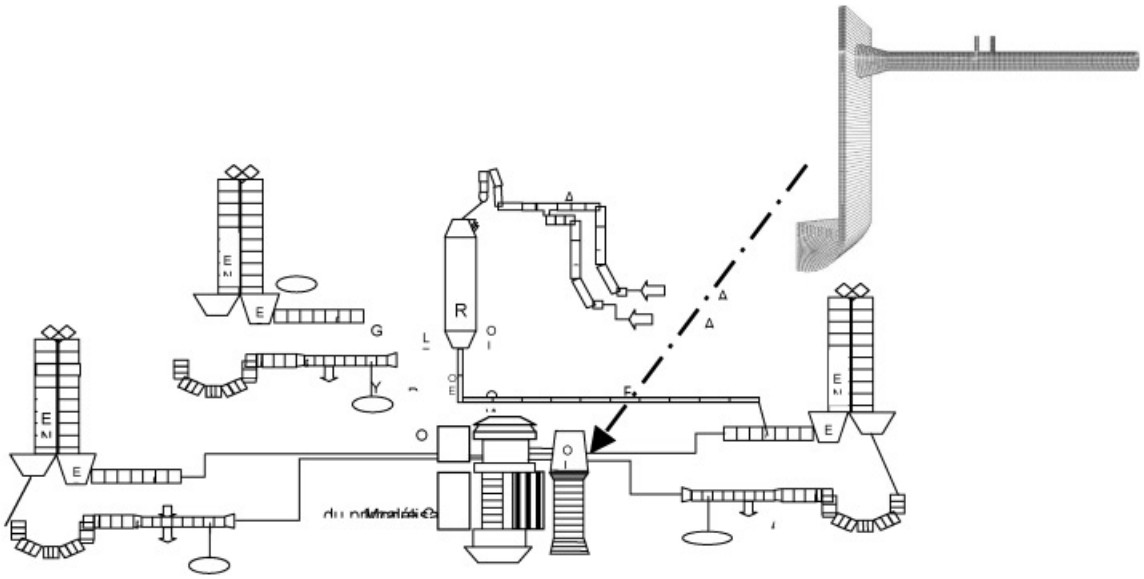

Fig. 19. PTS: system scale and CFD scale meshing.

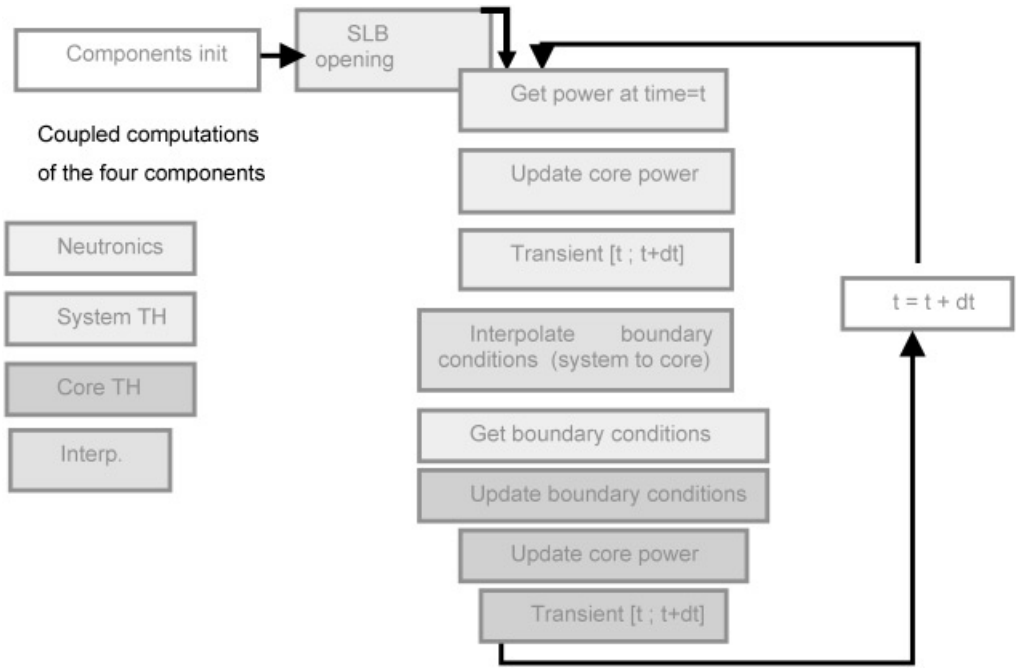

Fig. 20. Main SLB: transient supervision.

VI.C. NEPTUNE Software Architecture

From a general point of view, the main purpose of the NEPTUNE architecture is to provide rules and concepts to build a new platform in a new computational environment. However, this architecture must also take into account the preexisting thermal-hydraulic software. Many valuable and validated computational codes already exist, and they represent a considerable experience for the teams involved in the project. Thus, rather than starting from scratch, the NEPTUNE platform is being developed in a progressive way.

Technically, the NEPTUNE architecture has to fulfill the following requirements:

1. It allows one to reuse existing parts of source code written in different programming languages, mainly Fortran and C++.

2. It keeps the opportunity to make new developments using these languages; this is particularly important in order to include the physical or numerical R&D work.

3. It includes coupling mechanisms for multiscale and multiphysics applications.

4. It is compatible with the generic SALOME software platform developed by CEA and EDF for all the disciplines (thermal hydraulics, core physics, fuel mechanics, etc.).[62]

5. Last but not least, parallel computations are possible, as NEPTUNE applications generally need large CPU time and involve a large amount of data.

In order to satisfy these requirements, we have decided to build the NEPTUNE platform on a component architecture. We define "component" as a piece of software that gathers a set of functions that are specific to a clearly identified purpose, e.g., the computation of the thermodynamic properties of a fluid. The components are also defined by the way they are built: The development of a component should not depend on the development of another one; when a function is relevant to the purpose of a component, this function should always be developed inside this component. Finally, a component is only seen from outside by its interface: That is the way the component gets the information it needs to work and the way it returns the information it has computed. This information is organized by means of the object concept (we refer here to the classical object-oriented programming method).

The same component can also be used by different NEPTUNE applications. For instance the EOS component computes the thermodynamic properties of the fluids and also of some solids (for thermal coupling). The services of the EOS component can be called by different thermal-hydraulic solvers. The component concept applies from basic services (closure laws for example) to an entire application (NEPTUNE CFD as a whole can be seen as a large component).

To gather the components into an application we have retained two methods: wrapping using the C++ language or wrapping using the Python command language. In fact it is not necessary to build two different interfaces since, using the simple wrapper interface generator (SWIG) tools, the Python interface is automatically built from the C++ interface. So, a component will publish a C++ interface together with its corresponding Python interface. The use of source code written with the Fortran language is still possible; it must then be called by a C function.

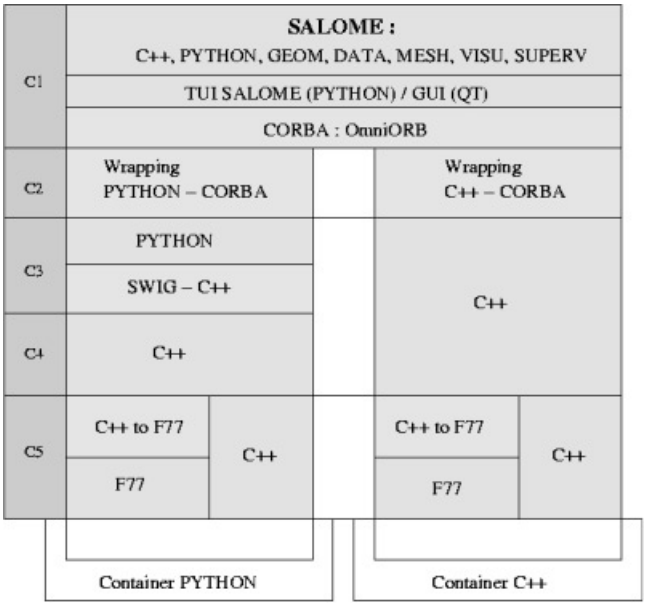

Fig. 21. The shell model of the NEPTUNE architecture.

The programming shell model of the NEPTUNE platform is summarized in Fig. 21.

VI.D. Numerical Methods: Unsteady Interfacial Coupling of Codes

This work package is ambitious. A quick glance in the standard literature enables one to check that little effort has been devoted so far to the problem of unsteady coupling of distinct codes through thin interfaces.

Though some other workers in the classical CFD community also try to combine LES and unsteady RANS approaches—for instance, when studying combustion patterns in a whole reactor (see Refs. 75, 76, and 77)—no theoretical approach clearly arises from the latter work that might be applicable in our framework. Since some predictive computations of the flow in the primary coolant circuit of a PWR also require the use of different codes involving different systems of partial differential equations (PDEs) on each side of a "fictitious" interface, the NEPTUNE project decided to start a deep investigation of this topic, as explained below.

In some applications, the model that is chosen to describe the flow in pipes may be a six-equation two-fluid model (CATHARE code for instance), whereas the one considered in the core (namely the THYC code or the FLICA code) may be a three-equation model (to account for total mass, total energy, and total momentum of the water-vapor mixture). Numerical methods in each code may rely on the use of either pressure-correction techniques or on upwinding techniques. Thus, the interfacial coupling techniques should only provide specific information through adequate fluxes that will be

imposed as flux boundary conditions for each code. This information should be provided by the theoretical approach.

The overall strategy of the NEPTUNE team within this field is the following. First of all, we decided to split the ultimate goal in a few basic problems that should be addressed one after another. More precisely, we decided to examine, successively, the following:

1. the coupling of flows between a free medium and a porous medium
2. the coupling of 1-D flows and 3-D flows
3. the influence of discontinuities in EOS
4. the coupling of relaxed and equilibrium models.

An "ultimate" goal obviously concerns the interfacial coupling of two-fluid models with homogeneous models.

The first item above is obviously motivated by the fact that THYC and FLICA component codes rely on the porous approach and may be used together with the CATHARE code in order to compute the whole coolant circuit. While doing that, one also couples a 3-D code with a 1-D code, which justifies investigating the second item. Another field of great interest corresponds to the third point, since different codes may apply for distinct thermodynamical tables, which may result in possible (assumed weak) discontinuities of coefficients in EOS. Last but not least, the influence of closure laws for mass transfer is expected to have a great impact on computations, and this has urged focusing on the fourth item. We emphasize once more that none of these problems has been examined in the open literature up to now.

For all of these problems, one needs to define suitable information to be exchanged at the coupling interface so that the following occurs:

1. The local pollution at the (steady) coupling interface is minimized.

2. The amplitude of transmitted and reflected waves is as low as possible.

3. The basic principles of conservation are not violated by the coupling algorithm.

4. Some elementary solutions, including pure contact waves, remain ghost solutions when passing through the coupling interface.

5. The stability of the coupled simulation is fulfilled.

From a practical point of view, the main guidelines rely on some previous work by Greenberg, Le Roux, Baraille, and Noussair for the numerical processing of source terms in hyperbolic conservation laws (see Refs. 78 and 79), and also on recent work by Godlewski, Raviart, and Le Tanh (see Refs. 80 and 81). Actually, the whole work owes much to the ongoing collaboration.[82] We also wish to mention the review by Ambroso,[83] which clearly states the problem and lists some possible approaches, on the basis of ideas arising from the literature.

In order to define coupling techniques, we need to rewrite governing equations of sole codes in the following way. If we assume that W_1 (or W_2) is the main unknown of the code on the left (or right) side of the interface, both W_1 and W_2 are governed by a convection-source-dominated set of equations ($k = 1, 2$):

$$\frac{\partial W_k}{\partial t} + \frac{\partial f_k(W_k)}{\partial n} = S_k(W_k) \ , \tag{44}$$

with $n < 0, t > 0$ ($k = 1$), $n > 0, t > 0$ ($k = 2$). W_1 and W_2 belong to $\mathbb{R}^p$ and $\mathbb{R}^q$, respectively, with $p \leq q$. Convective fluxes f_1 (or f_2) and locally stiff source terms S_1 (or S_2) also lie in $\mathbb{R}^p$ (and $\mathbb{R}^q$ respectively). The variable n stands for the normal direction through the interface. The latter systems may be rewritten in a slightly different form in order to upwind source terms (see Ref. 78):

$$\frac{\partial W_k}{\partial t} + \frac{\partial f_k(W_k)}{\partial n} - S_k(W_k)\frac{\partial a}{\partial n} = 0 \ , \tag{45}$$

where the function $a(n, t)$ is such that $a(n, t = 0)$ is piecewise constant on each cell ($a_i^0 mes(\omega_i) = \int_{\omega_i} n dn$) and is governed by:

$$\frac{\partial a}{\partial t} = 0 \ . \tag{46}$$

All systems to be coupled may thus be written in a nonconservative homogeneous form.

We summarize here very briefly some achievements for these basic coupling cases, and also some very recent ongoing work that is devoted to the coupling of two-fluid models with homogeneous models.

VI.D.1. The Coupling of Flows Between a Free Medium and a Porous Medium

This first problem requires the correct definition of information to be transmitted through a porous interface. The flow on the left side of a steady interface was assumed to be governed by standard Euler equations in a free medium, whereas it enters a porous medium on the right. Thus the only heterogeneity pertains to the porosity ϵ. An interface model is introduced according to ideas similar to those developed by Greenberg et al. This approach suggests a connection through the interface when genuinely nonlinear fields do not overlap the steady interface. Some possible numerical ways to account for this strategy have been defined and compared with approaches where the interface is thickened. When some genuinely nonlinear field overlaps the interface, the agreement of the numerical approximation with the entropy inequality has been checked for each scheme.[84]

VI.D.2. The Coupling of One-Dimensional Flows and Three-Dimensional Flows

When some genuinely nonlinear field overlaps the interface, one has to cope with a 1-D model (on the left side of a fictitious interface) that suddenly becomes 3-D. One may deduce that no problem will occur when the flow comes from the left to the right (in the common sense, i.e., $U > 0$), and that, on the contrary, some pollution of the numerical signal cannot be avoided when $U < 0$. Reference 85 partially investigates this topic and shows that previous ideas based on Greenberg et al. formalism, or on the Godlewski, Raviart, and Le Tanh approach, give fair results from an engineering point of view, and that both approaches may identify in some cases. It also provides some comparison between a fully conservative approach, and a nonconservative approach. It eventually suggests that the engineering "know-how" is grounded on relevant facts, and provides useful recommendations for practical purposes.

VI.D.3. The Influence of Inhomogeneities in Equations of State

This third item actually examines the sensibility of computational results with respect to the choice of EOS in codes. Various thermodynamical approaches have been implemented in internal softwares in different companies. One straightforward consequence is that the interfacial coupling of different codes involving these different softwares may result in unexpected disturbances around the interface, which in addition may propagate through (and reflect on) the fictitious boundary. Thus, the coupling of similar equations with distinct EOS has been examined in detail in Ref. 86. Reference 86 indeed confirms that this point should retain special care. It is expected that the standardization of thermodynamics software will obviously contribute to a decrease of problems arising in that case.

VI.D.4. The Influence of Mass Transfer Terms

This fourth point represents some preliminary work when aiming at defining the correct information to be exchanged between a six-equation two-fluid model (CATHARE code) and a four-equation homogeneous model (THYC or FLICA code). For that purpose, we have examined the coupling of an HRM with an HEM, which differ by the EOS and by the fact that the timescale of the mass transfer term is assumed to be null in the HEM. Though this does not correspond to a true coupling case in an industrial framework, it contains tough difficulties. This problem has been addressed and reported in Refs. 82, 87, and 88. A companion work[89] also suggests that different numerical approaches should be retained depending on whether one focuses on steady or unsteady coupling.

VI.D.5. A Preliminary Study on the Coupling of Two-Fluid Models and Homogeneous Models

Quite recently, a first strategy has been defined in order to achieve the interfacial coupling of a two-fluid six-equation model with the HRM model. The basic ideas rely on the use of relaxation techniques combined with upwinding algorithms applied to the seven-equation two-fluid two-pressure model (see Refs. 90, 91, and 92). Preliminary results are described in Ref. 93. These seem to confirm that the velocity imbalance has rather weak drawbacks compared with the imbalance connected with the mass transfer discussed in Sec. VI.D.4, at least when prescribing nominal coolant circuit parameters. The results displayed in Fig. 22 correspond to the computation of a traveling wave coming from the left code (two-fluid model) and propagating toward the right side of the coupling interface (located at $x = 50$).

VII. NEPTUNE LONG-TERM RESEARCH ACTIVITY

VII.A. Physical Modeling

The first applications of recent modeling advances in computational multifluid dynamics (CMFD) tools, as presented in previous sections, clearly reveal the rather low maturity of this new approach and show that the effort has to be considered as a long-term activity. Some directions to this CFD modeling activity are given here. It is also shown that DNS tools with ITM are now able to provide information on small-scale flow processes and may help to develop closure relations for CFD in this long-term perspective. Some examples are given here showing the capabilities of these tools, which are being developed in parallel to the averaged CFD models.

Additionally, present system codes are very mature and further progress will require new experimental data, together with modeling and validation effort. Considering the relative lower urgency of progressing in system codes and the need of new experiments, these modeling improvements are also planned in the long-term. Some future directions to this activity are also given here.

VII.A.1. Future Research for Developing and Using Two-Phase Computational Fluid Dynamics

The two-phase CFD (CMFD) module of NEPTUNE will be applied in the future to many reactor issues, with some priority given to the improvements of DNB and PTS investigations and with increasing effort dedicated to extending the application to more complex flows. Some of this activity will be performed in the frame of the NURESIM European project, in which 14 partners join their efforts in two-phase CFD application to direct

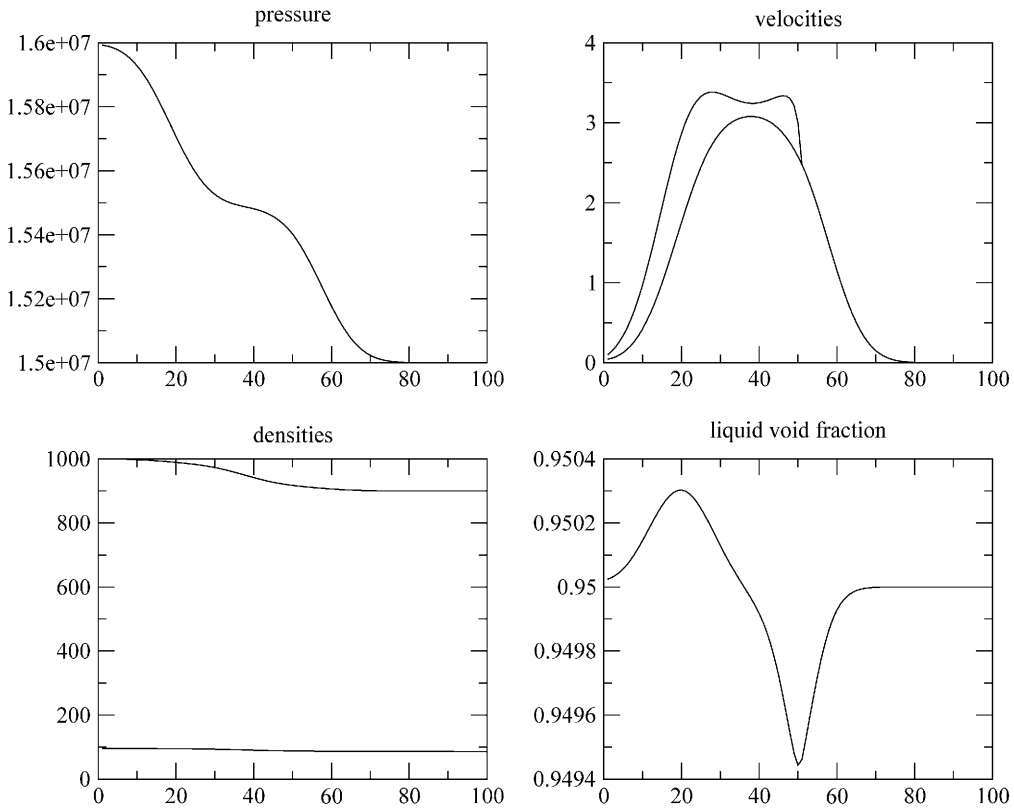

Fig. 22. Propagation of waves through the coupling interface when coupling a two-fluid model (left side) and a homogeneous model (right side).

contact condensation (DCC), PTS, and CHF. For DNB investigations the future modeling effort will address the following issues:

1. The turbulence modeling in bubbly flow should better take into account the different natures of the turbulence produced in wall shear layers and the turbulence produced in bubble wakes. More advanced turbulence modeling such as $R_{ij} - \epsilon$ could be necessary for rotating flow downstream from a grid with mixing vanes.

2. Modeling polydispersion effects either through multigroup or multifield, or by transport of statistical moments of the bubble size distribution, is necessary.

3. More generic models for lift and turbulent diffusion forces are still necessary.

4. Specific wall functions for momentum and energy equations are required for any two-phase flow conditions.

5. First attempts to develop a DNB correlation based on local parameters should be possible in the future.

Further effort is also required in the PTS investigations:

1. *Free surface*: Using an interface tracking technique to predict the exact position of the interface or adopting a simple interface sharpener technique remains an open question that requires further benchmarking.

2. *Turbulence modeling*: Beyond the $K - \epsilon$ model, other models may be evaluated to better deal with temperature stratification effects or for predicting large scale turbulence (i.e., LES).

3. *Interfacial transfers*: The liquid to interface heat transfer should be validated in both separate effect tests and more integral tests, and the formulation of the transfer should either allow a mesh convergence or not be too sensitive to the mesh size.

4. *ECCS jet*: The effects of the ECCS jet on local turbulence and on bubble entrainment require further validation.

It is clear that current two-phase CFD simulation tools are not as mature as in single-phase flows and are not able to predict all flow regimes and any interface structure. A rather long-term research effort will be necessary to extend the modeling for all two-phase flow regimes. More generally, efforts will be made to define a large-scale simulation approach that could be the equivalent in two-phase flow of the LES in single-phase flow. Such an approach seems necessary for two-phase flows with

complex interfacial structure such as churn flows, where small and very large and distorted bubbles coexist, or wavy stratified flows with possible entrainment of drop at wave crests and breaking of waves entraining bubbles in the liquid. In such complex flows, filtering all turbulent scales and two-phase intermittency scales would not make sense since the main characteristics of the flow would be lost, and no filtering at all would be too expensive in required CPU time.

VII.A.2. The Use of Direct Numerical Simulation Tools

DNS tools with ITM (pseudo-DNS would be a more appropriate term since subgrid models exist in these tools) were implemented in the TRIO-U code[94,95] and have now reached some maturity to be used for helping the modeling of averaged models of NEPTUNE CFD. These tools have already been able to simulate mono-site pool boiling,[95] and will be used to investigate multisite boiling[96] (Fig. 23) up to DNB. Microvisualisation experiments are also in progress to validate some aspects of the simulations.

DNB occurs at the very vicinity of the heating wall, and all small-scale phenomena occurring at the finest scale have to be taken into account: activation of nucleation sites, growing of attached bubbles, sliding of attached bubbles along the wall, coalescence of attached bubbles, bubble detachment, and wall rewetting after detachment. Calculations with DNS including ITM are necessary to predict such small-scale phenomena since detached bubbles have a diameter of a few tens of micrometers. However, today it may only be used for a very limited space domain. Such simulations may provide information on the bubble diameter when it leaves the wall, the frequency of bubble detachment, the heat transfer due to vaporization, liquid heating, and wall quenching after a bubble departure. Many sensitivity tests are possible, or will be possible in the future, to learn about the influence of the nucleation site density, of the geometrical characteristics of the metallic surface, and of the mechanisms leading to DNB. Is coalescence likely to occur before detachment? How may a bubble detachment affect the growing of neighboring bubbles? Such questions may be investigated through DNS and will help in developing adequate and physically based closure relations for the CMFD simulations. After bubble departure, bubbles are entrained in the flow and may grow or collapse by vaporization and condensation. They may also either coalesce or break up. Figure 24 shows a simulation of a bubble coalescence due to entrainment in the wake.[97] Figure 25 illustrates how a bubble can be distorted by turbulence up to breakup. Here the LES is used in the continuous phase together with a front tracking method.[98]

DNS methods for two-phase flow are still limited by the required computer power but progress is going on with improving efficiency of both numerical schemes and computer power. The methods used in the examples above are implemented with a parallel solver, and future applications on massive parallel computers will allow much more complex simulations. Such fine-scale simulations may also be of great interest for understanding the complex interactions at a free surface between friction forces, surface tension, wave propagation, condensation or vaporization,

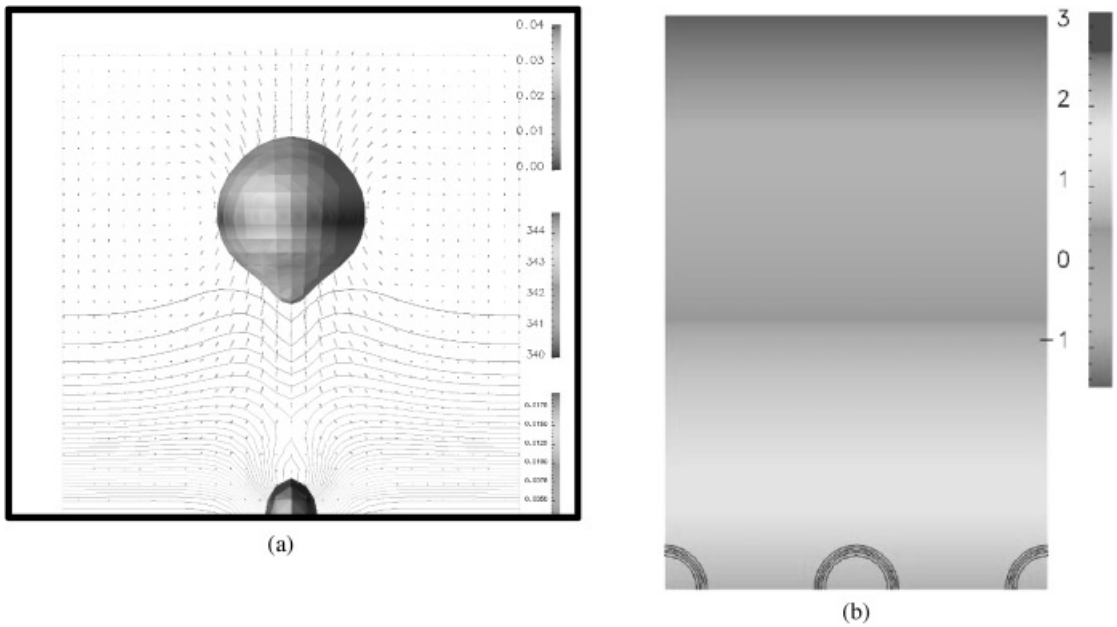

(a) (b)

Fig. 23. DNS simulation of (a) monosite boiling by Mathieu et al.,[95] and (b) multisite boiling by Fouillet.[96]

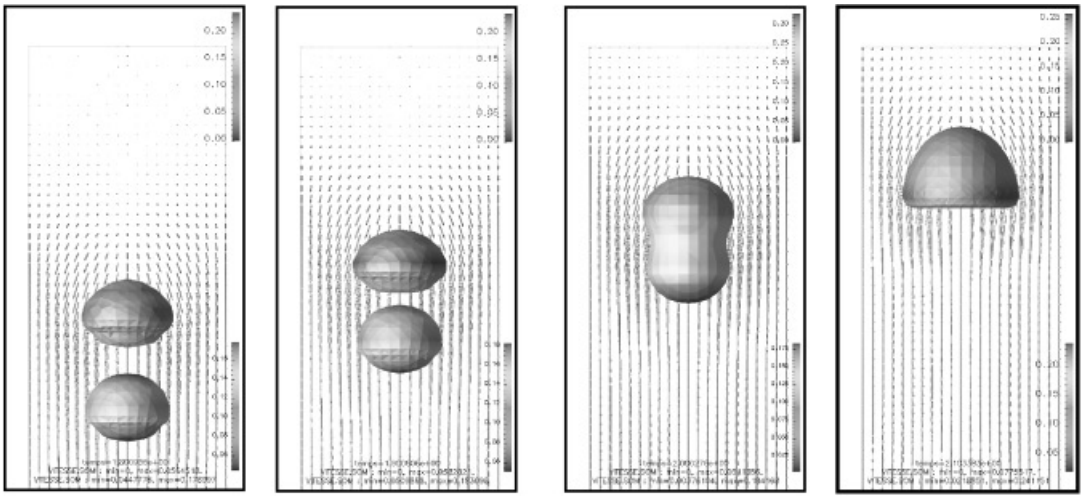

Fig. 24. DNS simulation of a coalescence of two bubbles (Mathieu[97]).

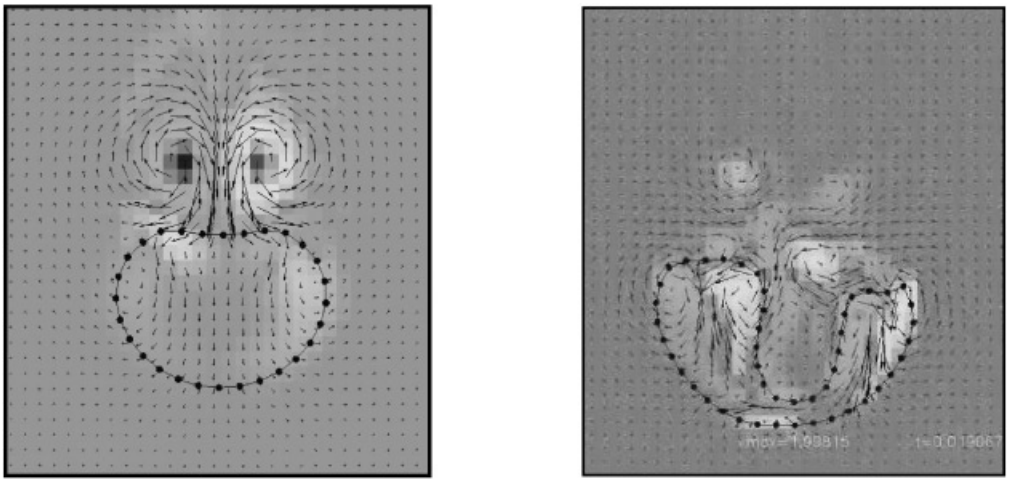

Fig. 25. Simulation with LES coupled to an interface tracking technique. Distortion of a bubble due to large-scale eddies (Labourasse et al.[98]).

and turbulence of both the gas and liquid flows. In support of the modeling of PTS, DNS and/or LES with ITM will be used for condensing flows with free surface. Lakehal et al.[99,100] have used LES along with ITM to investigate stratified countercurrent air-water flow with high interfacial shear and developed a specific subgrid scale modeling. These results of LES with ITM will be used for developing closure relations for CMFD in the frame of PTS modeling in the NURESIM project.

VII.A.3. Future Improvements in System and Component Scales

The intrinsic limitations of the two-fluid six-equation model were reached in the current generation of system code, and further progress is now mainly expected from multifield modeling, IAT, and modeling of turbulence effects (1-D and 3-D porous), with application to many accidental transients including the reflooding phase of LBLOCA and low-pressure transients where high steam velocity may create annular mist flow and stratified mist flows. In the component codes two-fluid and multifield models for porous medium will be further developed, with application to PWR core in operation and in accidental transients (e.g., SLB), critical power in BWRs, research reactors and propulsion reactors, steam generator tube vibrations, corrosion, etc. Then, new options will be progressively developed and implemented in NEPTUNE system and NEPTUNE component scales with these new capabilities. The multifield modeling will

focus on annular mist flow and stratified mist flow regimes for which two liquid fields are necessary. Such flow regimes are encountered in nominal conditions in BWRs, in many accident scenarios of PWRs such as low-pressure transients, and in the late phase of LOCAs including reflooding. Dynamic modeling of interfacial area and turbulence will focus on bubbly-slug-churn flows in reactor core and on the bubbly-to-stratified transition. Stratified flows are often encountered in the hot legs of a PWR. The following two-flow regime transitions may also occur in hot legs, which may play an important role in accident sequences:

1. transition from bubbly to stratified flow
2. transition from stratified to stratified mist flow.

Stratification of a bubbly flow in a horizontal channel also depends on a balance between turbulent dispersion force and the buoyancy force acting on the bubbles. In two-fluid six-equation models, only a very simplified formulation of both effects was possible in the CATHARE code,[101] and no relaxation time associated to the process could be properly described by an algebraic criterion. In this process, transport equations for turbulence and IAC are required to predict the evolution of the flow with bubble sedimentation and progressive appearance of a continuous gas field at the top of the pipe. A specific experimental program will be devoted to the investigation of such flow regime transitions (METERO experiment, CEA Grenoble). The transition from stratified to stratified mist flow is often treated by system codes using extrapolations of models for onset of droplet entrainment in vertical annular flow. Moreover, stratified mist flow also requires a two-liquid-field model to describe the separate behavior of droplets and continuous liquid. A specific experimental program will also be devoted to the investigation of stratified mist flow in a horizontal pipe with measurements of entrainment and deposition rates, and of the droplet size and velocity (REGARD facility, see Sec. VIII). The prediction of chocked flow by system codes still remains rather inaccurate. Flashing flows in a nozzle or at a break are nonestablished flows that require an accurate modeling of the flashing delay related to heterogeneous nucleation. It is expected that the activation of the nucleation sites depends on pressure turbulent fluctuations, which might be estimated by a proper modeling of turbulent scales. After nucleation, myriads of small bubbles grow by flashing and may break up when reaching a limit size. The convective heat transfer controls the thermal nonequilibrium, and the bubble size is the key parameter. Thus, using transport equations for turbulence intensity and IAC may allow a better prediction of flashing flows. Three-dimensional models in porous medium will also be further developed, and ongoing and future R&D will address the following issues:

1. mathematical derivation of two-fluid and multifield system of equations in a porous medium using a homogenization technique
2. development of wall friction and interfacial friction tensors, taking into account the nonisotropy of the porous medium.

VII.B. Numerical Methods

The long-term activities include the following items, which may be split into two parts. New modeling techniques are investigated within the first part, including the DNS models and the multipressure multifield models. The second part corresponds to other investigations, including the preconditioning techniques, the fictitious domain methods, and the finite volume element methods.

VII.B.1. Two-Fluid Two-Pressure Models

A new class of two-fluid models has emerged quite recently in the framework of gas-particle flows when focusing on deflagration to detonation transition.[102–105] More recently, similar models have been reexamined in order to check their ability to describe water-vapor flows.[91,92,106] This class of models requires defining in detail both the interfacial velocity and the interfacial pressure. Moreover, the source terms have to be defined, in agreement with preexistent two-fluid models.

In order to simplify the presentation, we neglect here the mass transfer terms and only retain momentum transfer effects. Hence, the governing equations are

$$\begin{cases} \dfrac{\partial \alpha_1}{\partial t} + v^{\text{int}} \dfrac{\partial \alpha_1}{\partial x} = \lambda (p_1 - p_2) \\ \dfrac{\partial m_k}{\partial t} + \dfrac{\partial m_k v_k}{\partial x} = 0 \\ \dfrac{\partial (m_k v_k)}{\partial t} + \dfrac{\partial (m_k v_k^2 + \alpha_k p_k)}{\partial x} - p^{\text{int}} \dfrac{\partial \alpha_k}{\partial x} = F_k \\ \dfrac{\partial (\alpha_k E_k)}{\partial t} + \dfrac{\partial (\alpha_k v_k (E_k + p_k))}{\partial x} + p^{\text{int}} \dfrac{\partial \alpha_k}{\partial t} = F_k v^{\text{int}}. \end{cases} \tag{47}$$

We still use standard notations here: The subscript $k \in \{1,2\}$ refers to phases 1 and 2, respectively; v_k, ρ_k, and p_k denote the velocity, the density, and the pressure, respectively, in phase k. The volume fraction in each phase is denoted by $\alpha_k \in [0,1]$, with $\alpha_1 + \alpha_2 = 1$; the partial masses are $m_k = \alpha_k \rho_k$; and $E_k = \rho_k u_k + (\rho_k v_k^2/2)$ stands for the total energy of phase k, where the internal energy is noted $u_k = u_k(p_k, \rho_k)$.

The interfacial velocity v^{int} and the interfacial pressure p^{int} are modeled in a classical way,[91,92,107] as follows:

$$v^{\text{int}} = \mu v_1 + (1 - \mu) v_2 \ , \tag{48}$$

where either $\mu(1-\mu)=0$ (see Ref. 102), or $\mu = m_1/(m_1+m_2)$ (see Ref. 92). Moreover,

$$p^{\text{int}} = \frac{(1-\mu)a_1p_1 + \mu a_2p_2}{(1-\mu)a_1 + \mu a_2} \ , \tag{49}$$

where $a_k = (\partial u_k(p_k,\rho_k)/\partial p_k)^{-1}\,(\partial Ln(s_k)(p_k,\rho_k)/\partial p_k)$, if s_k denotes the specific entropy such that

$$(c_k)^2\,\frac{\partial s_k}{\partial p_k} + \frac{\partial s_k}{\partial \rho_k} = 0 \ . \tag{50}$$

The main achievements in this area in the framework of the NEPTUNE project essentially concern the following:

1. the establishment of a meaningful relationship between the interfacial velocity and the interfacial pressure, so that a physically meaningful entropy inequality holds
2. a correct definition of the interfacial velocity, which ensures a unique set of meaningful jump conditions
3. the definition of interfacial source terms that comply with the entropy inequality
4. the construction of stable and accurate enough finite volume schemes to compute approximations of solutions of these models
5. a correct treatment of boundary conditions.

For further details on the closure laws, on the main properties of these models, and on some suitable algorithms, the reader is referred to Refs. 91, 92, and 108. A key point is that exact solutions of the 1-D Riemann problem associated with the convective subset are physically relevant, since partial masses, void fractions, and pressures remain in their physical domain. Some extension to the framework of turbulent flows is also discussed in Ref. 107. In a more recent work, which is closely connected with Ref. 109, we also give some unified strategy to compute two-fluid models,[90] and we also examine some possible drawbacks of standard two-fluid models (see also Refs. 110 and 111). Eventually, Ref. 112 provides a preliminary investigation of the problem of the mathematical modeling of three-phase (or three-field) flows. The whole confirms that this approach is indeed very promising.

VII.B.2. Interface Models

Another part of our investigation concerns the prediction of two-phase flows with sharp interfaces. For such a goal, focus is given to a class of five-equation models that accounts for the position of the interface (defining some parameter Z, $Z=0$ corresponding to the presence of the sole phase 2), the mean momentum, the mean total energy, and the mass conservation within each phase. A five-equation model has been introduced in Refs. 113 and 114, and the extension to the framework of two-phase flows with mass transfer has been achieved more recently in Ref. 115. The governing equations for Z and for mass conservation read:

$$\frac{\partial Z}{\partial t} + v_i\,\frac{\partial Z}{\partial x_i} = K(p_1-p_2) \ , \tag{51}$$

and (for $k=1,2$)

$$\frac{\partial m_k}{\partial t} + \frac{\partial m_k v_i}{\partial x_i} = (-1)^k\lambda(g_1-g_2) \ , \tag{52}$$

where the mean density and the mean pressure are $\rho = Z\rho_1 + (1-Z)\rho_2$ and $p = Zp_1 + (1-Z)p_2$, respectively. The Gibbs enthalpy is denoted g_k for $(k=1,2)$ as usual. The governing equation for the mean velocity v is of course given by

$$\frac{\partial \rho v_i}{\partial t} + \frac{\partial \rho v_i v_j}{\partial x_j} + \frac{\partial p}{\partial x_i} = 0 \ , \tag{53}$$

and the governing equation for the mean total energy E is

$$\frac{\partial \rho E}{\partial t} + \frac{\partial (\rho E + p)v_j}{\partial x_j} = 0 \ . \tag{54}$$

The resulting set of equations is hyperbolic (see Ref. 116), assuming finite or null timescales.

VII.B.3. Low Mach Number Methods and Preconditioning Techniques

Finite volume upwinding schemes provide stable approximations of solutions of hyperbolic sets of PDE. However, first-order explicit schemes give rather crude approximations on coarse meshes in very low Mach number regions. The L^1 norm of the error varies as $O(h/M)$, and thus the accuracy in low Mach regions is poor. Some recipes for steady computations have been proposed by Roe and Turckel some years ago, and Ref. 117 describes in detail the application of similar ideas to the exact Godunov scheme[118] or to the approximate Godunov scheme nicknamed VFRoe-ncv (Ref. 119).

The "pressure-based" algorithms always require preconditioning techniques in order to solve algebric systems associated with discrete elliptic problems on fine meshes. Clasical methods rely on the use of incomplete Choleski or polynomial preconditioners. An innovative approach based on the use of wavelets is discussed in Ref. 120. Another interesting way to speed up convergence consists in using multigrid algorithms. These may also be used to solve the full set of nonlinear equations.[121]

VII.B.4. Fictitious Domain Methods and Finite Volume Element Methods

Many recent CFD or CMFD codes are based on the use of unstructured meshes, because of the fact that one needs to deal with complex geometries to compute flows in cores or steam generators. They nonetheless may suffer from a few drawbacks. An important point, for instance, is that it is not so easy to derive convergent approximations of some simple diffusion problems when using finite volume techniques on triangular or tetrahedral meshes. It must also be emphasized that, because of indirect addressing of unknowns and complexity of flux formulas in an arbitrary reference frame, the CPU time required in some steps may increase rather quickly. The temptation is thus great to turn back to structured meshes, while using fictitious domain methods to account for complex geometries. Quite recently, these methods and their applications have been widely investigated. When applying for fictitious domain method[122] (FDM), the initial computational (or physical) domain must be immersed in a wider and geometrically simpler domain called the fictitious domain (for instance, a circular duct is plugged into a square domain). One needs to define a set of PDEs that coincides with the real set of PDEs that governs the flow in the physical domain, and also applies in the fictitious part of the domain. The new set must thus by some way impose the true boundary conditions on the border of the physical domain. An important point to note is the true CPU time, which is required by these FDMs for given accuracy, and the comparison with standard finite element methods or finite volume methods. References 123 and 124 focus on this approach and examine several ways to impose boundary conditions (see Ref. 125 also).

Another research topic concerns finite volume element techniques, which have already been proven to provide very accurate results for Stokes and Navier-Stokes equations (see Ref. 126). Since most of the time schemes in two-phase codes rely on a discretization of the coupled equations of total mass and total momentum, which results in an almost standard Navier-Stokes (or Stokes-like) problem, it seems natural to investigate the finite volume element approach in order to retrieve a fair accuracy on the mean velocity–mean pressure pair. This work is still on progress.

VIII. EXPERIMENTAL PROGRAMS

VIII.A. NEPTUNE Validation Plan

VIII.A.1. A Classical Application-Oriented Validation Methodology

The physical validation of NEPTUNE software is strongly oriented by the industrial applications the code has to deal with; in this frame, it is carried out according to a classical process characterized by the following three main features:

1. a validation specially relevant for the selected industrial applications
2. a two-step validation approach aiming at the assessment of the dominant basic models against separate-effect test data and of the whole code capability against integral-type test data
3. the use of actually relevant experimental data with respect to the validation aims.

On the basis of this general validation process, the following four-step generic work approach has been adopted to draw up dedicated validation plans and provide the required relevant validation data, possibly thanks to new experimental programs to be set up:

1. a thorough analysis of the concerned industrial applications, on a thermal-hydraulic modeling point of view;
2. an assessment of the involved dominant models according to the available pieces of information with respect to the model validation;
3. an inventory of existing relevant validation data;
4. eventually, the specification of the new experimental programs to be set up to provide the additional needed data.

VIII.A.2. Dedicated Validation Plans and Experimental Programs To Be Set Up

A thorough analysis of high-priority industrial applications has been carried out, in addition to the previous FASTNET and EUROFASTNET related analyses.[1,2] This analysis has recommended that the further activity focus on the following:

1. the open medium (3-D) CFD modeling, in connection with DNB in PWR cores and PTS applications (in the case of an SBLOCA scenario for PTS, and of bubbly flows for DNB)
2. the porous medium, multifield, and IAT modeling, in connection with the reflooding phase (in an LBLOCA situation).

VIII.A.2.a. DNB Application

The analysis of PWR in-core DNB application has pointed out that a step forward can be anticipated from the use of two-phase 3-D CFD modeling of boiling flows. Actually, the priority aim is to investigate a CHF (DNB-type) local predictive approach, which would provide CHF correlations based on local parameters as provided by the CFD modeling.

With respect to DNB phenomenon and bubbly boiling flow configuration on which we concentrate (in a first step), the key thermal-hydraulic parameters are the refined two-phase flow pattern, the liquid phase and bubble velocities, and the liquid phase and rod surface temperature. They must be accurately predicted; therefore, the CFD code has to reliably model the associated dominant physical phenomena, namely, the "flow-to-wall" interaction (nucleate boiling and turbulence) and the grid impact on two-phase flow along with the bubble radial displacement from the heated wall and the bubble coalescence, collapse, and breakup within the flow.

The assessment of NEPTUNE CFD key basic models has highlighted the great lack of existing validation support, and a dedicated validation plan involving the following two successive steps has been defined:

1. The first step deals with the information and validation of the models in parallel flows; the models related to the flow dynamics, the interfacial mass and energy transfers in sub-cooled boiling, and the wall-to-fluid heat transfer in nucleate boiling are concerned. An assessment of the whole modeling is also recommended in such a parallel flow configuration.

2. The second step aims at extending the first step's validation insights to complex geometry flows, such as those met in PWR cores. It involves the additional validation of the dynamics-related models as well as the assessment of the whole modeling in such complex geometries.

Because of a crucial lack of relevant experimental data (basically, liquid phase and bubble velocities, liquid phase and wall temperature, and void fraction and interfacial area, to be obtained in representative conditions), to comprehensively carry out this validation plan, six new experimental programs should be set up; they involve the following:

1. adiabatic two-phase flows, successively in parallel and complex geometry configurations, to assess the dynamics-related models without any mass transfer between the gas and liquid phases
2. adiabatic subcooled two-phase parallel flows, to deal with the mass transfer in a subcooled flow (steam bubble recondensation process in the subcooled liquid flow)
3. nucleate boiling conditions in parallel flows, to further develop/complement and validate a local wall-to-fluid heat transfer model that can be actually applied in industrial configurations
4. integral-type boiling conditions, both in parallel and complex geometry configurations, to check the correct ability of the whole modeling.

These experimental programs will be carried out on the following:

1. the EDF MEDOC test facility, which provides test sections with adiabatic "liquid water–gaseous R116" mixture flows. For a description of the MEDOC loop, see Ref. 127. The new CHAPTAL mock-up, which is being set up for NEPTUNE validation, is presented in Ref. 128
2. the CEA DEBORA and GRAZIELLA test facilities (see DEBORA description in Ref. 57), which allow R134A boiling flows.

They will provide data from 2007 until 2011.

VIII.A.2.b. PTS Application

SBLOCA scenarios may result in an injection of cold water in a partially uncovered cold leg, possibly leading to crucial PTSs on the RPV wall. Such a configuration involves a dispersed two-phase flow in the cold water impinging jet area and a downstream stratified two-phase flow along the cold leg to the RPV downcomer, both with DCC as a prime importance phenomenon; liquid phase turbulence and flow-to-wall heat transfer (mainly in the downcomer area, for the latter) are also dominant physical phenomena to be accurately modeled. With respect to the foreseen open medium CFD simulations of such a configuration, the key thermal-hydraulic parameters are the refined two-phase flow pattern, the liquid phase and bubble velocities, and the liquid phase and wall temperatures.

No comprehensive validation support exists for the related key basic models of the CFD modeling, and a two-fold validation plan has been defined; it aims at the following:

1. the development/closure and validation of these key models, successively in the impinging jet area, in the cold-leg area and in the downcomer area. The involved dominant physical phenomena are
   a. the turbulence source term, as well as the entrainment, breakup, and condensation of the steam phase, in the impinging jet area
   b. the direct contact condensation in stratified wavy flows and the turbulent diffusion in presence of density gradients, in the cold-leg area
   c. the wall-to-fluid heat transfer in the downcomer area, to a lesser extent
2. a global assessment of the whole modeling.

To fully carry out this validation plan, the following local data are required:

1. liquid and steam phase velocities and temperatures, void fraction and interfacial area, in the impinging jet area

2. liquid and steam phase velocities and temperatures, refined interfacial structure and condensation flux density close to the interface, for the stratified flow zone with density gradients
3. liquid velocities and temperatures in the downcomer, as well as wall temperature.

Actually, there is a lack of such relevant local data, and an integral-type experimentation with a refined instrumentation is currently being set up in the framework of a European collaboration involving FZR, PSI, AREVA NP, CEA, EDF, and IRSN. It is implemented on the FZR TOPFLOW test facility (see TOPFLOW description in Ref. 129) using the so-called "diving chamber technology"(which allows test performance in pressure equilibrium pressure with the outside). Its basic design is presently completed; it involves the following:

1. a 1:2.5 scaled down test section representing a cold leg and a part of the downcomer of French CPY 900 MWe NPPs
2. the implementation of microthermocouples, thermoneedle probes and wire mesh sensors, along with the use of IR and high-speed cameras; concurrently innovative measurement techniques are being assessed (particle image velocimetry) and developed (four-sensor electrical probe) for use in a further stage
3. the performance of both transient and steady-state tests, both in water-steam flow conditions (at pressures up to 50 bar) and in air-water flow conditions.

Test results are expected within the second half of 2007.

VIII.A.2.c. LBLOCA Application

The evaluation of the safety margin in relation to the peak cladding temperature during a hypothetical LOCA is mostly connected to an accurate prediction of the cooling of the cladding during the reflooding phase.

In that prospect, a three-field modeling (liquid and steam continuous fields, plus a dispersed liquid field) would help to reduce the prediction uncertainties associated to the current two-phase six-equations models, as well as to extend the modeling capability to different configurations. Furthermore, several phenomena do have a significant impact on the water drop size (coalescence and breakup within the steam flow, breakup across the grids, entrainment and deentrainment along the rods, the grids and the "liquid-steam" continuous field interface, a well as along the upper plenum structures), whereas this parameter is crucial for the in-core heat transfer and also for system-type effects; the development of an IAT equation is therefore recommended to fully take advantage of the three-field modeling.

As far as these modeling functionalities are concerned in relation with the reflooding phase of an LBLOCA, there is a need for a specific validation based on the use of a refined characterization of droplet size distributions in different test sections dealing with the relevant core, hot leg and upper plenum geometrical and thermal-hydraulic configurations.

For a few years, similar refined data have been obtained in a core-type test section in the framework of reflooding tests carried out at The Pennsylvania State University on the RBHT test facility; these RBHT data should be of great interest for the NEPTUNE project and have been made available to the project. With respect to the hot leg and upper plenum-type configurations, two new experimental programs (REGARD experiment) are planned on the CEA MHYRESA test facility, which has been formerly used for the CATHARE code validation[130]; test results for the hot-leg configuration are expected by the first half of 2007.

VIII.B. Instrumentation Techniques

The thorough analysis presented above clearly revealed the need for physical quantities to be locally measured in bulk flows. Among others, liquid velocity (both mean and turbulent values), IAC, and local void fraction are of crucial importance when considering the experimental validation of physical models that describe the phenomena governing two-phase flows.

Focused on the needs related to these physical quantities, the development and/or enhancement of three different measuring techniques has been undertaken, in the frame of the NEPTUNE project.

VIII.B.1. Hot-Film Anemometry

Hot-wire and hot-film anemometry is widely used in single-phase gas and liquid flows, and commercial systems are available.

In two-phase adiabatic flows, this measuring technique has been used already in various tests; however, it requires some specific adaptations, especially concerning signal processing, as compared to single-phase flow use. In order to extract, from the two-phase signals, the high-level portions that are relevant to the liquid phase, different filtering techniques have been tested, based on thresholding the signal itself, its derivative, and its instantaneous frequency. Junqua[131] used such developments to measure both vertical and horizontal components of the liquid velocity (mean and fluctuating values) in an air-water stratified flow.

When heat transfer occurs, and particularly in the vicinity of a heated wall, specific attention must be paid to how the measured velocity may be influenced by a strong temperature gradient. Numerical simulations have recently been achieved, and a dedicated experimental assessment is intended. In that objective, a

square test section with a heated wall is being set up. Validation will be achieved through comparisons with laser Doppler velocimetry and nuclear magnetic resonance measurements.

In the case of a nearly saturated flow, preliminary tests demonstrated that, if boiling occurs on the sensitive element of the probe (hot-film or hot-wire), the spectral signature of the fluctuations induced by bubble formation and detachment should be easily discriminated from the velocity fluctuations of the bulk flow, allowing the use of a simple filtering technique to remove related artifacts.

VIII.B.2. Four-Sensor Optical Probes

An optical probe detects the presence of liquid or gas at the tip of a fiber immersed in the flow, by detecting the changes of optical index. Single-sensor probes have been used for several decades to measure the local void fraction, in air-water and in Freon bubbly boiling flows. In same conditions, double-sensor optical probes are also used to measure the IAC and phase interface velocity, in 1-D flows with spherical bubbles. At the opposite, a four-sensor probe has the capability of measuring the local IAC with weaker restrictions concerning the flow direction and the bubble shape.

A four-sensor probe is composed of an upstream reference sensor and three downstream secondary sensors (Fig. 26). At CEA-Grenoble, particular attention has been devoted to the design and manufacturing of the probe itself. The conical shape of the tips are obtained by using a dedicated stretching machine. Learning from the realization of some preliminary prototypes, the optimization of the stretching parameters led to improvement of the sharpness of the glass tips, thus enhancing the interface piercing efficiency.

Starting from the four-sensor probe theory established by Ishii and Revankar, the algorithm used to process the four binary signals has been specially developed and assessed. The main efforts focused on the minimization of the "missing events" (i.e., the bubbles not intercepted by the four tips), the way to restore information for the latter, and on calculation speed. In a first step, simulations have been performed to numerically generate bubbly flows with imposed void fraction and bubble size distribution. By this way, artificial signals have been generated and processed. The comparison between the a priori known characteristics of the computed flow and the results provided by the signal processing algorithm contributed to validate the algorithm itself and to quantify its intrinsic accuracy. Moreover, several parametrical analyses revealed the influence of the flow characteristics, and helped to optimize the spatial arrangement of the four sensors. In a second step, an instrumental benchmark has been achieved at Purdue University, by comparing the measurements obtained by a four-sensor optical probe and a four-sensor electrical probe, mounted on the same test section.[132] Bubbly, slug, and churn air-water flows have been investigated in a vertical 5.08-cm (2-in.)-diam pipe (Fig. 27).

In a third step, experiments carried out at CEA-Grenoble and comparisons with high-speed imaging of a bubbly flow exhibited a relative measurement accuracy that is better than $\pm 1\%$ for void fraction and $\pm 8\%$ for IAC. It has been demonstrated that such performances were obtained even when the probe was inclined in the range of ± 30 deg with respect to the main direction of the flow. Calibration has also been performed in the wavy zone of a horizontal stratified flow, and the comparison with a capacitance wire probe revealed a $\pm 5\%$ relative accuracy for IAC measurement.[133]

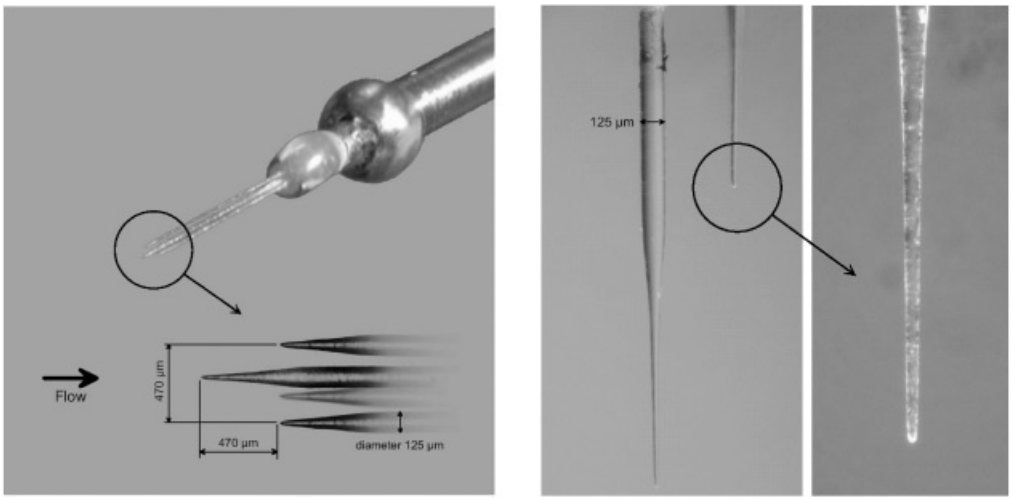

Fig. 26. First prototype of a four-sensor optical probe and close view of tips with improved sharpness.

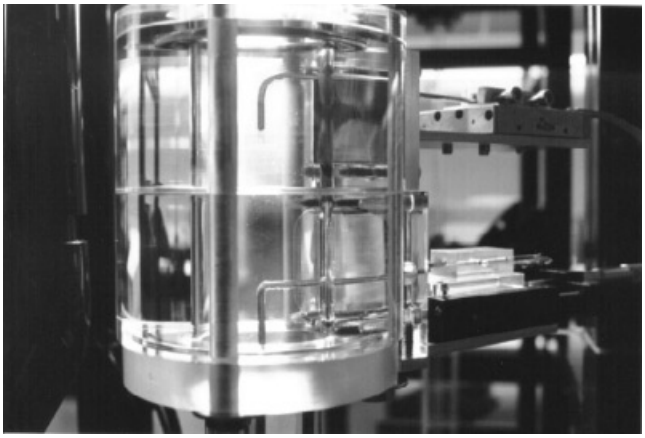

Fig. 27. Optical and electrical four-sensor probes in a vertical 5.08-cm (2-in.) test section.

VIII.B.3. X-Ray Tomography

Nonintrusive imaging techniques such as X-ray tomography become of great interest, especially to investigate domains containing internal structures and obstacles such as rod bundles. X-ray absorption has been widely used to obtain time- and space-averaged void fraction in various two-phase systems. However, the present work concerns the development of a local measuring technique with a high spatial resolution and giving access to a quantitative value of the local void fraction in flows exhibiting large amplitude fluctuations. In the frame of the NEPTUNE project, the development of such a new tomograph required focus on the two following topics: the measurement bench and the reconstruction algorithm.

The fan-beam X-ray 2-D tomographic bench is designed to investigate static targets by moving an X-ray source and a linear multipixel detector around them. It is mainly composed of an X-ray generator (160 kV/30 mA) equipped with a thin collimating slit, a Thomson TH9560 linear wide dynamic sensor (1536 pixels), and a tomographic rotating bearing. The latter, entrained by a stepper motor, allows positioning of the detector and X-ray source around the test section with a better than 0.01-deg absolute accuracy.

Figure 28 provides a global view of the bench. A more detailed description can be found in Ref. 134.

Concerning the numerical inversion method, the algebraic reconstruction technique (ART) has been chosen because of its flexibility regarding the projection geometry. In the category of ART, different algorithms have been compared and a conjugate gradient least squares algorithm has been preferred because of its higher accuracy, higher convergence efficiency, lower CPU cost, and lower noise sensitivity. Because of oscillations and artifacts exhibited by reconstructions obtained with these algorithms in their standard version, a regularization process has been included in the linear system inversion. However, this regularization process leads to a poor reconstruction accuracy near the walls. To overcome this difficulty, an adaptative regularization method restricted to the regions of interest has been developed. Its efficiency has been demonstrated with simulations and

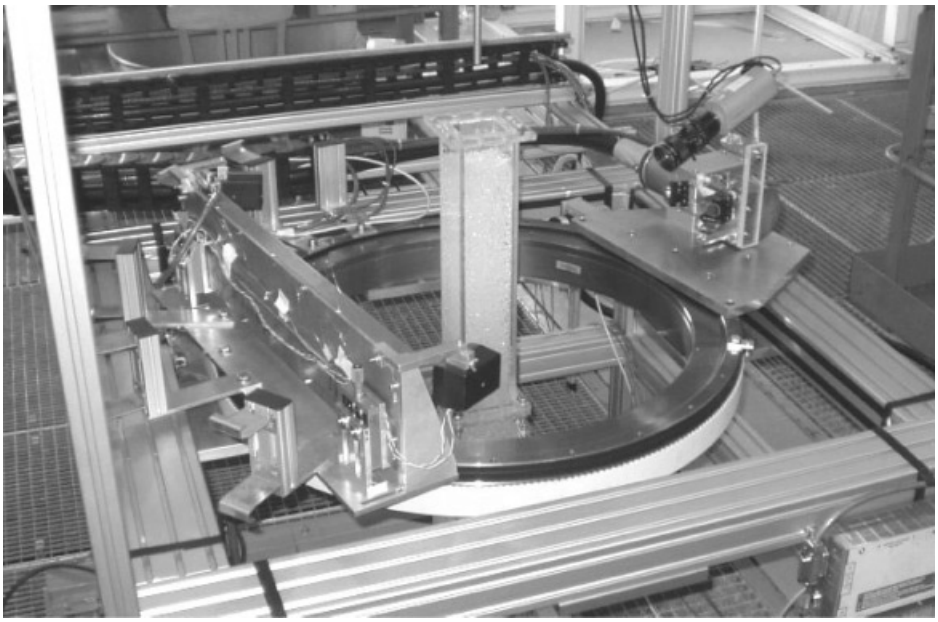

Fig. 28. Global view of the X-ray tomographic bench.

reconstruction tests performed on static phantoms and real two-phase flows. All these developments are detailed in Ref. 135 and summarized in Ref. 136. In particular, the validation of the tomograph has been achieved on a bubble column. A movable optical probe was plunged inside the pipe and measured the local void fraction 5 mm above the X-ray beam crossing the flow. By this way, void fraction maps provided by X-ray tomography and optical probe were obtained. A pixel-by-pixel comparison reveals that the void fraction discrepancy does not exceed 2% (absolute value) in the core of the pipe and near the walls, except in the corners where the void fraction overestimation (by X-ray tomography) reaches 6% because of beam-hardening effects that had not been taken into account in this series of tests. The low and uniform discrepancy observed illustrates the benefit provided by the reconstruction algorithm enhancements.

NOMENCLATURE

a_i = interfacial area concentration

$\boldsymbol{D}$ = approximate velocity derivative in function of pressure (notation for numerics)

D = diameter

e = internal energy

F = force (general)

F' = interfacial momentum transfer (notation for numerics)

g = gravity acceleration

H = total enthalpy

h = enthalpy

K = turbulent kinetic energy

M = interfacial momentum transfer

P = production term (in $K - \epsilon$ equations)

Pr = Prandtl number

p = pressure

Q = heat source

q = internal heat flux

$\boldsymbol{R}$ = approximate velocity derivative in function of volume fraction (notation for numerics)

S = source term (general)

S' = generalized source term (notation for numerics)

$\overline{\overline{T}}$ = stress tensor

t = time

$\vec{v}$ = velocity

$\vec{w}$ = auxiliary velocity (notation for numerics)

Greek

α = volume fraction

Γ = interfacial mass transfer

ϵ = turbulent dissipation rate

ν = kinematic viscosity

ρ = density

Subscripts

exp = relative to an explicit form (time discretization)

g = relative to gas phase

i = relative to interface

K = relative to turbulent kinetic energy

k = relative to phase k

l = relative to liquid phase

ϵ = relative to turbulent dissipation

Superscripts

ext = relative to external force or heat source

IAC = relative to interfacial area coalescence

(i) = relative to the (i) (current) stage of the fractions-pressure-energy algorithm

$(i + \frac{1}{2})$ = relative to an intermediate stage of the fractions-pressure-energy algorithm

$(i + 1)$ = relative to the $(i + 1)$ stage of the fractions-pressure-energy algorithm

m = relative to molecular forces

n = relative to time-step number n (explicit form)

$n + 1$ = relative to time-step number $n + 1$ (implicit form)

$n + \frac{1}{2}$ = relative to an intermediate step between time-steps n and $n + 1$

Re = relative to Reynolds stress

t = relative to turbulence

$*$ = intermediate values for velocities (velocity prediction step of NEPTUNE_CFD)

Symbols

∇ = gradient operator

$\nabla\cdot$ = divergence operator

$\wedge$ = vector product

$\otimes$ = tensor product

REFERENCES

1. D. BESTION, P. CLÉMENT, J. CAMINADE, J. DELHAYE, P. DUMAZ, J. GARNIER, D. GRAND, E. HERVIEU, O. LEBAIGUE, H. LEMONNIER, C. LHUILLIER, J. PAGES, I. TOUMI, and I. VILLAND, "A Proposal for a Ten-Year Effort in Thermal-Hydraulic Research," *Multiphase Sci. Technol.*, **11**, 79 (1999).

2. D. BESTION, A. LATROBE, H. PAILLÈRE, A. LAPORTA, V. TESCHENDORFF, H. STAEDTKE, N. AKSAN, F. D'AURIA, J. VIHAVAINEN, P. MELONI, G. HEWITT, J. LILLINGTON, B. MAVKO, A. PROSEK, J. MACEK, M. MALACKA, F. CAMOUS, F. FICHOT, and D. MONHARDT, "European Project for Future Advances in Science and Technology for Nuclear Engineering Thermal-Hydraulics (EUROFASTNET), Final Report," Technical Report, Commission of the European Communities (2002).

3. "Research and Training in the Field of Nuclear Energy," Commission of the European Communities; available on the Internet at http://www.cordis.lu/fp5-euratom (2007).

4. "Working Group on the Analysis and Management of Accidents (GAMA)," Organisation for Economic Co-operation and Development/Nuclear Energy Agency; available on the Internet at http://www.nea.fr/html/nsd/csni/gama.html (2007).

5. "NURESIM—European Platform for Nuclear Reactor Simulation (Contract Number 516560)," Technical Report, Commission of the European Communities (2005).

6. "NURESIM Project," Commission of the European Communities; available on the Internet at http://www.nuresim.com (2007).

7. M. ROBERT, M. FARVACQUE, M. PARENT, and B. FAYDIDE, "CATHARE 2 V2.5: A Fully Validated CATHARE Version for Various Applications," *Proc. 10th Int. Topl. Mtg. Nuclear Reactor Thermal Hydraulics (NURETH 10)*, Seoul, Republic of Korea, October 5–9, 2003.

8. "TRACE: TRAC/RELAP Advanced Computational Engine," U.S. Nuclear Regulatory Commission; available on the Internet at http://www.nrc.gov (2007).

9. I. TOUMI, A. BERGERON, D. GALLO, E. ROYER, and D. CARUGE, "FLICA-4: A 3D Two-Phase Flow Computer Code with Advanced Numerical Methods for Nuclear Applications," *Nucl. Eng. Des.*, **200**, 139 (2000).

10. P. OBRY, J. CHEISSOUX, M. GRANDOTTO, J. GAILLARD, E. DE LANGRE, and M. BERNARD, "An Advanced Steam Generator Design 3D Code," *Proc. Thermal-Hydraulics of Advanced Heat Exchangers, ASME Annual Winter Meeting*, Dallas, Texas, November 25–30, 1990, American Society of Mechanical Engineers (1990).

11. S. AUBRY, C. CARÉMOLI, J. OLIVE, and P. RASCLE, "The THYC Three-Dimensional Thermal-Hydraulic Code for Rod Bundles: Recent Developments and Validation Tests," *Nucl. Technol.*, **112**, *3*, 331 (1995).

12. C. PAIK, L. HOCHREITER, J. KELLY, and R. KOHRT, "Analysis of FLECHT-SEASET 163—Rod Blocked Bundle Data Using COBRA-TF," Technical Report, NUREG/CR-4166, U.S. Nuclear Regulatory Commission (1985).

13. H. NINOKATA, T. ANEGAWA, M. ARITOMI, T. HARA, H. KAMO, S. KUSUNO, K. MISHIMA, S. MOROOKA, K. NISHIDA, M. SADATOMI, A. SOU, Y. YABUSHITA, and Y. YAMAMOTO, "Development of the NASCA code for Predicting Transient BT Phenomena in BWR Rod Bundles," *Proc. OECD/CSNI Workshop on Advanced Thermal-Hydraulic and Neutronic Codes Application*, Barcelona, Spain, April 10–13, 2000, Organisation for Economic Co-operation and Development/Committee on the Safety of Nuclear Installations (2000).

14. "ATHOS/SGAP V3.0," Electric Power Research Institute; available on the Internet at http://www.epri.com (Nov. 2003).

15. D. BESTION, "On the Application of Two-Phase CFD to Nuclear Reactor Thermal-Hydraulics," *Proc. 11th Int. Topl. Mtg. Nuclear Reactor Thermal Hydraulics (NURETH 11)*, Avignon, France, October 2–6, 2005.

16. M. THURGOOD, J. KELLY, T. GUIDOTTI, R. KOHRT, and K. CROWELL, "COBRA/TRAC—A Thermal Hydraulics Code for Transient Analysis of Nuclear Reactor Vessels and Primary Coolant," Technical Report, NUREG/CR-3046, U.S. Nuclear Regulatory Commission (1983).

17. E. ROYER and I. TOUMI, "CATHARE-CRONOS-FLICA Coupling with ISAS: A Powerful Tool for Nuclear Studies," *Proc. 6th Int. Conf. Nuclear Engineering (ICONE 6)*, San Diego, California, May 10–15, 1998, American Society of Mechanical Engineers (1998).

18. D. AUMILLER, E. TOMLINSON, and W. WEAVER, "An Integrated RELAP5-3D and Multiphase CFD Code System Utilizing the Semi-Implicit Coupling Technique," *Nucl. Eng. Des.*, **216**, 77 (2002).

19. T. SOFU, D. WEBER, H. JOO, T. CHUN, T. DOWNAR, J. THOMAS, and Z. ZHONG, "Development of a Comprehensive Modeling Capability Based on a Rigorous Treatment of Multi-Physics Phenomena Influencing Reactor Core Design," *Proc. Int. Congress on Advances in Nuclear Power Plants (ICAPP '04)*, Pittsburgh, Pennsylvania, June 13–17, 2004, American Nuclear Society (2004).

20. "OASIS Software," Centre Européen de Recherche et Formation Avancée en Calcul Scientifique; available on the Internet at http://www.cerfacs.fr/globc/software/oasis (Sep. 2006).

21. M. ISHII and T. HIBIKI, *Thermo-Fluid Dynamics of Two-Phase Flows*, Springer, New York (2005).

22. J. FERZIGER and M. PERIC, *Computational Methods for Fluid Dynamics*, Springer, New York (1996).

23. N. MECHITOUA, M. BOUCKER, J. LAVIÉVILLE, J. HÉRARD, S. PIGNY, and G. SERRE, "An Unstructured Finite Volume Solver for Two-Phase Water-Vapour Flows Based on an Elliptic Oriented Fractional Step Method," *Proc. 10th Int. Topl. Mtg. Nuclear Reactor Thermal Hydraulics (NURETH 10)*, Seoul, Republic of Korea, October 5–9, 2003.

24. R. EYMARD, T. GALLOUET, and R. HERBIN, in "Finite Volume Methods," *Handbook for Numerical Analysis*, **VII**, 723, P. G. CIARLET and P. L. LIONS, Eds., North-Holland Publishing Co., Amsterdam (2000).

25. M. CARVER, "Numerical Computation of Phase Separation in Two-Fluid Flow," *J. Fluids Eng*., **106**, 147 (1984).

26. S. MUSAFERIJA and D. GOSMAN, "Finite Volume CFD Procedure and Adaptive Error Control Strategy for Grids of Arbitrary Topology," *J. Comput. Phys*., **138**, 766 (1997).

27. F. ARCHAMBEAU, N. MÉCHITOUA, and M. SAKIZ, "Code-Saturne: A Finite Volume Code for the Computation of Turbulent Incompressible Flows—Industrial Applications," *Int. J. Finite Volumes*, **1**; available on the Internet at http://averoes.math.univ-paris13.fr (2004).

28. A. KUMBARO and M. PODOWSKI, "The Effect of Bubble/Bubble Interactions on Local Void Distribution in Two-Phase Flows," *Proc. 13th Int. Heat Transfer Conf*., Sydney, Australia, August 13–18, 2006.

29. P. ROE, "Approximate Riemann Solvers, Parameter Vectors and Difference Schemes," *J. Comput. Phys*., **43**, 357 (1981).

30. I. TOUMI and A. KUMBARO, "An Approximate Linearized Riemann Solver of a Two-Fluid Model," *J. Comput. Phys*., **124**, 286 (1996).

31. J. GHIDAGLIA, A. KUMBARO, and G. L. COQ, "On the Numerical Solution to Two Fluid Models via a Cell Center Finite Volume Method," *Eur. J. Mech./B Fluids*, **20**, 841 (2001).

32. M. NDJINGA, A. KUMBARO, P. LAURENT-GENGOUX, and F. D. VUYST, "Fast and Robust Computation of the Matrix Absolute Value Function—Application to Roe Solver for the Numerical Simulation of Two-Phase Flow Models," *Proc. 14th Int. Conf. Nuclear Engineering (ICONE 14)*, Miami, Florida, July 17–20, 2006, American Society of Mechanical Engineers (2006).

33. A. KUMBARO, "Simulation of Two-Phase Flows using a Multi-Size Group Model," *Proc. 3rd Int. Symp. Two-Phase Flow Modelling and Experimentation*, Pisa, Italy, September 22–25, 2004.

34. A. KUMBARO, "Flux Schemes: A Method for General Non-Conservative Two-Fluid Systems," *Proc. 8th Int. Symp. Gas-Liquid Flows*, Honolulu, Hawaii, July 6–10, 2003 (2003).

35. C. MOREL, W. YAO, and D. BESTION, "Three-Dimensional Modeling of Boiling Flow," *Proc. 10th Int. Topl. Mtg. Nuclear Reactor Thermal Hydraulics (NURETH 10)*, Seoul, Republic of Korea, October 5–9, 2003.

36. C. MOREL, "Turbulence Modeling and First Numerical Simulations in Turbulent Two-Phase Flows," *Proc. 11th Symp. Turbulent Shear Flows*, Grenoble, France, September 8–11, 1997, Vol. 3, Poster Session 3, pp. 10–15.

37. W. YAO and C. MOREL, "Volumetric Interfacial Area Prediction in Upward Bubbly Two-Phase Flow," *Int. J. Heat Mass Transfer*, **47**, 307 (2004).

38. W. YAO and C. MOREL, "Prediction of Parameters Distribution of Upward Boiling Two-Phase Flow with Two-Fluid Models," *Proc. 10th Int. Conf. Nuclear Engineering (ICONE 10)*, Washington, D.C., April 14–18, 2002, American Society of Mechanical Engineers (2002).

39. R. SCHIESTEL, *Modélisation et simulation des écoulements turbulents*, Hermès, Paris (1993).

40. N. KURUL and M. PODOWSKI, "Multidimensional Effects in Forced Convection Subcooled Boiling," *Proc. 9th Int. Heat Transfer Conf.*, Jerusalem, Israel, August 19–24, 1990, Vol. 1, p. 21 (1990).

41. P. HAYNES, "Contribution à la modélisation de la turbulence pour les écoulements à bulles: proposition d'un modèle K-epsilon multi-échelles diphasique," PhD Thesis, Institut National Polytechnique de Toulouse/Electricité de France/Institut de Mécanique des Fluides de Toulouse/Commissariat à l'Énergie Atomique (2004).

42. "Comparison Report of RPV Pressurised Thermal Shock—International Comparative Assessment Study (PTS ICAS)," Technical Report, Organisation for Economic Co-operation and Development/Nuclear Energy Agency/Committee on the Safety of Nuclear Installations (1999).

43. E. KEIM, C. SCHMIDT, A. SCHÖPPER, and R. HERTLEIN, "Life Management of Reactor Pressure Vessels Under Pressurized Thermal Shock Next Term Loading: Deterministic Procedure and Application to Western and Eastern Type of Reactors," *Int. J. Press. Vessels Piping*, **78**, 85 (2001).

44. A. MARTIN and S. BELLET, "CFD-Tools Qualification for Thermal-Hydraulics Pressurised Thermal Shock Analysis," *Proc. ASME Pressure Vessels and Piping Conference*, Vancouver, British Columbia, Canada, August 4–8, 2002, American Society of Mechanical Engineers (2002).

45. M. BOUCKER, J. LAVIÉVILLE, A. MARTIN, and C. BÉCHAUD, "Preliminary Applications of the New NEPTUNE Two-Phase CFD Solver to Pressurized Thermal Shock Investigations," *Proc. 12th Int. Conf. Nuclear Engineering (ICONE 12)*, Arlington, Virginia, April 25–29, 2004, American Society of Mechanical Engineers (2004).

46. W. YAO, P. COSTE, D. BESTION, and M. BOUCKER, "Two-Phase Pressurized Thermal Shock Investigations Using a 3D Two-Fluid Modeling of Stratified Flow with Condensation," *Proc. 10th Int. Topl. Mtg. Nuclear Reactor Thermal Hydraulics (NURETH 10)*, Seoul, Republic of Korea, October 5–9, 2003.

47. C. JAYATILLEKE, "The Influence of Prandtl Number and Surface Roughness on the Resistance of the Laminar Sublayer to Momentum and Heat Transfer," *Prog. Heat Mass Transfer*, **1**, 193 (1969).

48. L. SHEN, G. S.TRIANTAFYLLOU, and D. YUE, "Turbulent Diffusion Near a Free Surface," *J. Fluid Mech.*, **407**, 145 (2000).

49. E. HUGHES and R. DUFFEY, "Direct Contact Condensation and Momentum Transfer in Turbulent Separated Flows," *Int. J. Multiphase Flow*, **17**, *5*, 599 (1991).

50. J. FABRE, L. MASBERNAT, and C. SUZANNE, "Stratified Flow, Part 1: Local Structure," *Multiphase Sci. Technol.*, **3**, 285 (1987).

51. I. LIM, R. TANKIN, and M. YUEN, "Condensation Measurement of Horizontal Concurrent Steam-Water Flow," *J. Heat Transfer*, **106**, 425 (1984).

52. S. PIGNY, M. BOUCKER, J. LAVIÉVILLE, and N. MÉCHITOUA, "Extensive Assessment of the Numerical Method of the New NEPTUNE Two-Phase CFD Solver on Numerical Benchmark Exercises for Steam-Water Flows," *Proc. 5th Int. Conf. Multiphase Flow (ICMF5)*, Yokohama, Japan, May 30–June 4, 2004, International Information Center for Multiphase Flow (2004).

53. B. RIEGEL, "Supercanon," Technical Report, Commissariat à l'Énergie Atomique (1979).

54. W. MASCHEK, A. ROTH, M. KIRSTAHLER, and L. MEYER, "Simulation Experiments for Centralized Liquid Sloshing Motions," KfK-5090, Kernforschungszentrum Karlsruhe (1992).

55. R. B. FDHILA, "Analyse expérimentale et modélisation d'un écoulement vertical à bulles dans un élargissement brusque," PhD Thesis, Institut National Polytechnique de Toulouse (1991).

56. C. MOREL, J. POUVREAU, J. LAVIÉVILLE, and M. BOUCKER, "Numerical Simulations of a Bubbly Flow in a Sudden Expansion with the NEPTUNE Code," *Proc. 3rd Int. Symp. Two-Phase Flow Modeling and Experimentation*, Pisa, Italy, September 22–25, 2004.

57. J. GARNIER, E. MANON, and G. CUBIZOLLES, "Local Measurements on Flow Boiling of Refrigerant 12 in a Vertical Tube," *Multiphase Sci. Technol.*, **13**, 1 (2001).

58. C. MOREL, S. MIMOUNI, J. LAVIÉVILLE, and M. BOUCKER, "R113 Boiling Bubbly Flow in an Annular Geometry Simulated with the NEPTUNE Code," *Proc. 11th Int. Topl. Mtg. Nuclear Reactor Thermal Hydraulics (NURETH 11)*, Avignon, France, October 2–6, 2005.

59. S. MIMOUNI, "Validation partielle du code NEPTUNE 3D local V1.0 sur les essais DEDALE, DEBORA, AGATE promoteur et DEBORA promoteur," Technical Report, Electricité de France (2004).

60. D. BESTION and J. G. D'AILLON, "Condensation Tests Analysis and Correlation for the CATHARE Code," *Proc. 4th Int. Topl. Mtg. Nuclear Reactor Thermal Hydraulics (NURETH 4)*, Karlsruhe, Germany, October 10–13, 1989.

61. A. JANICOT and D. BESTION, "Condensation Modeling for ECC Injection," *Nucl. Eng. Des.*, **145**, 37 (1993).

62. "SALOME: The Open Source Integration Platform for Numerical Simulation," Open CASCADE S.A.S.; available on the Internet at http://www.salome-platform.org (2006).

63. J. LAUTARD, D. SCHNEIDER, and A. BAUDRON, "Mixed Dual Methods for Neutronic Reactor Core Calculation in the CRONOS System," *Proc. Int. Conf. Mathematics and Computation, Reactor Physics and Environmental Analysis in Nuclear Applications (M&C 1999)*, Madrid, Spain, September 27–30, 1999, American Nuclear Society (1999).

64. C. FEDON-MAGNAUD et al., "Mixed Dual Methods for Neutronic Reactor Core Calculation in the CRONOS System," *Proc. Int. Mtg. Nuclear Mathematical and Computational Sciences (M&C 2003)*, Gatlinburg, Tennessee, April 6–11, 2003, American Nuclear Society (2003).

65. G. PETIT, C. COLLIGNON, J. FEBURIE, E. GARCIA, and C. ACKERMANN, "COCCINELLE V3.4, Manuel d'utilisation," Technical Report, Electricité de France (2002).

66. C. CAREMOLI and J. BERTHOU, "CALCIUM V2, Guide d'utilisation," Technical Report, Electricité de France (1996).

67. B. AKHERRAZ, J. LAUTARD, and P. ERHARD, "An Object-Oriented 3D Nodal Finite Element Solver for Neutron Transport Calculations in the Descartes Project," *Proc. Int. Conf. Supercomputing in Nuclear Applications (SNA 2003)*, Paris, France, September 22–24, 2003.

68. G. SERRE and D. BESTION, "Progress in Improving Two-Fluid Model in System Code Using Turbulence and Interfacial Area Equation," *Proc. 11th Int. Topl. Mtg. Nuclear Reactor Thermal Hydraulics (NURETH 11)*, Avignon, France, October 2–6, 2005.

69. M. VALETTE and S. JAYANTI, "Annular Dispersed Flow Calculations with a Two-Phase Three-Field Model," *Proc. 41st European Two-Phase Flow Group Meeting*, Trondheim, Norway, May 11–14, 2003.

70. S. JAYANTI and M. VALETTE, "Prediction of Dry-Out and Post Dry-Out Heat Transfer at High Pressure Using a One-Dimensional Three-Field Model," *Int. J. Heat Mass Transfer*, **47**, 4895 (2004).

71. S. JAYANTI and M. VALETTE, "Calculation of Dry-Out and Post Dry-Out Heat Transfer in Rod Bundles Using a Three-Field Model," *Int. J. Heat Mass Transfer*, **48**, 1825 (2005).

72. G. YODER, D. MORRIS, C. MULLINS, and L. OTT, "Dispersed-Flow Film Boiling Heat Transfer Data Near Spacer Grids in a Rod Bundle," *Nucl. Technol.*, **60**, 304 (1983).

73. D. BESTION and A. GUELFI, "Multi-Scale Analysis of Nuclear Reactor Thermal-Hydraulics—The NEPTUNE Project," *Proc. SHF/AIRH Conf. Advances in the Modeling Methodologies of Two-Phase Flows*, November 2004.

74. M. GRANDOTTO, C. BÉCHAUD, M. BOUCKER, A. DOUCE, and M. TAJCHMAN, "A Component Architecture for the Two-Phase Flow Simulation System NEPTUNE," *Proc. Supercomputing in Nuclear Applications (SNA 2003)*, Paris, France, September 22–24, 2003.

75. J. SCHLUTER, "Consistent Boundary Conditions for Integrated RANS/LES Simulations: LES Inflow Conditions," AIAA paper 2003-3971, American Institute of Aeronautics and Astronautics (2003).

76. J. SCHLUTER, H. PITSCH, and P. MOIN, "Consistent Boundary Conditions for Integrated RANS/LES Simulations: LES Outflow Conditions," AIAA paper 2002-3121, American Institute of Aeronautics and Astronautics (2002).

77. J. BLAZEK, "Comparison of Two Conservative Coupling Algorithms for Structured/Unstructured Grid Interfaces," AIAA paper 2003-3536, American Institute of Aeronautics and Astronautics (2003).

78. J. GREENBERG and A. LE ROUX, "A Well Balanced Scheme for the Numerical Processing of Source Terms in Hyperbolic Equation," *SIAM J. Numer. Anal.*, **33**, *1*, 1 (1996).

79. J. GREENBERG, A. LE ROUX, R. BARAILLE, and A. NOUSSAIR, "Analysis and Approximation of Conservation Laws with Source Terms," *SIAM J. Numer. Anal.*, **34**, *5*, 1980 (1997).

80. E. GODLEWSKI and P. RAVIART, "The Numerical Coupling of Non-Linear Hyperbolic Systems of Conservation Laws—The Scalar Case," *Numerische Mathematik*, **97**, 81 (2004).

81. E. GODLEWSKI, K. LE TANH, and P. RAVIART, "The Numerical Coupling of Non-Linear Hyperbolic Systems of Conservation Laws—The System Case," *Math. Models Numer. Anal.*, **39**, 649 (2005).

82. A. AMBROSO, F. COQUEL, C. CHALONS, E. GODLEWSKI, F. LAGOUTIERE, and P. RAVIART, CEA-SFME/JLL Working Group on the Coupling of Models in Thermohydraulics (2003).

83. A. AMBROSO, "An Introduction to the Problem of Interfacial Coupling of Thermohydraulic Models," Internal Report SFME/LETR/RT/04-008/A, Commissariat à l'Énergie Atomique (2004).

84. J. HÉRARD, "Naive Schemes to Compute Isentropic Flows Between Free and Porous Medium," Report HI81/04/008/A, Electricité de France; see also *Int. J. Finite Vol.*, **3**, *2* (2006); available on the Internet at http://www.latp.univ-mrs.fr/IJFV/.

85. J. HÉRARD and O. HURISSE, "Coupling Two and One-Dimensional Unsteady Euler Equations Through a Thin Interface," *Comput. Fluids*, **36**, *4*, 651 (2007).

86. A. AMBROSO, C. CHALONS, F. COQUEL, E. GODLEWSKI, F. LAGOUTIERE, and P. RAVIART, "Coupling of Multi-Phase Flow Models," *Proc. 11th Int. Topl. Mtg. Nuclear Reactor Thermal Hydraulics (NURETH 11)*, Avignon, France, October 2–6, 2005.

87. A. AMBROSO, C. CHALONS, F. COQUEL, E. GODLEWSKI, F. LAGOUTIERE, P. RAVIART, and N. SEGUIN, "Homogeneous Two-Phase Flow Models: Coupling by Finite Volume Methods," *Proc. 4th Int. Symp. Finite Volume for Complex Applications (FVCA 4)*, Marrakech, Morocco, July 4–8, 2005; see also *Int. J. Finite Vol.*, **4**, *1* (2007); available on the Internet at http://www.latp.univ-mrs.fr/IJFV/.

88. A. AMBROSO, J. HÉRARD, and O. HURISSE, "A Method to Couple Two-Phase Flow Models," AIAA paper 2006-3900, American Institute of Aeronautics and Astronautics (2006).

89. J. HÉRARD and O. HURISSE, "A Few Schemes to Compute Hyperbolic Systems with Source Terms," Report HI81/04/007/A, Electricité de France (2004); published in revised form in CALCOLO, **43**, *4*, 217 (2006).

90. J. HÉRARD and O. HURISSE, "A Relaxation Method to Compute Two Fluid Models," *Int. J. Comput. Fluid Dyn.*, **19**, 475 (2005).

91. T. GALLOUET, J. HÉRARD, and N. SEGUIN, "Numerical Modelling of Two-Phase Flows Using the Two-Fluid Two-Pressure Approach," *Math. Models Methods Appl. Sci.*, **14**, 663 (2004).

92. F. COQUEL, T. GALLOUET, J. HÉRARD, and N. SEGUIN, "Closure Laws for a Two-Fluid Two Pressure Model," *Comptes Rendus de l'Académie des Sciences*, **I-334**, 927 (2002).

93. J. HÉRARD and O. HURISSE, "A Method to Couple Two-Fluid Models and Homogeneous Models," Report H181/2006/04691/FR, Electricité de France (2006).

94. D. JAMET and P. RUYER, "A Quasi-Incompressible Model Dedicated to the Direct Numerical Simulation of Liquid-Vapour Flow with Phase Change," *Proc. 5th Int. Conf. Multiphase Flow (ICMF5)*, Yokohama, Japan, May 30–June 4, 2004, International Information Center for Multiphase Flow (2004).

95. B. MATHIEU, O. LEBAIGUE, and L. TADRIST, "Influence of Dynamic Contact Line Model on the Characteristics of Nucleate Wall Boiling Computed with a DNS Approach," *Proc. 5th Int. Conf. Multiphase Flow (ICMF5)*, Yokohama, Japan, May 30–June 4, 2004, International Information Center for Multiphase Flow (2004).

96. C. FOUILLET, "Généralisation à des mélanges binaires de la méthode du second gradient et application à la simulation numérique directe de l'ébullition nucléée," PhD Thesis, Université Paris VI/Commissariat à l'Énergie Atomique-Grenoble (2003).

97. B. MATHIEU, "Etude physique, expérimentale et numérique des mécanismes de base intervenant dans les écoulements diphasiques," PhD Thesis, Université de Provence/Commissariat à l'Énergie Atomique-Grenoble (2003).

98. E. LABOURASSE, A. TOUTANT, and O. LEBAIGUE, "Bubble Interface-Turbulence Interaction," *Proc. 5th Int. Conf. Multiphase Flow (ICMF5)*, Yokohama, Japan, May 30–June 4, 2004, International Information Center for Multiphase Flow (2004).

99. D. LAKEHAL, B. SMITH, and M. MILELLI, "Large-Eddy Simulation of Bubble Turbulent Shear Flows," *IOP J. Turbulence*, **3**, 1 (2002).

100. D. LAKEHAL, S. REBOUX, and P. LIOVIC, "Subgrid Scale Modeling for the LES of Interfacial Gas-Liquid Flows," *Proc. SHF/AIRH Conf. Advances in the Modeling Methodologies of Two-Phase Flows*, November 2004; see also *La Houille Blanche*, **6** (2005).

101. D. BESTION, "The Physical Closure Laws in the CATHARE Code," *Nucl. Eng. Des*., **124**, 229 (1990).

102. M. BAER and J. NUNZIATO, "A Two Phase Mixture Theory for the Deflagration to Detonation (DDT) Transition in Reactive Granular Materials," *Int. J. Multiphase Flow*, **12**, *6*, 861 (1986).

103. A. KAPILA, S. SON, J. BDZIL, R. MENIKOFF, and D. STEWART, Two-Phase Modelling of DDT: Structure of the Velocity Relaxation Zone," *Phys. Fluids*, **9**, 3885 (1997).

104. J. GLIMM, D. SALTZ, and D. SHARP, "Renormalization Group Solution of Two Phase Flow Equations for Rayleigh-Taylor Mixing," *Phys. Lett., A*, **222**, 171 (1996).

105. R. SAUREL and R. ABGRALL, "A Multiphase Godunov Method for Compressible Multifluid and Multiphase Flows," *J. Comput. Phys*., **150**, 425 (1999).

106. S. GAVRILYUK and R. SAUREL, "Mathematical and Numerical Modelling of Two Phase Compressible Flows with Inertia," *J. Comput. Phys*., **175**, 326 (2002).

107. J. HÉRARD, "Numerical Modelling of Turbulent Two Phase Flows Using the Two Fluid Approach," AIAA paper 2003-4113, American Institute of Aeronautics and Astronautics (2003).

108. T. GALLOUET, J. HÉRARD, R. HERBIN, N. JULLIAN, and N. SEGUIN, "Upwind Finite Volume Schemes for One and Two Dimensional Euler Equations," AIAA paper 2003-4122, American Institute of Aeronautics and Astronautics (2003).

109. F. COQUEL, K. E. AMINE, E. GODLEWSKI, B. PERTHAME, and P. RASCLE, "A Numerical Method Using Upwind Schemes for the Resolution of Two Phase Flows," *J. Comput. Phys*., **136**, 272 (1997).

110. I. TISELJ and S. PETELIN, "Modelling of Two-Phase Flow with Second Accurate Scheme," *J. Comput. Phys*., **136**, 503 (1997).

111. H. STAEDTKE, "Remarks on Single Pressure Two-Fluid Model and Hyperbolicity," Contribution to the ASTAR project (Aug. 2002) (unpublished).

112. J. HÉRARD, "An Hyperbolic Three-Phase Flow Model," *Comptes Rendus de l'Académie des Sciences de Paris*, **I-342**, 779 (2006).

113. G. ALLAIRE, S. CLERC, and S. KOKH, "A Five-Equation Model for the Numerical Solution of Interfaces in Two Phase Flows," *Comptes Rendus de l'Académie des Sciences de Paris*, **I-331**, 1017 (2000).

114. G. ALLAIRE, S. CLERC, and S. KOKH, "A Five-Equation Model for the Simulation of Interfaces Between Compressible Fluids," *J. Comput. Phys*., **181**, 577 (2002).

115. F. CARO, F. COQUEL, D. JAMET, and S. KOKH, "A Simple Finite Volume Method for Compressible Isothermal Two-Phase Flow Simulations," *Int. J. Finite Volumes*, **3**; available on the Internet at http://averoes.math.univ-paris13.fr (2006).

116. F. CARO, "Modélisation et simulation numérique des transitions de phase liquide-vapeur," PhD Thesis, Ecole Polytechnique, Palaiseau, France (Nov. 24, 2004).

117. H. GUILLARD and A. MURONNE, "On the Behaviour of Upwind Schemes in the Low Mach Number Limit: II. Godunov Type Schemes," *Comput. Fluids*, **33**, 655 (2004).

118. S. GODUNOV, "A Difference Method for Numerical Calculation of Discontinuous Equations of Hydrodynamics," *Sbornik*, pp. 271–300 (1959).

119. T. BUFFARD, T. GALLOUET, and J. HÉRARD, "A Sequel to a Rough Godunov Scheme. Application to Real Gases," *Comput. Fluids*, **29**, *7*, 813 (2000).

120. M. BELLIARD and C. CRYPPA, "Comparaison de méthodes de résolution du système linéaire en pression de PyGene pour un grand nombre d'éléments," Internal Report NT/DTN/SMTM/2004-16, Commissariat à l'Énergie Atomique (2004).

121. M. BELLIARD and M. GRANDOTTO, "Multigrid Preconditioning of the Steam Generator Two Phase Mixture Balance Equations in the GENEPI Software," *Proc. 10th Int. Topl. Mtg. Nuclear Reactor Thermal Hydraulics (NURETH 10)*, Seoul, Republic of Korea, October 5–9, 2003.

122. P. ANGOT, C. BRUNEAU, and P. FABRIE, "A Penalization Method to Take into Account Obstacles in Incompressible Viscous Flows," *Numerische Mathematik*, **81**, 497 (1999).

123. I. RAMIÈRE, P. ANGOT, and M. BELLIARD, "Fictitious Domain Methods to Solve Convection Diffusion Problems with General Boundary Conditions," AIAA paper 2005-4709, American Institute of Aeronautics and Astronautics (2005).

124. I. RAMIÈRE, M. BELLIARD, and P. ANGOT, "On the Simulation of Nuclear Power Plant Components Using a Fictitious Domain Approach," *Proc. 11th Int. Topl. Mtg. Nuclear Reactor Thermal Hydraulics (NURETH 11)*, Avignon, France, October 2–6, 2005.

125. I. RAMIÈRE, "Méthodes de domaine fictif pour des problèmes elliptiques avec conditions aux limites générales en vue de la simulation numérique d'écoulements diphasiques," PhD Thesis, Université Aix Marseille I, Marseille, France (2006).

126. T. FORTIN, "Une methode Eléments Finis à décomposition L2 d'ordre élevé motivée par la simulation d'écoulements diphasiques Bas Mach," PhD Thesis, Université Paris VI, France, (May 5, 2006).

127. G. PIÉROTTI and P. DÉCEMBRE, "Experimental Studies of Two-Phase Flow Across Tube Support and Distribution Plates," *Proc. 11th ASME Winter Annual Meeting*, Dallas, Texas, November 25–December 1, 1990.

128. P. HAYNES, P. PETURAUD, M. MONTOUT, and E. HERVIEU, "Strategy for the Development of a DNB Local Predictive Approach Based on the NEPTUNE CFD Software," *Proc. 14th Int. Conf. Nuclear Engineering (ICONE 14)*, Miami, Florida, July 17–20, 2006, American Society of Mechanical Engineers (2006).

129. A. SCHAFFRATH, A. KRÜSSENBERG, F. WEISS, E. HICKEN, M. BEYER, H. CARL, H. PRASSER, J. SCHUSTER, P. SCHÜTZ, M. TAMME, and W. ZIMMERMANN, "TOPFLOW, A New Multipurpose Thermal-Hydraulic Test Facility for the Investigation of Steady State and Transient Two-Phase Flow Phenomena," *Kerntechnik*, **66**, 209 (2001).

130. G. GEFFRAYE, S. LAROCHE, B. FAYDIDE, and G. RATEL, "CATHARE Assessment on MHYRESA Tests," *Proc. 8th Int. Conf. Nuclear Engineering (ICONE 8)*, Baltimore, Maryland, April 2–6, 2000, American Society of Mechanical Engineers (2000).

131. A. JUNQUA, "Détermination expérimentale et modélisation de la concentration d'aire interfaciale en écoulement stratifié horizontal," PhD Thesis, Institut National Polytechnique de Grenoble (2003).

132. J. L. CORRE, E. HERVIEU, M. ISHII, and J. DELHAYE "Benchmarking and Improvements of Measurement Techniques for Local-Time-Averaged Two-Phase Flow Parameters," *Exp. Fluids*, **35**, 448 (2003).

133. E. HERVIEU and A. JUNQUA, "Using and Assessing Four-Sensor Optical Probe of an X-Ray Tomograph for Two-Phase Flows," *Proc. 5th Int. Conf. Multiphase Flow (ICMF5)*, Yokohama, Japan, May 30–June 4, 2004, International Information Center for Multiphase Flow (2004).

134. P. MATHIEU and E. HERVIEU, "Development of an X-Ray Tomograph for Two-Phase Flows Void Fraction Measurement," *Proc. 41st European Two-Phase Flow Group Meeting*, Trondheim, Norway, May 11–14, 2003.

135. E. JOUET, "Mise au point et qualification d'une technique de mesure du taux de présence local par tomographie à rayons X," PhD Thesis, Institut National Polytechnique de Grenoble (2001).

136. E. HERVIEU, E. JOUET, and L. DESBAT, "Development and Validation of an X-Ray Tomograph for Two-Phase Flows," *Proc. 1st Int. Symp. Visualization and Imaging Transport Phenomena (VIM01)*, Antalya, Turkey, May 5–10, 2002, International Center for Heat and Mass Transfer (2002).